New Applications of Covariance NMR and Experimental Development for Measurements of Homonuclear Coupling Constants in Overlapping Signals

André Roberto de Oliveira Fredi

Universitat Autònoma de Barcelona

New Applications of Covariance NMR and Experimental Development for Measurements of Homonuclear Coupling Constants in Overlapping Signals

André Roberto de Oliveira Fredi

Doctoral thesis

Ph.D. in Chemistry

Director:

Dr. Teodor Parella Coll, Dr. Pau Nolis Fañanas

Tutor: Dr. Albert Virgili Moya

Chemistry Department

Faculty of Science

2018

Universitat Autònoma de Barcelona

Memòria presentada per aspirar al Grau de Doctor per André Roberto de Oliveira Fredi

Vist i plau,

Dr. Teodor Parella Coll

Dr. Pau Nolis Fañanas

Dr. Albert Virgili Moya

André Roberto de Oliveira Fredi

Bellaterra, 20 de febrer de 2018

ACKNOWLEDGMENT

I would like to thank the financial aid of different institutions for the realization of this thesis.

- *Conselho Nacional de Desenvolvimento Científico e Tecnológico* (CNPq) for the help with the doctoral scholarship and the accomplishment of this thesis.
- *Universitat Autònoma de Barcelona* (UAB) and Chemistry Department for all activities involving classes and conferences that helped me very much with the growth of my knowledge.
- *Servei de Ressonància Magnètica Nuclear* (SeRMN) for offering me optimum working conditions and the use of all its equipment and facilities.
- Projects CTQ2012-32436 and CTQ2015-64436-P from the Spanish MINECO.
- *Grupo Especializado de Resonancia Magnética Nuclear* (GERMN) for financial help with travel to conferences and courses.

Agradeço ao meu orientador Dr. Teodor Parella pela oportunidade de desenvolver este trabalho e por me ensinar sobre as maravilhas da RMN. Obrigado!

Também quero agradecer Pau Nolis por ter me ajudado muito com o desenvolvimento de novas sequências e por estar próximo me ensinando e ajudando.

Em especial eu agradeço aos meus pais. Sem eles, eu não seria quem eu sou hoje. Com eles aprendi a apreciar a importância e o valor da família.

À minha mãe que sempre me apoiou em todos esses meus anos longe de casa estudando e por seu carinho e amor. A minha irmã Juliana, a minha avó Dores, meu tio Evandro, meu Pai que me ajudaram diretamente com apoio e motivação para a conclusão deste trabalho.

Aos meus amigos de laboratório, Núria Marcó, Kumar Motiram, Laura Castañar pelo incentivo e distração no dia-a-dia.

Aos técnicos do SerRMN Eva Monteagudo, Miquel Cabañas, Miriam Perez, Silvia Lope e Esperanza Ramirez pela ajuda com os espectrômetros, por compartilhar seus conhecimentos e por me receberem muito bem no laboratório onde me senti muito a vontade, como uma segunda casa.

Aos funcionários do Departamento de Química por toda ajuda com as burocracias.

A todos que trabalham na companhia Mestrelab por ajudar com as dúvidas sobre o software, pela boa conversa e tempos que passamos juntos.

Aos meus cachorros Whisky, Vida, Tieta, Raja e Bia que sempre estiveram nos meus pensamentos e até hoje estão.

SUMMARY

LIST OF ABBREVIATIONS

λ	matrix power
δ	chemical shift
2D	two-dimensional
BASH	BAnd-Selective Homonuclear
BIRD	BIlinear Rotational Decoupling
COSY	COrrelation SpectroscopY
CPMG	Carr-Purcell-Meiboom-Gill
DC	Direct Covariance
DIAG	2D F1-homodecoupled ^{1}H-^{1}H DIAGonal correlation
DIC	Doubly Indirect Covariance
DOSY	Diffusion-Ordered SpectroscopY
DSE	Double-Spin Echo
EA	Echo/Anti-Echo
Eq.	Equation
FID	Free Induction Decay
FT	Fourier Transformation
GIC	Generalized Indirect Covariance
GSD	Global Spectral Deconvolution
G-SERF	Gradient-encoded SERF experiment
H2BC	Heteronuclear 2-Bond Correlation
HOBS	HOmodecoupled Band-Selective
HSQC	Heteronuclear Single Quantum Coherence

HSQMBC	Heteronuclear Single Quantum Multiple Bond Coherence
IC	Indirect Covariance
INADEQUATE	Incredible Natural Abundance DoublE QUAntum transfEr
IDR	Inverse Direct Response
J	scalar coupling
J_{HH}	Proton-proton scalar coupling
J-res	*J*-resolved
ME	Multiplicity-Edited
MRI	Magnetic Resonance Imaging
NMR	Nuclear Magnetic Resonance
NOESY	Nuclear Overhauser Effect SpectroscopY
NUS	Non-Uniform Sampling
PFG	Pulse-Field Gradient
ps	Pure-Shift
psNMR	Pure-Shift NMR
psGIC	Pure-Shift NMR spectra by using Generalized Indirect Covariance
PSYCHE	Pure Shift Yielded by CHirp Excitation
PSYCHEDELIC	Pure Shift Yielded by CHirp Excitation to DELiver Individual Couplings
rf	radiofrequency
SelTOCSY	Selective TOtal Correlation SpectroscopY
SERF	SElective ReFocusing
SNR	Signal-to-Noise Ratio

TOCSY	Total Correlation SpectroscopY
UIC	Unsymmetrical Indirect Covariance
ZQ	Zero-Quantum Coherence
ZQF	Zero-Quantum Filter
ZS	Zangger-Sterk

1. INTRODUCTION

1.1. Covariance NMR

1.1.1. Basic Concepts

Nuclear Magnetic Resonance (NMR) spectroscopy is one of the most widely used techniques for studying structural determination, conformational analysis and dynamic properties of molecules in solution. Indeed, instrument developments in the last five decades culminated in the positioning of NMR as the primary analytical technique to characterize organic compounds and biomolecules in solution- and solid-state conditions. Besides that, NMR is a quantitative and non-destructive analytical tool also applied to many other fields of science. In 1966, the application of the Fourier Transformation (FT) for efficient NMR data processing represented a significant advance that revolutionized the concept of fast NMR. Its general implementation allowed the design and development of a high number of different pulses sequences.[1] Some years later, two-dimensional (2D) NMR was initially projected by Jeener and experimentally implemented by Ernst and their collaborators in the so-called COrrelation SpectroscopY (COSY) experiment.[2] With these fundamentals and with the help of technological enhancements that have been appearing over time (higher magnetic fields, improved probe heads and more robust electronic devices), an extensive library of new and increasingly sophisticated NMR experiments are now available for a wide range of NMR and Magnetic Resonance Imaging (MRI) applications.

Figure 1 shows a general pulse sequence scheme to acquire a 2D NMR experiment. The nuclei of interest are initially excited during the preparation period, and the corresponding transverse magnetization evolves during a variable t_1 period with a ω_1 frequency (that affords the indirect dimension (F1) after FT). After that, transfer polarization between different nuclei takes place during the mixing time which defines the type of the NMR experiment to be performed. Finally, all schemes finish with the acquisition of the Free Induction Decay (FID) of the signal monitored during a detection t_2 period with a ω_2 frequency (that generates the direct dimension (F2) after FT).

The resulting 2D spectrum displays signal intensities as a function of two correlated ω_1 and ω_2 frequencies involved in the mentioned t_1 and t_2 periods, respectively.

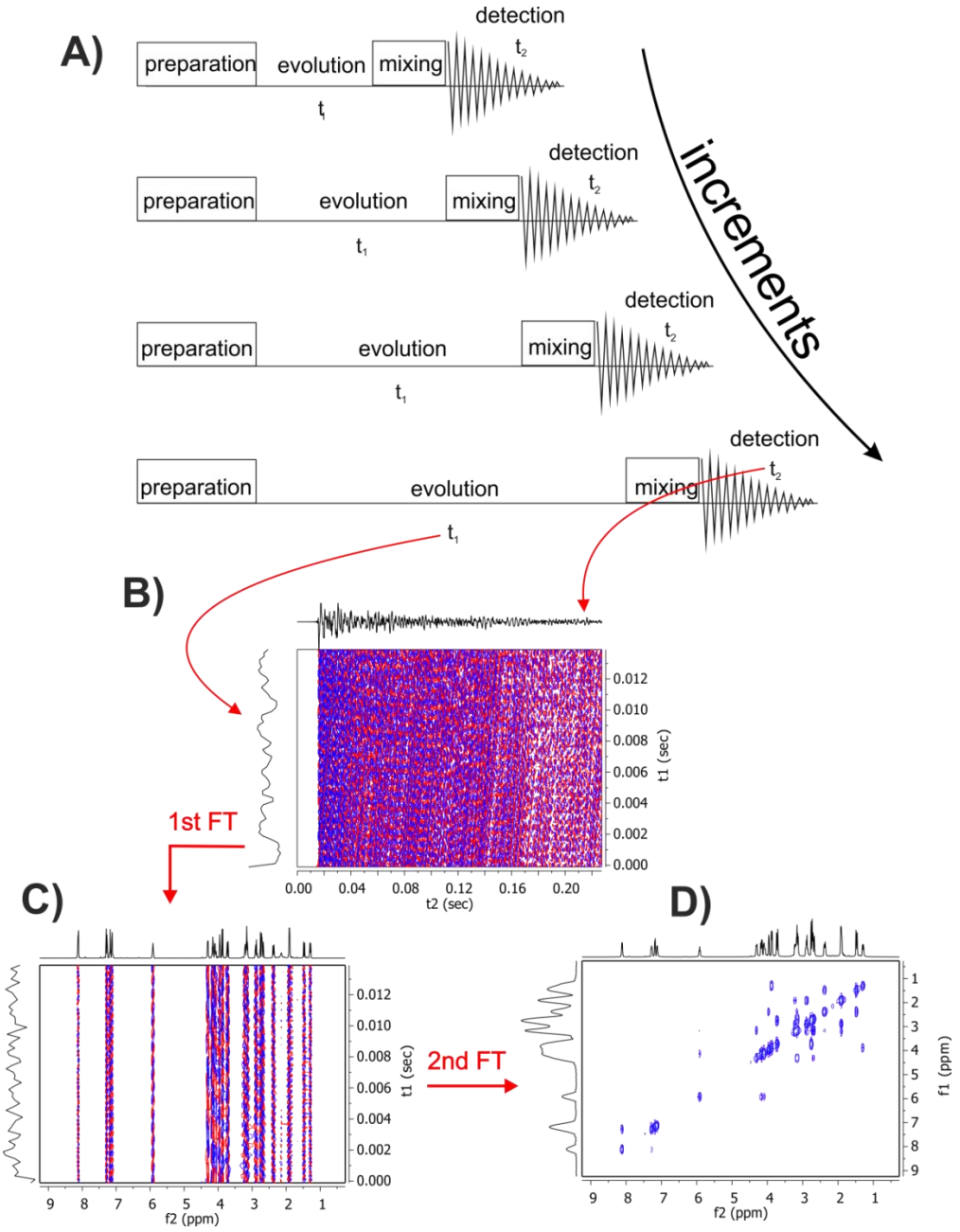

Figure 1: (A) Generalized scheme for the acquisition of a 2D NMR experiment. The pulse sequence is repeated *n* times by incrementing the t_1 period that provides the F1 dimension. On the other hand, the detection t_2 period generates the F2 dimension; (B-D) Generalized scheme for data processing of a 2D NMR dataset: (B) The full-time t_1 and t_2 domains; (C) after the first FT, the time-dependent F2 dimension is transformed to frequencies (columns); and similarly, (D) a second FT is subsequently applied to generate the F1 dimension (rows).

The time-dependent 2D NMR data set is represented by a 2D data matrix which is processed with a double FT to obtain an interpretable 2D spectrum. The first step applies FT in F2 (columns) of the 2D matrix (Figure 1C) and then, a second FT is executed for transform the signals in F1 (rows), as shown in Figure 1D. Usually, standard 2D experiments are collected with a relatively high resolution in F2 (for instance 2048 data points) and a lower resolution in F1 (64, 128 or 256 data t_1 points). As a significant drawback of 2D and higher dimensional NMR experiments, the overall experimental time is proportional to the number of incrementable t_1 increments to be recorded. Therefore, a resolution improvement in the F1 dimension is, in principle, only feasible by a proportional increase of the spectrometer time. Due to the mathematical nature of NMR data, other complementary data processing treatments are also available to increase spectral resolution per time unit. Some examples of current powerful tools are the use of window functions,[3] linear prediction,[4] Non-Uniform Sampling (NUS)[5–7] or Covariance co-processing.[8] In statistical terms, the Covariance is defined as the measurement of the variability of two or more variables. In practice, Covariance in NMR spectroscopy is associated with the combination of different dimensions of the same or different NMR spectra (Covariance mapping), with the aim to reconstruct a new spectral representation. This reconstruction avoids the necessary spectrometer time for data acquisition or generates new spectra that are difficult or impossible to obtain by experimental NMR pulse sequence acquisition. For a better understanding, the different types of Covariance NMR are briefly explained in the next section.

1.1.2. Types and applications of Covariance NMR

Covariance NMR methods are divided into two groups: Direct Covariance (DC) and Indirect Covariance (IC). In general, DC transfers the information available in F1 onto the F2 dimension of the same spectrum whereas that IC does the reverse process. As an extension of IC co-processing, other Covariance methods (Doubly Indirect Covariance (DIC), Unsymmetrical Indirect Covariance (UIC), and Generalized Indirect Covariance (GIC)) have

been further developed to combine dimensions from different 2D spectra. All these new co-processing tools allow different spectral reconstruction strategies while the presence of potential artefacts are minimized.

The utility of covariance NMR co-processing has been demonstrated in several studies devoted to structural elucidation,[9] quantitative NMR,[10] complex mixture analysis,[11,12] and the reconstruction of NMR spectra that are difficult or even impossible to acquire experimentally by pulse sequence design. Covariance is also compatible with other mathematical treatments, including deconvolution or NUS.[13,14] Covariance NMR is currently available in different commercial or open software tools. In this work, the covariance module included in the MNova software (version 11.0.0) package by Mestrelab Research[15] was used to reconstruct all spectra. Table 1 summarizes some *pros* and *cons* of each type of covariance processing.

Table 1: *Pros* and *cons* of Covariance NMR.

Types of covariance	*Pros*	*Cons*
Direct Covariance (DC)	- Enhanced F1 resolution.	- Only applicable in 2D homonuclear spectra. - Do not combine different NMR spectra.
Indirect Covariance (IC)	- Reconstruction of ^{13}C–^{13}C correlations spectra. - Higher sensitivity than experimental acquisition.	- Reduced F2 resolution. - Good F1 resolution is required (long acquisition times). - Do not combine different spectra.
Double Indirect Covariance (DIC)	- Combine the F1 dimensions from two different spectra. - Reconstruction of ^{13}C – ^{13}C correlations spectrum.	- Limited to homonuclear reconstructions.
Unsymmetrical Indirect Covariance (UIC)	- Reconstruction of a heteronuclear 2D spectrum from two different F1 dimensions. - Reconstruction of 2D NMR spectra faster than experimental acquisition.	- It does not apply matrix-square root. - Take care of the possible presence of artefacts.
Generalized Indirect Covariance (GIC)	- All pros of UIC. - Reconstruction of experiments that are difficult or even impossible to obtain experimentally. - Reduction of artefacts concerning UIC. - Applying different values of matrix power (λ) is possible.	- Take care of the possible presence of artefacts.

Direct Covariance

Brüschweiler and collaborators initially developed DC[16] with the aim to find alternative mathematical processing tools to the second FT in 2D experiments. DC co-processing captures the information of the high-resolved F2 dimension and transfers it onto the F1 dimension of the same spectrum, thus increasing resolution in F1 dimension and offering a valuable spectrometer time-saving. This kind of covariance only works in 2D homonuclear

experiments, like COSY, where both dimensions have the same properties and nuclei. The DC works with the following equation:

$$\boldsymbol{C^2} = A^T A \tag{1}$$

where ***C*** is the covariance map, ***A*** is the matrix data of the original spectrum and $\mathbf{A}^{\boldsymbol{T}}$ is the matrix transpose of ***A***. The F2 dimension of a 2D spectrum is called **donator** dimension because it donates its information to F1 dimension, the **acceptor** dimension.[17]

Different NMR spectra of the target molecule strychnine **1** dissolved in $CDCl_3$ are used in the following descriptions to explain the different types of existing covariance procedures. Figure 2 shows the benefits of using DC co-processing in a regular COSY spectrum acquired with an original digital resolution of 2048 (F2) x 64 (F1) complex points (Figure 2A). The increased resolution of the reconstructed COSY spectrum, with a symmetrical resolution of 2048 (F2) x 2048 (F1), is evidenced observing the resulting 2D cross-peaks and the F1 spectrum projection (Figure 2B). Regarding spectrometer time, the experimental COSY was acquired in 10 minutes whereas the equivalent spectrum with 2048 t_1 increments would last more than 6 hours of overall experimental time. Thus, the reconstruction of 2D homonuclear spectra by DC affords improved F1 resolution without additional spectrometer time. The DC co-processing has been successfully applied to enhance resolution in different homonuclear experiments, as reported for TOCSY,[18] NOESY,[16,19] COSY[19,20] and INADEQUATE[21] spectra.

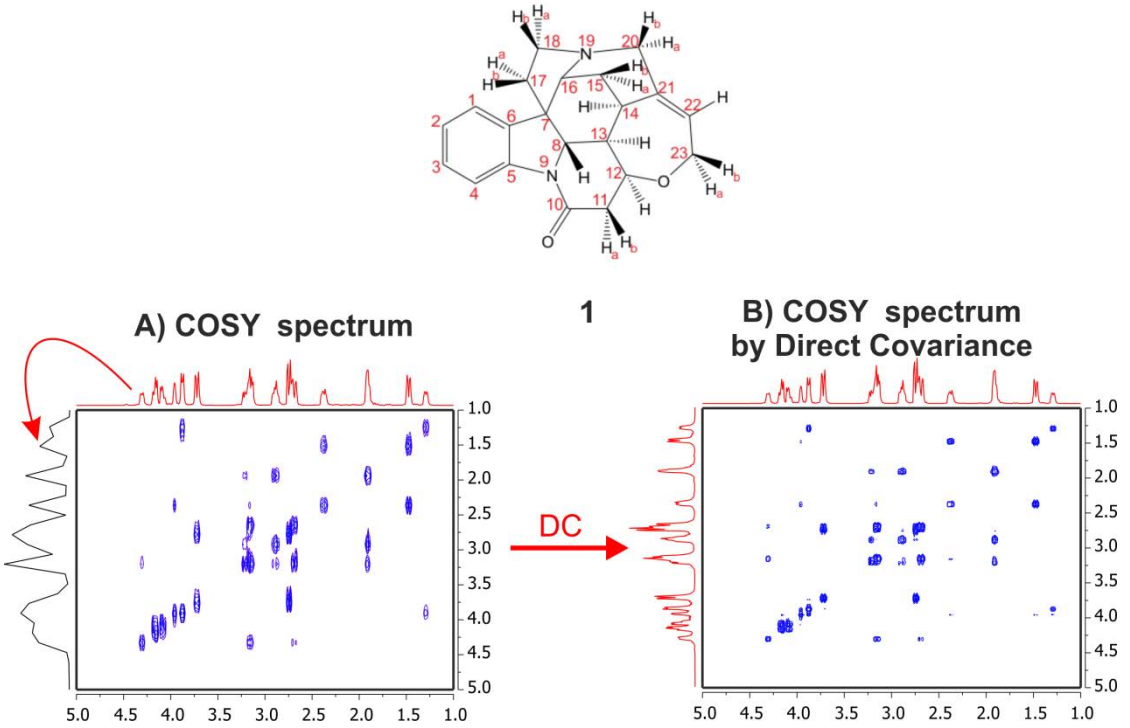

Figure 2: Example of Direct Covariance co-processing where the F2 resolution is transferred to the F1 dimension. (A) Conventional 500 MHz COSY spectrum of strychnine **1** (in $CDCl_3$) acquired with a matrix resolution of 2048 (F2) x 64 in F2 (F1), respectively, eight scans, 64 t_1 increments and 10 min. of overall experimental time. (B) After DC co-processing, the reconstructed COSY spectrum presents an improved matrix resolution of 2048 (F2) x 2048 (F1).

Indirect Covariance

Zhang and Brüschweiler announced IC[22] which works in the opposite sense of DC. IC transfers the information from F1 to F2 dimension, generating an unwanted reduction of F2 resolution. As an advantage, IC co-processing works on both 2D homonuclear and heteronuclear datasets. For instance, IC on the heteronuclear 2D $^{1}H–^{13}C$ HSQC-TOCSY spectrum of **1** (Figure 3A) transfers the information and features of the nucleus of the F1 (^{13}C) to F2 dimension. The result is a reconstructed homonuclear 2D $^{13}C–^{13}C$ TOCSY spectrum (Figure 3B) without having to detect ^{13}C directly. It is important to remark that time-consuming $^{13}C–^{13}C$ or $^{15}N–^{15}N$ correlation NMR experiments are not commonly recorded because they have a very low sensitivity (low

isotopic natural abundance of 1.1% for ^{13}C and 0.36% for ^{15}N), requiring ultra-long acquisition times or expensive ^{13}C isotopic enrichment.[17,23]

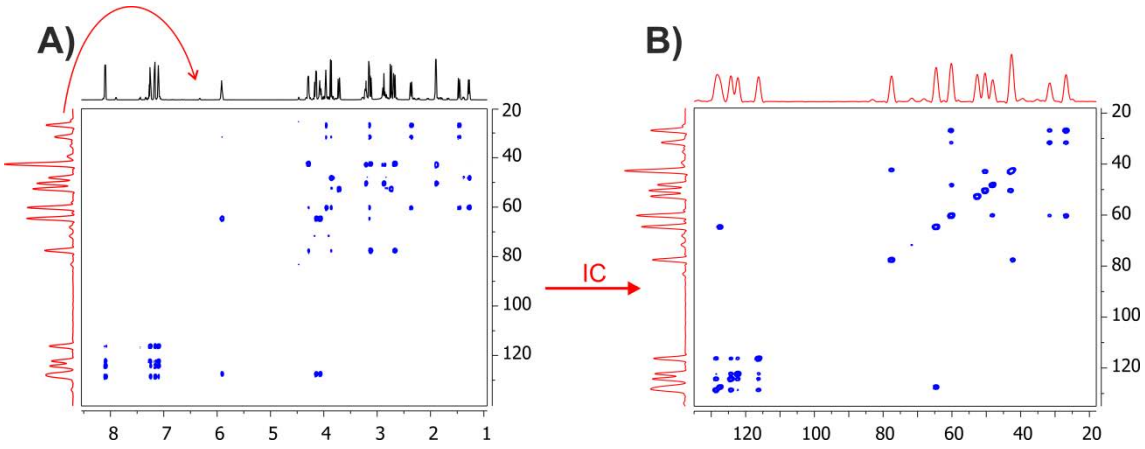

Figure 3: (A) standard 2D ^{1}H-^{13}C HSQC-TOCSY spectrum of **1** acquired in a 600 MHz spectrometer with 16 scans, 2048 complex points, and 256 t_1 increments (overall experimental time of 1 hour and 23 minutes). (B) IC processing quickly affords a novel ^{13}C-^{13}C TOCSY spectral representation.

Several spectral reconstruction examples involving IC have been reported such as the above-mentioned ^{13}C-^{13}C TOCSY spectra from ^{1}H–^{13}C HSQC-TOCSY.[22] Inspired in that example, Blinov *et al.*[24] investigated the presence of artefacts in ^{1}H–^{13}C HSQC-TOCSY and Inverse Direct Response (IDR) HSQC-TOCSY spectra that revealed that most of the artefacts are caused by overlapping signals. On the other hand, reconstructed long-range ^{13}C-^{13}C or ^{1}H-^{1}H correlation spectra can be derived from standard HMBC spectra.[25] Recently, Morris *et al.*[26] published a new F1-homodecoupled TOCSY (Figure 4A) experiment for achieving high levels of signal resolution in F1. The subsequent IC co-processing transfers the information from the F1 to F2 dimension to afford homodecoupled features in both dimensions (Figure 4B). The same idea has been extended to homodecoupled versions of the COSY and NOESY experiments. [27,28]

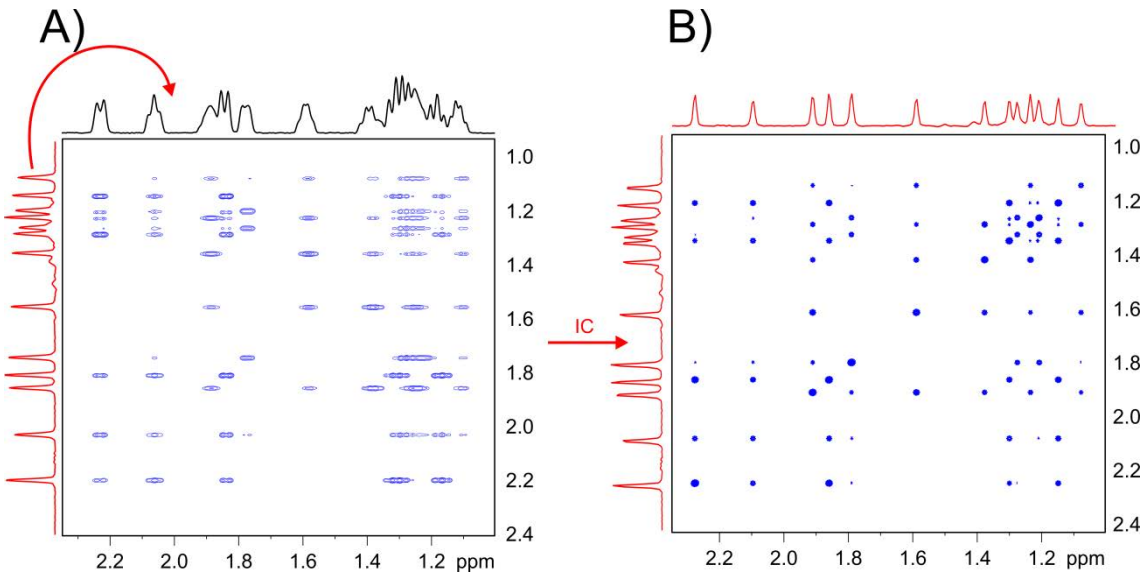

Figure 4: (A) 2D F1-homodecoupled TOCSY spectrum of estradiol **2** acquired in a 600 MHz spectrometer with four scans, 2048 complex points in F2 and 512 increments in F1. (B) IC transfers the information in the F1 to F2 dimension affording a 2D spectral representation homodeclouped in both dimensions.

Doubly Indirect Covariance

Until now, the described Covariance methods have combined the F1 and F2 dimensions of the same spectrum. On the other hand, the DIC is a double-step extension of IC that uses an intermediate step to take information from a different second spectrum. The DIC is defined as:

$$\boldsymbol{C^2} = A.B.A^T \tag{2}$$

As an example, when **A** is a ^{1}H–^{13}C HSQC (Figure 5A) and **B** is a ^{1}H–^{1}H COSY (Figure 5B), DIC first combines the F1 dimension of HSQC and COSY spectra and, then with the transpose of HSQC spectrum (**A**$^{\mathbf{T}}$), yielding a spectral reconstruction with the F1 dimension of HSQC in both dimensions togother with the information of COSY spectrum. Thus, the resulting DIC reconstructed spectrum affords a 2D ^{13}C–^{13}C COSY correlation map (Figure 5C). The benefit of such combination is that the experimental time of an experimental 2D ^{13}C–^{13}C COSY is much larger than the experimental time of two separate HSQC and COSY experiments. Furthermore, to acquire a

spectrum $^{13}C–^{13}C$ the molecule under study must be enriched with ^{13}C in order to detect such a nucleus with such low isotopic abundance. The DIC $^{13}C–^{13}C$ COSY spectrum presents a diagonal in which indicate the protonated carbons and the off-diagonal peaks correlates two directly connected carbons, but as a drawback, only protonated carbons are correlated while non-protonated carbons correlations are missing. To solve this problem, an alternative combination using $^{1}H–^{13}C$ HMBC and $^{1}H–^{1}H$ COSY spectra would afford long-range $^{13}C–^{13}C$ correlations involving both protonated and non-protonated carbons.[17]

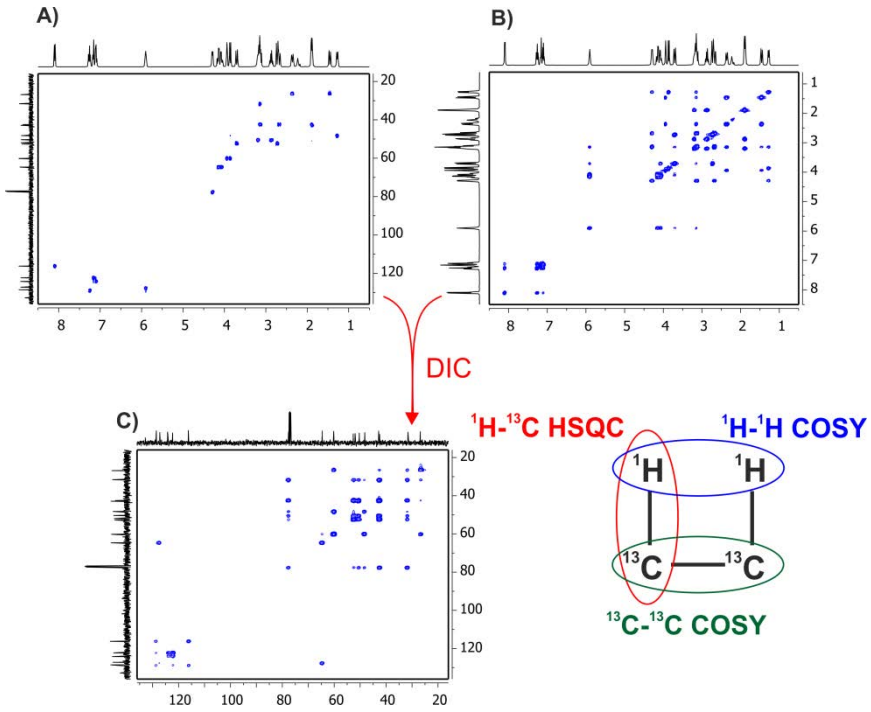

Figure 5: Experimental (A) 2D $^{1}H–^{13}C$ HSQC and (B) 2D $^{1}H–^{1}H$ COSY spectra of **1**. Both spectra were acquired in a 400 MHz NMR spectrometer using two scans, 2048 complex points in F2 and 256 t_1 increments (overall experimental time for each 2D experiment was about 10 minutes). (C) DIC quickly reconstructs a 2D $^{13}C –^{13}C$ COSY spectrum that affords the connections between directly attached protonated carbons.

Unsymmetrical Indirect Covariance

Until here, all the reconstruction covariance methods yielded spectra where both dimensions share the same resolution, the same nucleus and the same sweep widths. Martin and coworkers[29,30] created a new type of

covariance, named UIC, which combines two F1 dimensions containing different information of two different NMR spectra. UIC NMR is defined as [30]

$$\boldsymbol{C} = AB^T \tag{3}$$

For example, ^{1}H-^{13}C HSQC and ^{1}H-^{1}H COSY can be quickly combined by UIC to yield a ^{1}H-^{13}C HSQC-COSY representation without the need of additional spectrometer time. This HSQC-COSY spectrum is generated from the F1 dimension of the HSQC (**red colour**) and the F2 dimension of the transposed COSY dataset (**violet colour**) (Figure 6 A and B, respectively). ^{1}H-^{13}C HSQC-COSY is a useful spectrum because correlates carbon and protons separated by two bonds (like an H2BC experiment) or more bonds depending on how many correlations the COSY spectrum has.

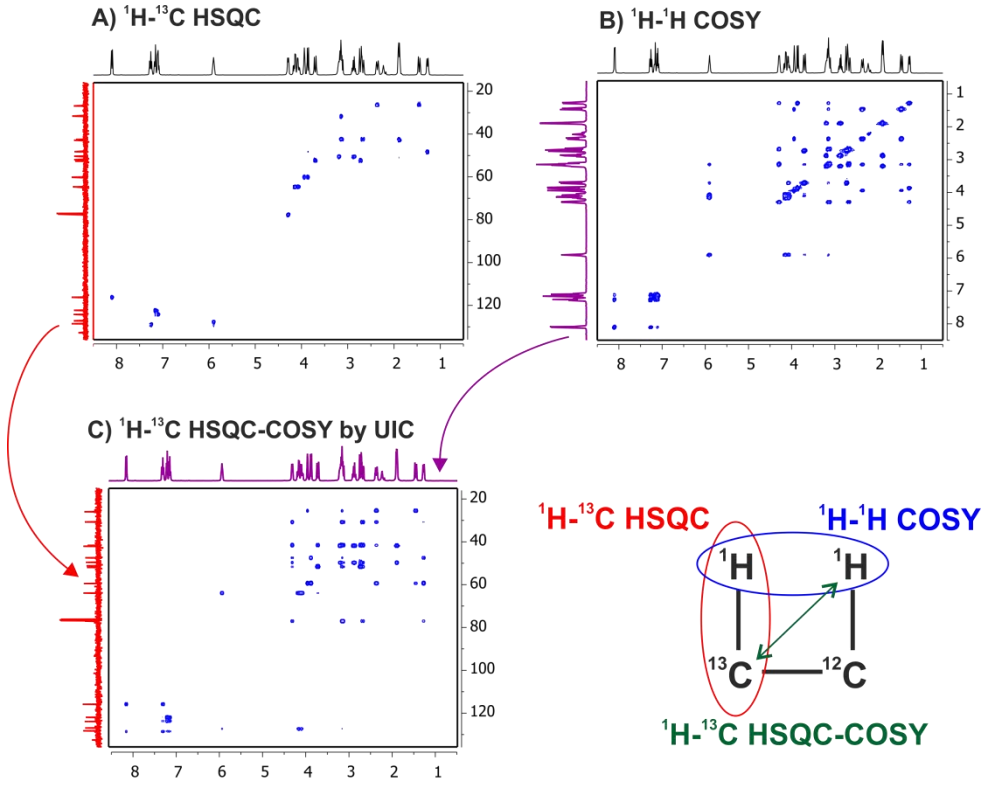

Figure 6: Experimental 400 MHz (A) 2D ^{1}H-^{13}C HSQC and (B) ^{1}H-^{1}H COSY spectra of **1** acquired with two scans, 2048 complex points in F2 and 256 t_1 increments. (C) UIC co-processing affords a 2D ^{1}H-^{13}C HSQC-COSY spectrum that draws the correlations between two-bonded protonated carbons and protons signals.

Many other UIC co-processing combinations are feasible to afford highly demanding experiments. For example, Martin *et al*.[31] combine multiplicity-edited ^{1}H-^{13}C HSQC and 1,1-ADEQUATE experiments by UIC to yield a ^{13}C-^{13}C correlation plot with resolution and sensitivity levels comparable to the original HSQC. Another possibility is the combination of HSQC and HMBC by UIC to reconstruct long-range ^{13}C-^{13}C correlations similar to the ADEQUATE experiment with higher sensitivity.[32] Similar ^{13}C-^{13}C correlations were obtained from IDR HSQC-TOCSY and HMBC to yield reconstructed HSQC-TOCSY-HMBC spectra.[33] The UIC can also be used to reconstruct insensitive spectra between nuclei that have a low gyromagnetic ratio. For example, the ^{1}H-^{13}C HSQC and ^{1}H-^{15}N HMBC can be combined by UIC to generate synthetic ^{13}C-^{15}N HSQC/HMBC spectra, affording $^{2}J_{CN}$ and $^{3}J_{CN}$ correlations.[29,34]

UIC co-processing works very well but as the Eq. 3 not lead a square root operation and it is not symmetrical operation, the generation of some unwanted artefacts must be checked with caution.[13,17]

Generalized Indirect Covariance

Snyder and Brüschweiler proposed the GIC co-processing as a better mathematical algorithm to UIC.[35] This method involves submatrices and a matrix power (λ) that plays an essential role to reduce artefacts generation.[13,17] GIC co-processing is defined as:

$$C^{\lambda} = \left\{ \begin{bmatrix} A \\ B \end{bmatrix} \begin{bmatrix} A^T & B^T \end{bmatrix} \right\}^{\lambda} \tag{4}$$

The experimental set-up of λ value is a useful parameter to detect the presence of false positives (artefacts) by observing decreased intensity when using low λ values.[35,36] The GIC co-processing can be exemplified using ^{1}H-^{13}C HSQC and ^{1}H-^{1}H TOCSY (**A** and **B** respectively in eq. 4). The ^{1}H information contained in the F1 dimension of TOCSY is transferred to the F2 dimension of the new spectrum, whereas the ^{13}C information in the F1 dimension of the

HSQC is transferred to the F1 dimension of the new spectrum, generating a new reconstructed 2D ^{1}H-^{13}C HSQC-TOCSY spectrum (Figure 7). High resolution in the F1 dimensions of the two original datasets is recommended to obtain optimum high-resolved reconstructed NMR spectra.

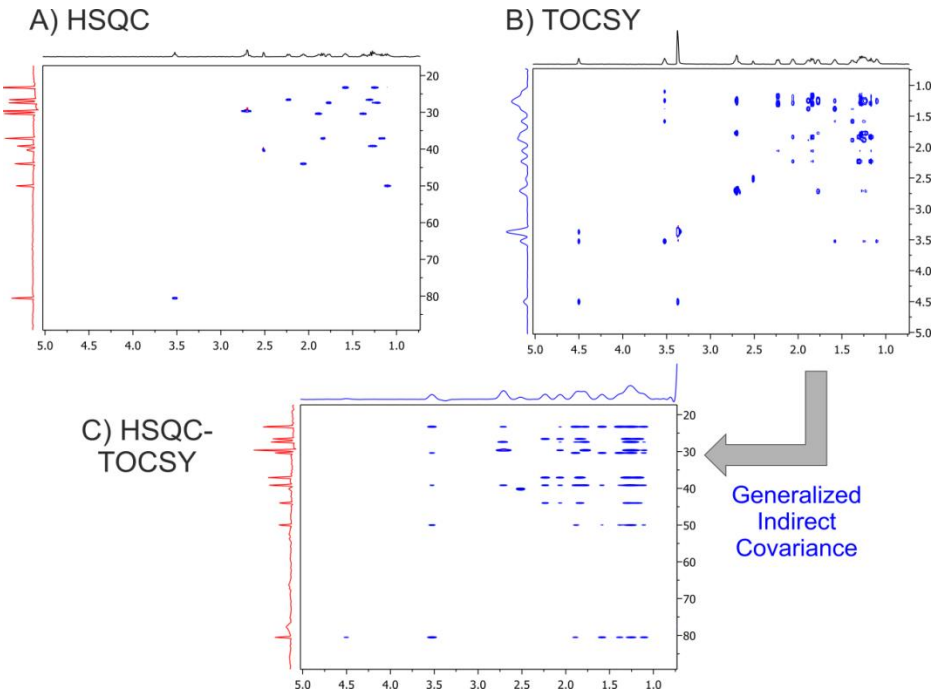

Figure 7: Experimental 400 MHz (A) ^{1}H-^{13}C HSQC and (B) ^{1}H–^{1}H TOCSY spectra (60 ms DIPSI-2 mixing period) of **1** (in $CDCl_3$) acquired with four scans, 2048 complex points in F2 and 512 t_1 increments. (C) These spectra can be combined by GIC (λ = 1.0) to reconstruct a ^{1}H-^{13}C HSQC-TOCSY spectrum.

A general drawback of any covariance method is the possible generation of unwanted artefacts due to signal overlapping.[24,37] The combination of spectra is performed using the rows of one spectrum and the columns of the other one, as schematically represented in Figure 8. Some artefacts are easily detected by visual inspection because they appear with inverted phase about the rest of signals. However, other artefacts are more difficult to distinguish because they have the same relative phase as correct signals.[24]

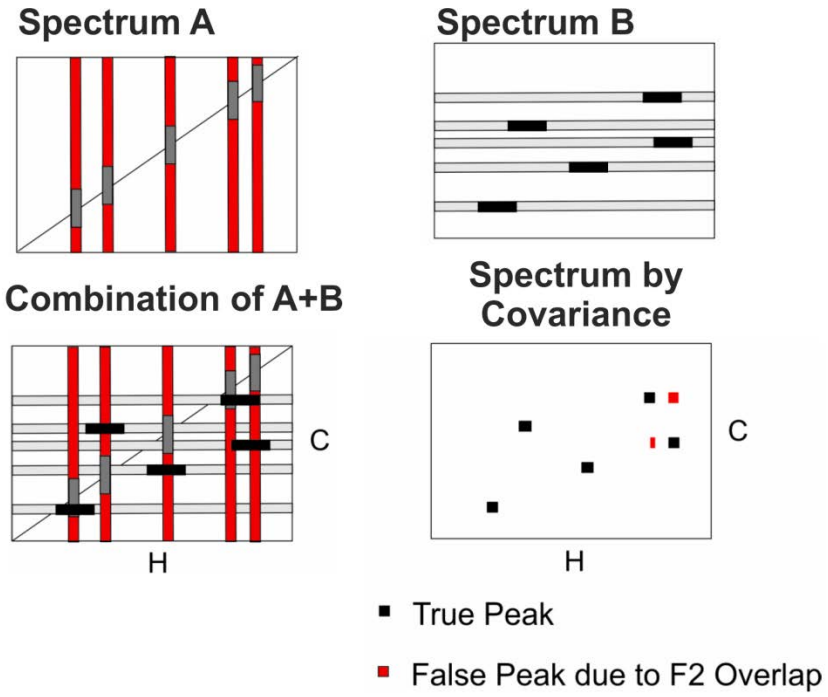

Figure 8: Graphic representation explaining the generation of false peaks during GIC covariance co-processing due to the presence of accidental signal overlapping along the F2 dimension.

1.2. Pure-Shift NMR

1.2.1. Introduction to Pure-Shift NMR

Scalar proton-proton couplings (J_{HH}) provide valuable information about the structure of molecules. The splitting of the NMR signal by *J* coupling can generate wide multiplets (up to 30-50 Hz) with characteristic and sometimes complex multiplicity patterns, increasing the probability of signal overlapping with other resonances. For years, the advantages to decouple J_{HH} in ^{1}H NMR spectroscopy has been recognized since spectra that exclusively contain chemical shift (δ) information should be more readily analyzed. This approach, known as Pure-Shift NMR (psNMR) or as broadband homodecoupled NMR, collapses characteristic ^{1}H multiplet *J* patterns into singlet signals, increasing signal resolution by several orders of magnitude. This spectral simplification can facilitate the analysis and the assignment of overcrowded areas, as observed in

the aliphatic region of the steroid estradiol **2** (Figure 9). Unfortunately, a frequent drawback related to the most psNMR techniques is their decreased sensitivity compared to conventional ones.

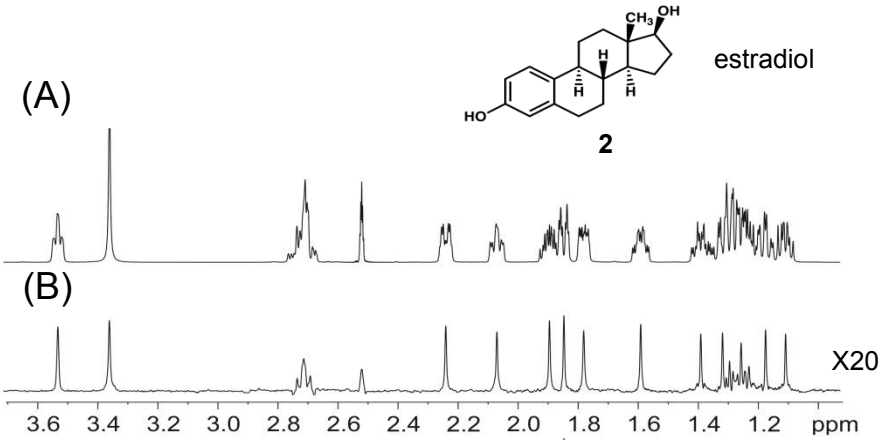

Figure 9: (A) 600 MHz ^{1}H NMR spectrum of estradiol **2** (in DMSO-d6); (B) ps ^{1}H spectrum showing a simplified singlet signal for each proton resonance.

Since the beginning of the high-resolution NMR, it was already recognized that the decoupling of J_{HH} would be of great help to simplify, analyze and interpret ^{1}H NMR spectra. In 1976, Ernst and co-workers developed the first approach for obtaining a fully homodecoupled 1D ^{1}H spectrum, by extracting the F2 projection of a 2D *J*-resolved (*J*-res) spectrum.[38] After that, different strategies were proposed, but a general solution did not succeed. Recently, the idea of broadband homodecoupling has resurrected, and the development of new psNMR methods and applications have taken a significant leap as shown for the increased number of publications and citations appeared in the period 2014-2017 (Figure 10).[39–42]

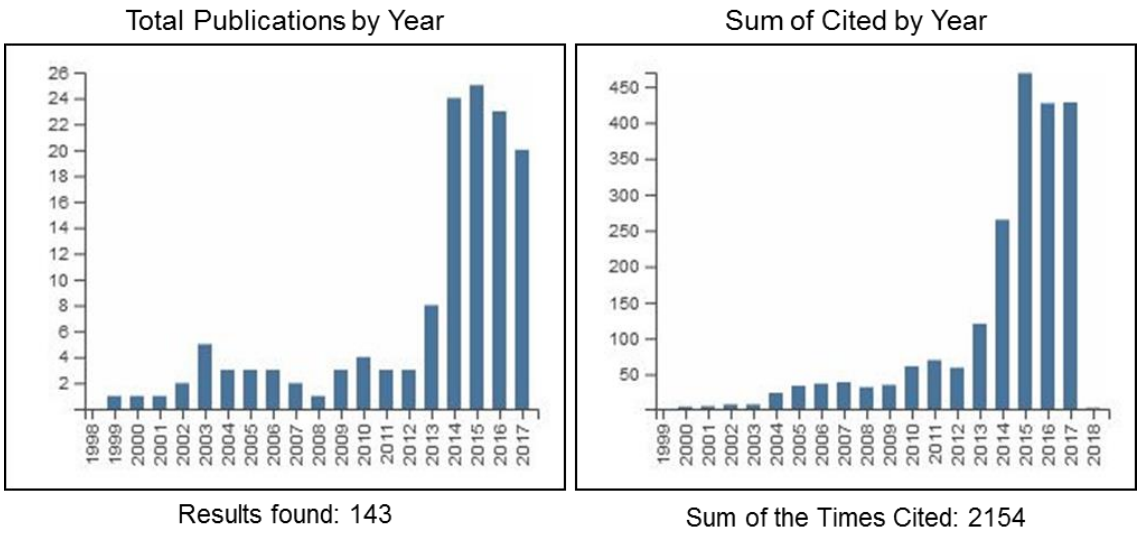

Figure 10: (A) Number of scientific publications and (B) citations per year including the term psNMR appeared in the last ten years. The search was performed on the Web of Knowledge database using the keywords "pure-shift NMR", “Homodecoupling” and/or “pure chemical shift”.

1.2.2. Concepts in Pure-Shift NMR

The development of new strategies and methods related to psNMR is nowadays an active area of research in small molecule NMR. Some current challenges to solve are: i) to enhance the sensitivity of the existing techniques (depending on the method, the available sensitivity is only around 1-10% of the conventional ones); ii) to design automated, user-friendly protocols without need of troublesome acquisition or processing set-ups; iii) to offer general implementation on a wide range of traditional 1D and 2D NMR experiments; iv) to speed-up data acquisition; v) to improve spectral quality; and vi) to minimise strong coupling effects and undesired artefacts such as decoupling sidebands.[41]

Homonuclear building blocks in Pure-Shift NMR

The key to success in obtaining a fully-decoupled NMR spectrum is to refocus the *J* coupling information while δ evolves freely. The most basic NMR building blocks are summarized in Figure 11.[41]

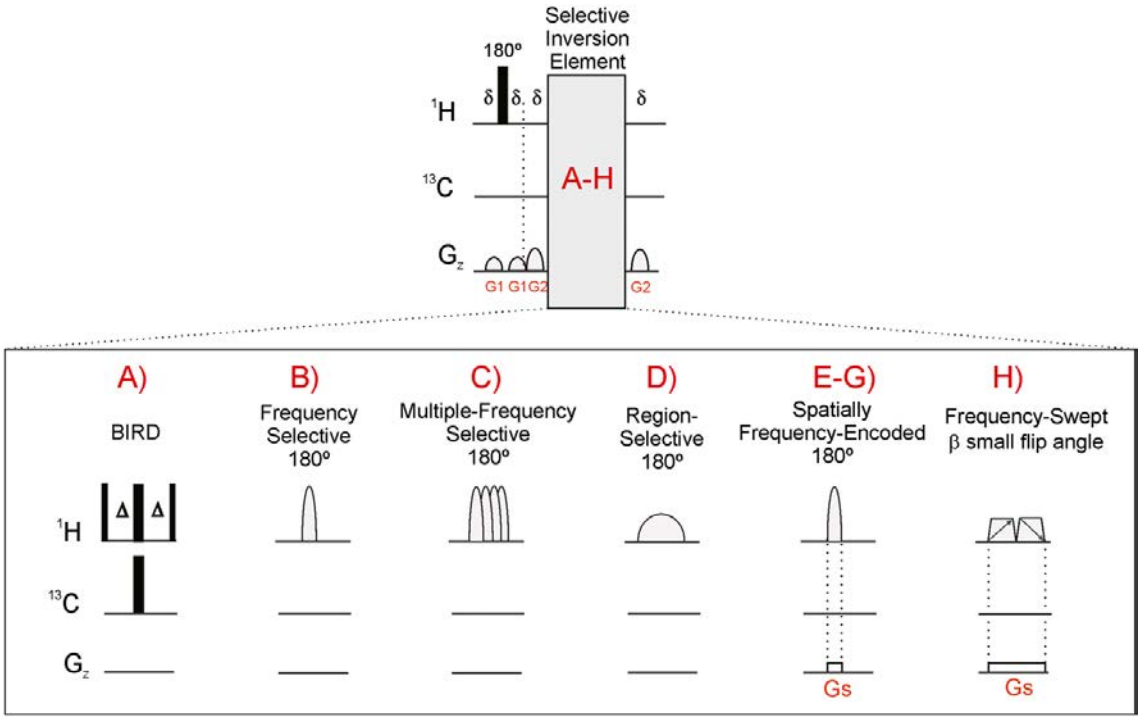

Figure 11: NMR building blocks used for homonuclear decoupling: (A) isotopic BIRD editing; (B-D) frequency-selective 180º pulse; (E-G) slice-selection elements that promote spatial-encoding along the z-axis due to the simultaneous application of one gradient (G_s) and a single-, multiple- or region-selective 180º pulse; (H) the spatially-encoding PSYCHE element which consists of a pair of small flip angle frequency-swept adiabatic pulses combined with an encoding *G*s gradient.[41]

The BIRD homodecoupling block (Figure 11A) is based on the presence of ^{13}C nuclei and was introduced by Garbow and coworkers more than 30 years ago.[43] The BIRD element selects the protons that are attached with ^{13}C while suppressing the ^{12}C-attached protons, or vice-versa. BIRD editing is very efficient and robust, but it can also suffer some drawbacks. First, the sensitivity of the experiment is limited to 1.1% of the full signal, because of the natural-abundance ^{13}C isotopic ratio. Secondly, the decoupling of diastereotopic

protons in prochiral CH_2 groups is not possible because BIRD cannot distinguish protons directly bond to the same ^{13}C nucleus. Thus, a doublet due to the geminal $^2J_{HH}$ remains in BIRD-based psNMR spectra. The BIRD building block has been implemented in 1D ^1H pure-shift [44–46] and 2D psHSQC[47] experiments, which are powerful tools in current structural elucidation studies.[48–53]

Another type of homodecoupling block uses selective 180º pulses to refocus the *J* coupling in the middle of the evolution time. Several options are feasible including single frequency (Figure 11B), multiple-frequency (Figure 11C) or band-selection (Figure 11D). Band-Selective Homodecoupled (BASH)[54] and HOmodecoupled Band-Selective (HOBS)[55] blocks work applying one band-selective 180º pulses in a specific region on the spectrum. This method retains full sensitivity and affords a better SNR with respect other homodecoupling elements like slice selection or BIRD. Besides that, HOBS have an easy set-up, fast acquisition and easy implementation as demonstrated for different 2D experiments, such as shown for the HOBS versions of the TOCSY, HSQC,[55] CPMG,[56] HSQMBC,[57] and HSQC-TOCSY[58] experiments. The main drawback of this method is that pure-shift features are restricted to spectral regions where all protons do not have a mutual coupling. In practice, the duration of the selective 180º pulse can become critical and short lengths of 5– 15 ms are required for real-time homodecoupling methods.

The standard homodecoupling method, known as Zangger-Sterk (ZS), uses the slice-selective element depicted in Figure 11E.[59] This spatial encoding concept was originally exploited in *in-vivo* MRI studies[60] but, in the recent years, it has found an enormous utility in psNMR applications.[41,42] The simultaneous application of a selective 180º (sel180º) pulse together with a weak Pulse-Field Gradient (PFG) causes a spatially-encoded selective decoupling of different signals placed at different z-slices of the NMR sample tube. This spatial encoding causes a location-dependent shift of all signals in different slices of the NMR tube, as indicated Figure 12.[41,42] The duration of the sel180º pulse influences the width of the slices. Pulses with long durations generate smaller slices whereas short pulses generate thinners slices that increase the experimental sensitivity.

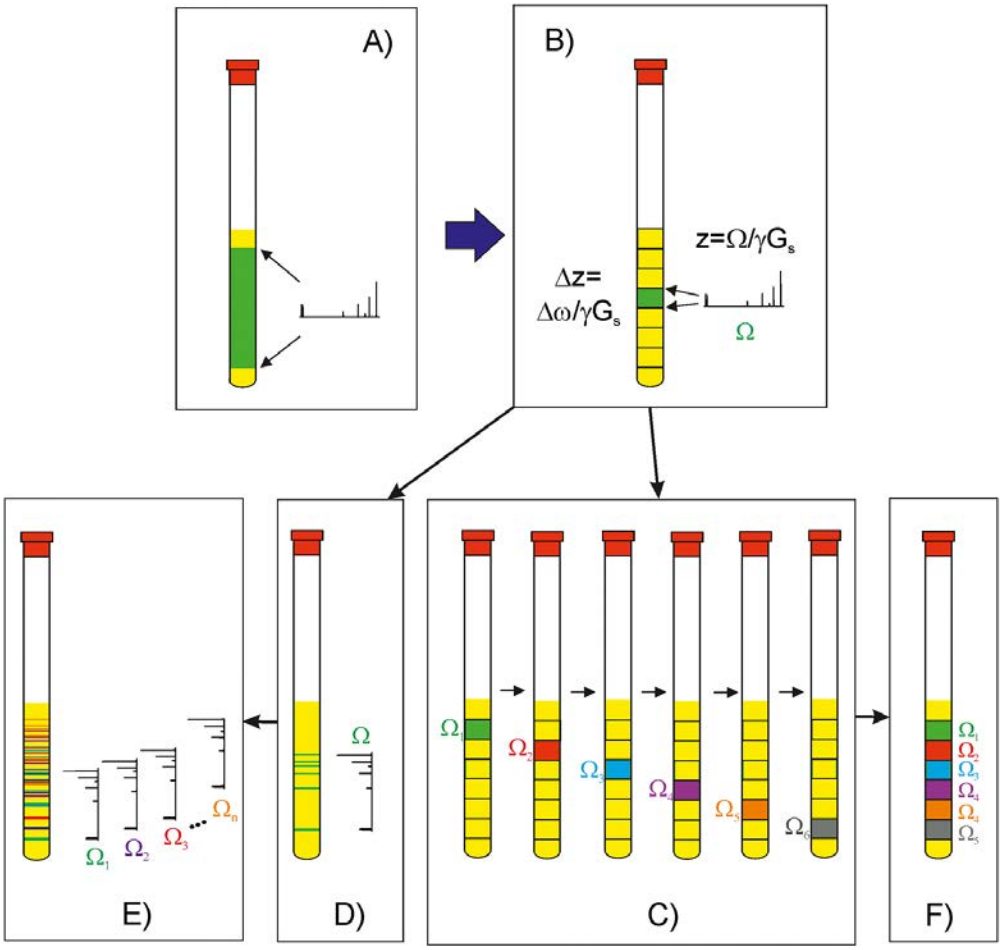

Figure 12: Different strategies to induce spatial selection along the z-axis of an NMR tube: (A) standard excitation/detection over the entire coil; (B) single-slice selection; (C) sequential spatial selection; (D) frequency-selective spatial selection; (E) simultaneous multiple frequency-selective spatial selection; (F) simultaneous multiple-slice excitation/detection.[41]

An excellent approach for homonuclear broadband decoupling is the Pure Shift Yielded by CHirp Excitation (PSYCHE) experiment.[61] This method uses two symmetrical low flips (β°) frequency-swept chirp pulses[62] which are applied during a weak PFG to refocus the passive spins while leaving the active ones undisturbed. PSYCHE experiment is a statistical approach that runs through the NMR tube in a random way exciting only one frequency of each proton without being coupled with another proton.[27,42] The use of frequency-swept pulse with gradient applying at the same time cause the suppression of zero-quantum coherences (ZQ) by superposing different ZQ evolutions from

different NMR tube regions.[39,41,42] Experimentally, the sensitivity of PSYCHE-based experiments depend on the βº flip angle used, that provides optimum results when βº=15-20º. In practice, the sensitivity in PSYCHE experiment is reduced to about 10% compared with the original 1D ^{1}H spectrum but is higher than those pure-shift methods based on BIRD- or slice-selection homodecoupling (Figure 13). PSYCHE has been recently incorporated into some 1D, and 2D homodecoupling experiments like 1D homodecoupling,[61] 1D selTOCSY,[63] 2D DOSY,[64] and 2D TOCSY[27] experiments. The PSYCHE element is incompatible with real-time homodecoupling techniques and only is efficient in interferogram-based NMR methods acquired as more time-consuming pseudo-2D or pseudo-3D datasets.

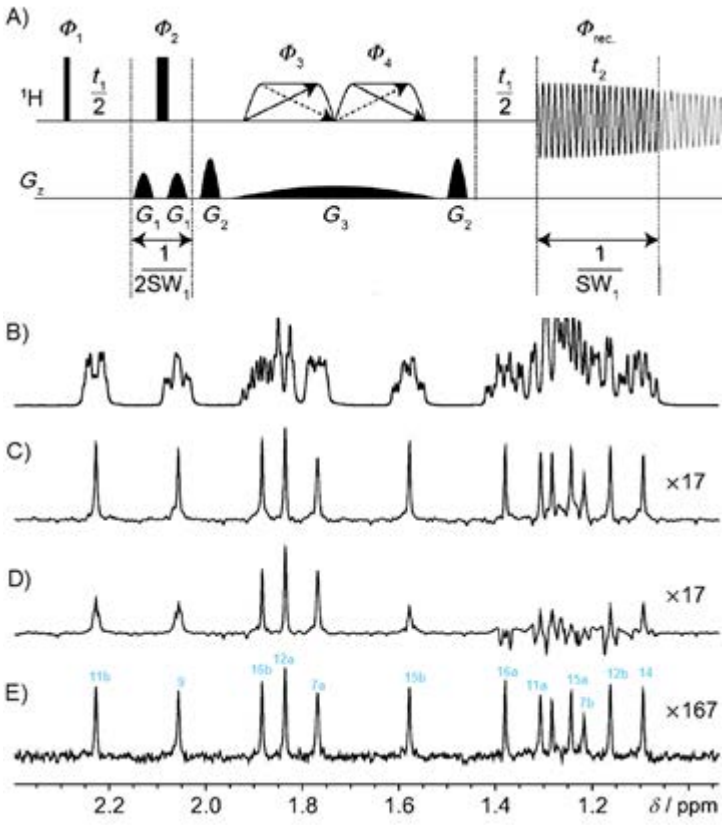

Figure 13: (A) Pulse scheme of the ZS-based PSYCHE experiment that uses a pair of low-power frequency-swept chirp pulses and a weak gradient as a selective inversion element. (B) 600-MHz ^{1}H NMR spectrum of the sex hormone estradiol **2** in DMSO-d_6; (C) PSYCHE spectrum obtained with two chirp pulses of 15ms (β= 20°); Original ZS spectra using (D) 12 ms and (E) 100ms Rsnob 180° ^{1}H pulses. Adapted from reference.[51]

Acquisition mode in Pure-Shift NMR

There are two acquisition strategies in psNMR: Interferogram-based pseudo-2D and Real-Time. The first method (the original ZS experiment) uses a conventional t_1-incremented 2D acquisition followed by a data reconstruction processing to generate a 1D homodecoupled FID (Figure 14A).[59] Any homodecoupling block depicted in Figure 11 can be applied in the middle of the incremented delay to refocus any J_{HH} evolution. The FID reconstruction is performed by concatenating the first ~10ms (data chunk) from the FID of each sequential increment, and the final homodecoupled ^{1}H spectrum is obtained after conventional Fourier transformation (Figure 14A). The size of the data chunk is 1/*SW* (F1) (typically, *SW* (F1) is set to 40–100 Hz) and 16–32 t_1 increments give reasonable results in 5–10 minutes with several milligrams of sample.[23] This process is efficient because the temporal evolution of *J* coupling is much slower than the chemical shift. However, a certain amount of the *J* coupling evolution does occur for the data block length of 10 ms, introducing some extra line broadening. Furthermore, some artefacts appear typically in the form of the sidebands peaks at multiples of *SW*, around each decoupled signal. The intensity of the sidebands is proportional to the square of 1/*SW,* sometimes comparable to that of the ^{13}C satellites.[41,23] Because of the 2D acquisition mode, this pseudo-2D strategy expends more time than a standard 1D experiment which is proportional to the number of collected t_1 increments. This point is more critical for homodecoupled 2D spectra acquired with this ZS method because a time-consuming pseudo-3D dataset recording is required.

Real-time homodecoupling works in a different way than pseudo-2D. In this method, the homodecoupled FID is directly recorded in a single scan with brief interruptions into the FID (chunks) to refocus scalar coupling (Figure 14B). The τ period is the duration of the data chunk, and this is defined as AQ/2*n,* where AQ is the acquisition time and *n* the number of loops. The data chunks of the FID are concatenated to make a fully-homodecoupled FID. In fact, real-time homodecoupled experiments reduce the experimental time compared to the pseudo-2D method. However, some limitations are present depending on the inversion element involved: i) the duration of data chunks is limited to some ms; ii) it can present poor selectivity; iii) severe sensitivity losses are achieved when

slice-selection is applied; iv) broader signals due to shorter T_2 relaxation or inefficient homodecoupling can be obtained; v) signals for strongly coupled nuclei cannot be efficiently decoupled; vi) the interruption of the FID causes a discontinuity, causing the presence of sidebands artefacts around the signals.[41,42]

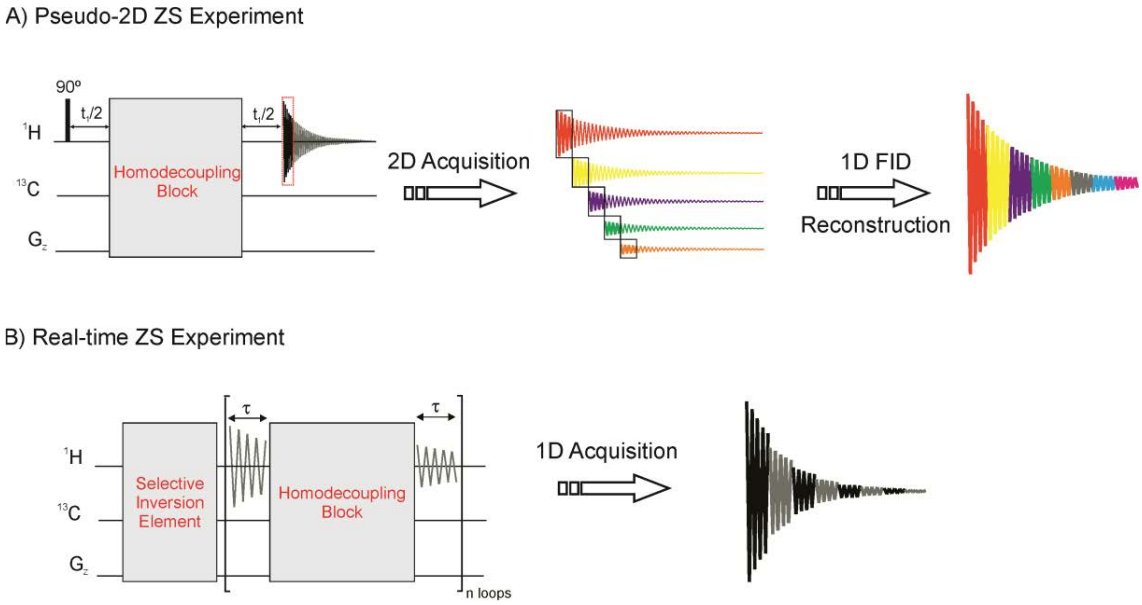

Figure 14: Generic schemes for the acquisition of 1D homodecoupled ^{1}H NMR spectra. (A) Pseudo-2D acquisition mode that consists on the recording of a 2D dataset followed by an FID reconstruction from the initial data chunks of each increment; (B) Real-Time acquisition mode that includes concatenated FID chunks flanking the incorporation of the homodecoupling block. [41]

In summary, both real-time and pseudo-2D homodecoupling acquisition modes (described in Fig. 14) can be combined with the different homodecoupling blocks, as shown in Figure 15. It is worth remembering that no technique is better than the other and all psNMR approaches present particular advantages and disadvantages, also depending on the molecules or spin systems under analysis. Table 2 summarizes pros and cons of each approach.

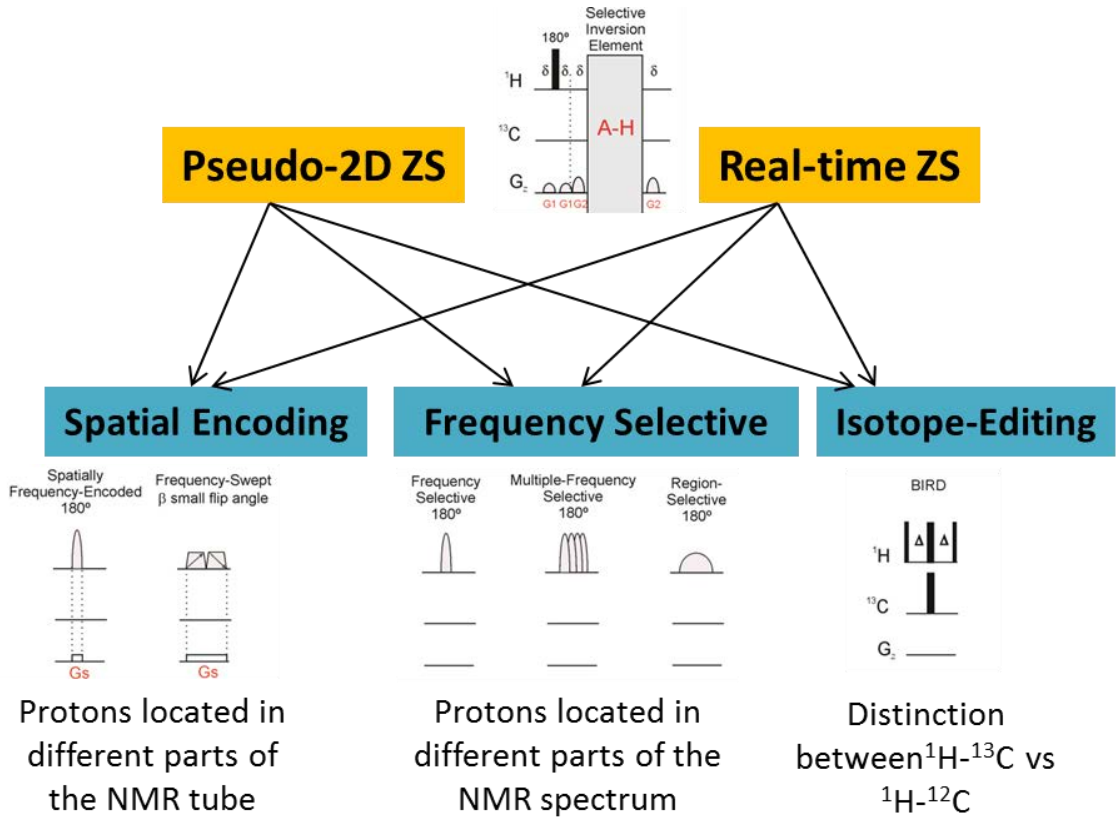

Figure 15: Different strategies for developing psNMR techniques by combining homodecoupling blocks with real-time or pseudo-2D acquisition modes.

Table 2: Summary of pros and cons of the different homodecoupling methods.

PS TECHNIQUES	PROS	CONS
HOMODECOUPLING BUILDING BLOCKS		
BIRD	- Both acquisition modes. - Easy set-up. - Retains maximum sensitivity in HSQC. - Single scan.	- Does not work for diastereotopic CH_2 protons. - Low sensitivity due to isotopic ^{13}C natural abundance.
HOBS	- Both acquisition modes. - Maximum sensitivity. - Single scan.	- It is not broadband. - Does not work for mutually coupled spins.
Slice-selection	- Both acquisition modes.	- Fail with strongly coupled protons. - Low sensitivity. - Careful set-up is required to optimise sensitivity.
PSYCHE	- Highest sensitivity in broadband homodecoupling. - Easy set-up and automation - Excellent tolerance to strong coupling effects.	- Only works in pseudo-2D acquisition mode. - Presence of unwanted sidebands.
ACQUISITION MODES		
Pseudo-2D	- Compatibility with any homodecoupling block.	- Longer acquisition time. - Special processing.
Real-time	- Single scan. - Faster acquisition mode.	- Poorer selectivity. - Broader signals. - Presence of artefacts. - Does not work with PSYCHE.

1.3. 2D *J*-resolved and SERF experiment

1.3.1. Introduction of *J*-resolved

The homonuclear J_{HH} or other heteronuclear couplings cause a split of signals into multiplets. Besides that, the range of spectral width in the 1D ^{1}H spectrum is small, typically between 10-12 ppm, and therefore the probability of signal overlapping becomes high in complex molecules or mixtures. On the other hand, multidimensional methods are powerful tools to obtain more efficient information about δ and *J*. The 2D *J*-res experiment[38] provides a simple tool to solve signal overlapped problems by separating δ of the detected nucleus along F2 dimension while the orthogonal F1 dimension displays *J* couplings patterns. The original *J*-res experiment is based on the 1D spin-echo pulse sequence that was reported in 1950 by Hahn to measure relaxation times.[65] Figure 16 shows the pulse sequence and the vector representation of the spin-echo experiment.

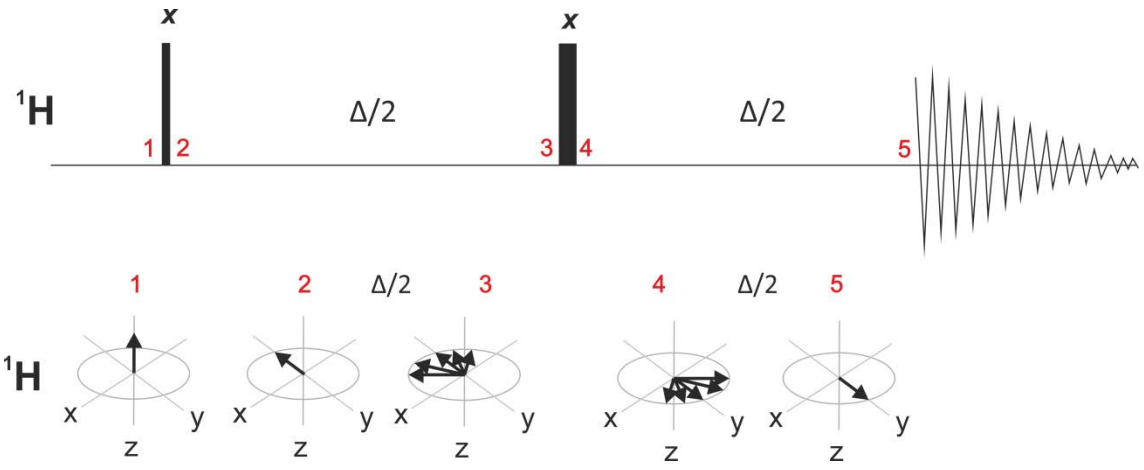

Figure 16: The spin-echo pulse sequence starts with an initial 90º pulse followed by a central 180º pulse placed between two evolution times $\Delta/2$. The vector representation gives a visual and intuitive model representation of the magnetization behaviour during the pulse sequence.

The spin-echo experiment starts with an initial 90º(x) pulse which placed the magnetization along $-y$ axis. After this, the magnetization evolves

during the first Δ/2 delay, from $-y$ towards to x-axis. The central 180º pulse is applied to rotate the magnetization in which ends up in mirror image position with respect to the xz-plane. During the second Δ/2 delay, the magnetization evolves with the same angle as in the first delay, and end up being refocused. If the Δ/2 delay is set to ½*J*, the magnetization is completely refocused and ends in the $+y$ axis. The 180º pulse is called a **refocusing pulse** because it causes the magnetization to be refocused at the end of the second delay. In this experiment is possible to monitor different evolution modulations and that was the origin of the CPMG experiment to measure T_2 relaxation times.[65,3] As a summary, an spin-echo NMR element refocuses δ(^{1}H) effects while allows the evolution of J_{HH} coupling during the entire Δ period. The homonuclear spin-echo experiment is known as *J-modulated spin-echo*.[3]

1.3.2. *J*-resolved pulse sequence

Aue and co-workers proposed the 2D spin-echo version, known as *J*-res experiment, for the first time in 1976 (Figure 17A).[38] Unlike conventional 2D correlation NMR experiments, 2D *J*-res separates δ and *J* couplings into two independent dimensions. After tilting, 2D *J*-res spectra show only singlets for each nucleus in F2 and *J* coupling patterns in F1, making the interpretation and measurements of *J* couplings easy and intuitive (Figure 17C) thanks to the high digital resolution and the short spectral width (50 Hz or less) defined in the indirect F1 dimension.[38]

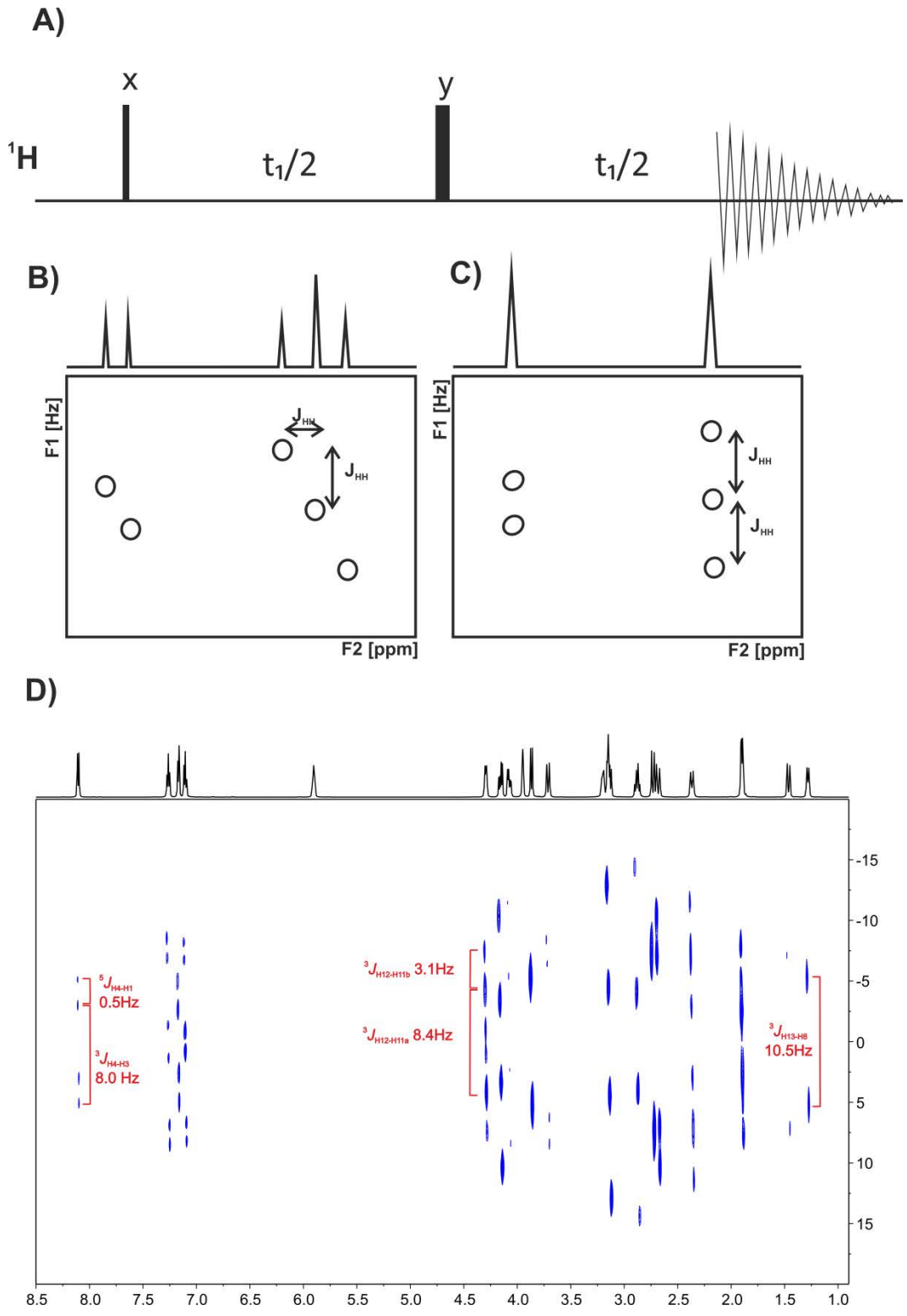

Figure 17: (A) 2D *J*-res pulse sequence; Schematic 2D *J*-res spectrum (B) before and (C) after the 45º tilting process. (D) Experimental 2D *J*-res spectrum of **1** acquired in a 600 MHz spectrometer with 16 scans, 2048 complex points, and 64 t_1 increments. In the 2D *J*-res, the spectral width in the F1 dimension is 40-60 Hz which provides a high F1 resolution.

Signals in the 2D *J*-res spectrum appear 45º tilted due to J_{HH} evolution in both dimensions (Figure 17B). A tilting post-processing algorithm is applied to align signals along the F2 dimension (Figure 17C). As shown in the experimental 2D *J*-res spectrum of **1** (Figure 17D), *J*-coupling patterns for each ^{1}H signal can be extracted in the F1 dimension. On the other hand, phase modulation during the incrementable t_1 delay generates "phase-twisted" lineshapes. For this reason, 2D *J*-res datasets are best processed in magnitude mode, causing an undesired line broadening of the signals. Different modifications in pulse schemes[66–68] or data processing strategies[69] have been proposed to obtain pure-absorption mode *J*-res spectra. A first solution was the modification reported by Thippleton and Keeler[66] based on the incorporation of slice-selection[59] and the separate acquisition of the *P*- or *N*-type data sets varying the sign of the gradient,[3] better known as Echo/Anti-Echo (EA) mode. Due to its slice selection scheme, the method suffers a severe sensitivity penalty. Recently, *J*-res versions using PSYCHE instead of slice-selection have been proposed to improve sensitivity, robust performance and to offer better tolerance to strong coupling effects.[70] In 2005 Keeler *et al.*[68] proposed the minimization of strong coupling artefacts by using the Double Spin Echo (DSE) pulse sequence.

Another solution to obtain pure-absorption *J*-res spectra adds a Zero-Quantum Filter (ZQF)[71] just before the acquisition.[67] The ZQF consists of an adiabatic 180º pulse applied simultaneously with a weak gradient both flanked by 90º pulses. The ZQF eliminates the antiphase contributions effectively, providing clear in-phase signals. An essential advantage of this approach is that only one scan per each t_1 increment is required, allowing fast acquisition times. Besides that, a *J*-pattern processing algorithm must be applied to obtain homonuclear decoupled signals along the detected F2 dimension.

1.3.3. Selective homonuclear *J-res* experiments

The *J*-res experiments afford full *J* couplings patterns in F1 dimension, and for complex multiplets or large molecules, the extraction of *J* values can

become a challenging task. The use of selective pulses instead of hard pulses can bring a significant simplification of the resulting *J*-res spectra. The 2D SElective ReFocusing (SERF)[72] experiment (Figure 18A) was proposed in 1995 by Fäcke and Berger to measure a specific *J* coupling between two protons. Two selective 180º pulses are applied on different *I,* and *S* spins, respectively, for efficient refocusing of δ and all other undesired *J* couplings to the rest of spins. Thus, the original SERF spectrum (Figure 18C) provides a simple doublet splitting along F1 corresponding to the coupling between the selected spins. Phase-sensitive SERF experiments were also designed by adding a z-filter before the acquisition.[73,74]

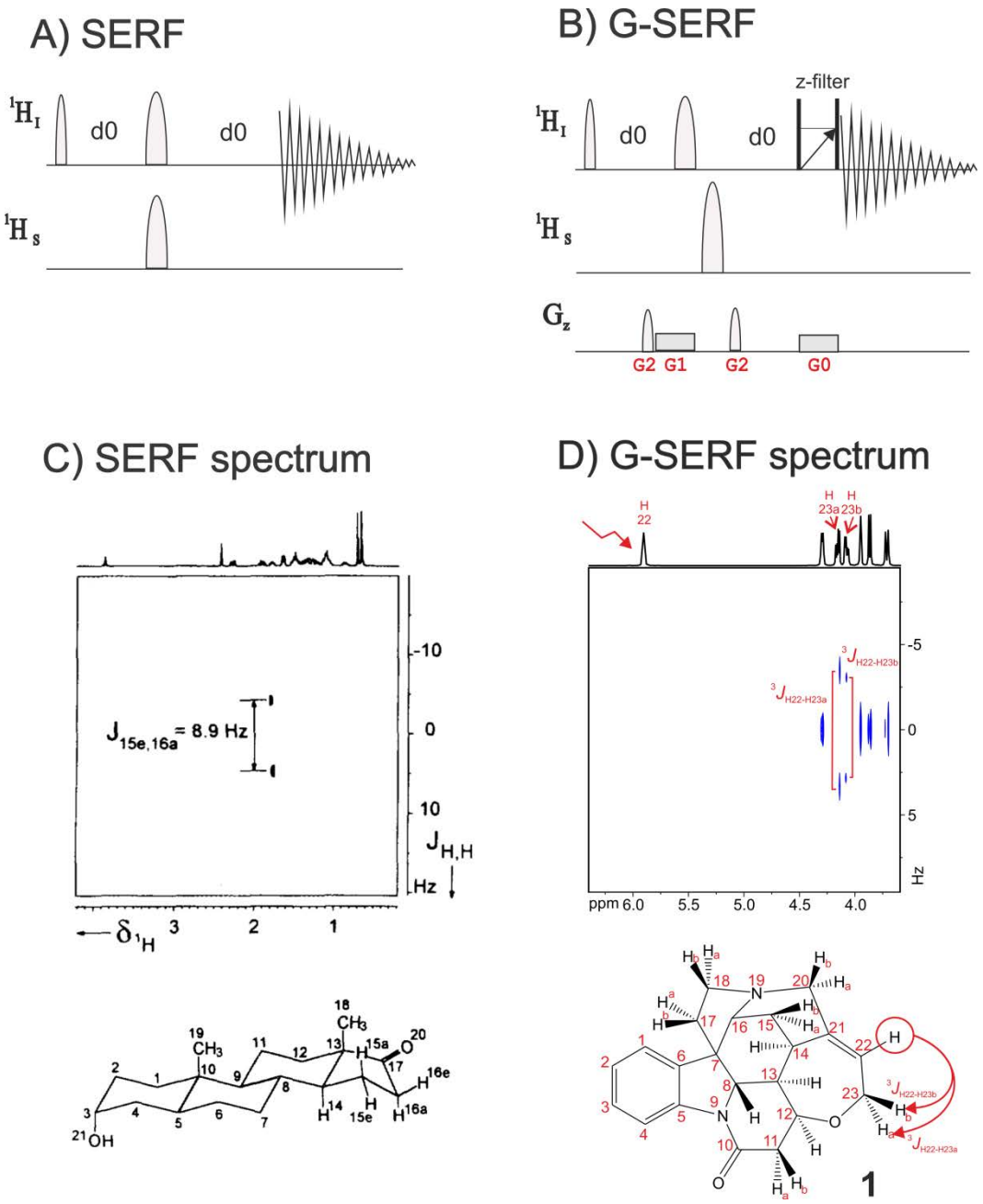

Figure 18: (A) The original SERF pulse sequence uses two different selective 180º pulses to determine the *J* coupling between the selected two protons. (B) G-SERF pulse sequence with a ZQF that uses spatial encoding element to extract all J_{HH} of the chosen proton signal. (C) SERF spectrum adapted from[72]. (D) 2D G-SERF spectrum of **1** acquired in a 600 MHz spectrometer with 16 scans, 2048 complex points, and 64 t_1 increments. H_{22} is the *I* proton selected by the sel180º pulse, and H_{23a} and H_{23b} are the passive *S* protons chosen by the slice-selective element .

Giraud and co-workers proposed an improved Gradient encoded SERF experiment (G-SERF) experiment[75] which uses the slice selection block as a refocusing element to allow the measurement of the magnitude of all J_{HH} couplings of the selected proton (Figure 18B). The major drawback is that sensitivity of the experiment is about only 1-3% of the maximum signal intensity. As an example, the G-SERF spectrum after selecting the H22 proton of **1** allows the accurate measurement of $^{3}J_{H22\text{-}H23a}$ and $^{3}J_{H22\text{-}H23b}$ (Figure 18D). Recently, a Clean G-SERF version has been proposed to obtain a much cleaner spectrum.[76]

An exciting improvement of the G-SERF has been the Pure Shift Yielded by CHirp Excitation to DELiver Individual Couplings (PSYCHEDELIC) experiment[77] where all ^{1}H signals are fully homodecoupled in F2 (Figure 19). The PSYCHEDELIC experiment uses the PSYCHE element instead of band-selective or slice selection elements, and the EA mode to obtain absorption mode line shapes. The use of the PSYCHE pulses provide an increase of sensitive compared to slice selection, but the inconvenient is its pseudo-3D acquisition mode requiring longer experimental time compared to other G-SERF versions.

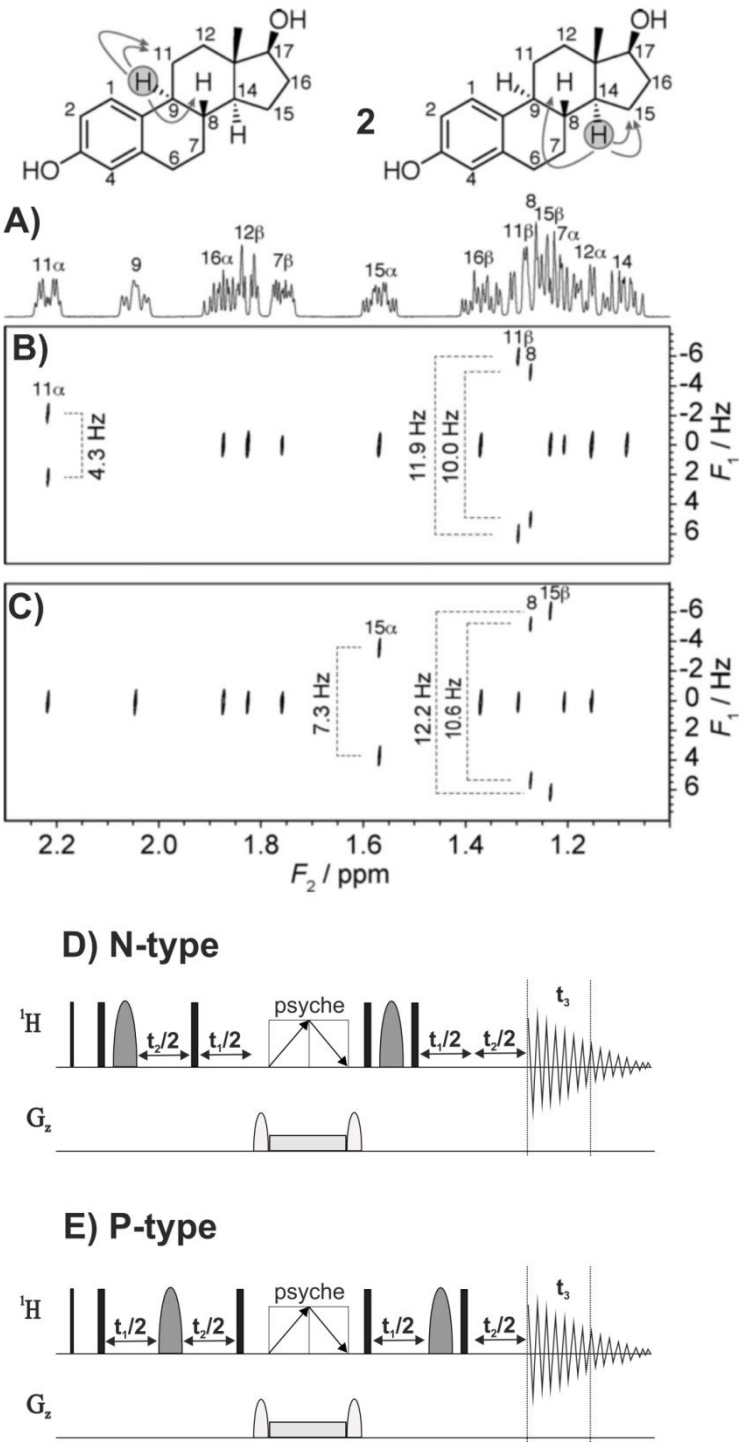

Figure 19: (A) 1D ^{1}H NMR spectrum of **2**, showing a crowed region with overlapping signals between 1.0 and 1.4 ppm. Experimental 2D PSYCHEDELIC spectrum showing the *J's* of selected H9 (B) and selected H14 (C). Pseudo-3D PSYCHEDELIC pulse sequence designed to measure J_{HH} using the EA approach: (D) N-type and (E) P-type. The narrow and wide black bars represent hard 90º and 180º pulses, respectively. The sel180º pulse is represented by the shaped gray pulse. The chunk of the FID has the duration of $1/SW_2$ for each increment t_1. Figure adapted from[77].

Other G-SERF-based methods have been reported incorporating homodecoupling in F2.[78] On the other hand, the Quick G-SERF experiment[79] is a faster 1D broadband homodecoupled version which affords a ps1D ^{1}H spectrum only displaying doublets with the active *J* coupling of the selected proton. This experiment relies on the use of real-time homodecoupling acquisition mode, and therefore broader linewidths can hamper the measurement of small *J* values. Another drawback is the requirement for a selective pulse which limits its application to isolated proton resonances.

2. OBJECTIVES

The primary objectives of this thesis were:

- Understand the theoretical and practical concepts of modern NMR techniques.

- Specialization in the design of new acquisition NMR pulse sequences and in the performance of several NMR data processing protocols.

- Evaluation of existing NMR experiments to know how to set up them, as well as to understand how it works and which are their advantages/drawbacks with the goal to improve them.

- Open a new research line on the potential of mathematical data post-processing treatments as a cheap approach to obtaining reconstructed NMR spectra without using spectrometer time.

- Use of Covariance NMR to evaluate and solve some current drawbacks related to psNMR: a) their relative low-sensitivity; b) their long acquisition times; c) the presence of unwanted strong coupling effects and sidebands; d) the presence of geminal coupling effects between diastereotopic CH_2 in heteronuclear psNMR experiments; e) the obtention of some psNMR spectra which has never been designed experimentally.

- Development of new pulse sequences to facilitate the measurement of homo- and heteronuclear *J* couplings.

3. RESULTS AND DISCUSSION

In this section, the experimental results obtained in this thesis are presented in the form of three papers published in NMR specialised scientific peer-reviewed journals. Two articles dela with the use of covariance NMR as a general method to generate novel psNMR spectra. The last work describes a new selTOCSY G-SERF experiment, for accurately measuring J_{HH} in overlapped regions.

Publication 1 describes a novel general protocol to generate psNMR spectra by Covariance NMR. This new approach is unique in NMR spectroscopy; giving a cheap, fast an easy way to reconstruct psNMR spectra without spending time in the spectrometer. This new strategy has been referenced to as psNMR Covariance.

The concept of psNMR Covariance has been extended in **Publication 2** by inserting Multiplicity-Edited (ME) information into 2D experiments that are difficult or even impossible to achieve experimentally. It is shown how the ME information can be efficiently transferred to a set of homonuclear and heteronuclear 2D NMR spectra by Covariance processing, reconstructing new psME spectra in a fast way.

Finally, G-SERF and related methods only work for isolated ^{1}H signals on which selective excitation can be successfully applied. Unfortunately, as it happens in other frequency-selective experiments, this approach fails for overlapped signals. A doubly-selective TOCSY G-SERF scheme is presented in the **Publication 3** to circumvent this limitation, by measuring J_{HH} efficiently even for protons resonating in crowded regions.

PUBLICATION 1

Exploring the use of Generalized Indirect Covariance to reconstruct pure shift NMR spectra: Current Pros and Cons

André Fredi[a], Pau Nolis[a], Carlos Cobas[b], Gary E. Martin[c], TeodorParella[a]

[a]Servei de RessonànciaMagnètica Nuclear, UniversitatAutònoma de Barcelona, Catalonia,

[b]MestrelabResearch, Santiago de Compostela, E-15706 A Coruña, Spain

[c]NMRStructureElucidation, Process&AnalyticalChemistry, Merck &Co. Inc., United States

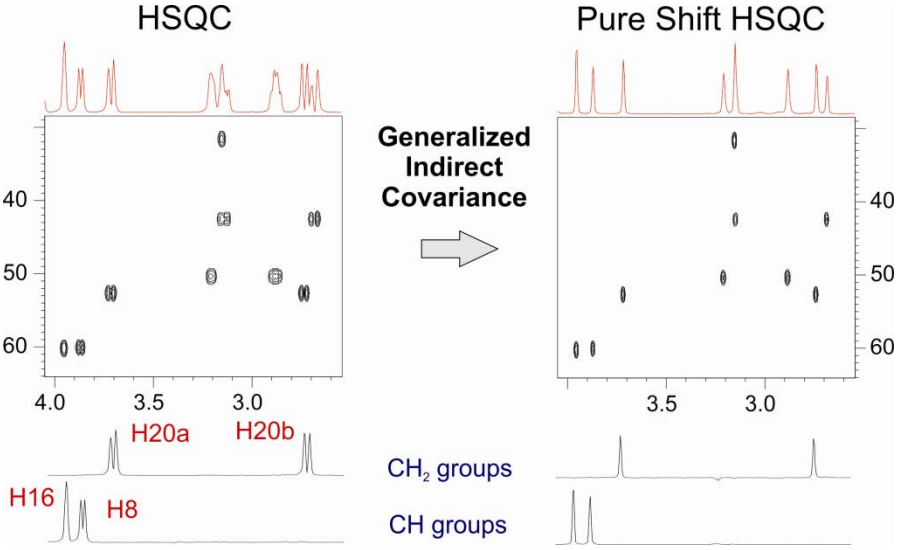

Introduction

The development of novel experimental strategies to significantly enhance signal resolution by broadband homodecoupling is a current topic of high interest in ^{1}H NMR spectroscopy.[39,41,42] For instance, the original ZS experiment has been modified and improved in several ways. All of these homodecoupling techniques have been implemented in many 1D and 2D homo- and heteronuclear pulse schemes to provide resolution-enhanced pure chemical shift ^{1}H NMR spectra, where common multiplet *J* patterns appear collapsed to singlet signals. However, not all traditional NMR experiments can be successfully converted to their homodecoupled counterparts.

On the other hand, covariance processing methods have been used to generate new and challenging NMR spectral representations.[59] We present here the first attempts towards a general solution to create *Pure-Shift NMR spectra by using Generalized Indirect Covariance* (psGIC). The current strategy is based on the calculation of a new 2D psGIC spectrum from the combination of a parent homo- or heteronuclear spectrum and a reference 2D F1-homodecoupled ^{1}H-^{1}H correlation spectrum only showing diagonal cross-peaks (DIAG), which share a characteristic ^{1}H frequency dimension. It is shown how the features of the F1 dimension in the DIAG spectrum can be transferred to the F2 dimension of the target spectrum using psGIC, thus generating a new ps2D spectrum. Examples are provided for a set of homonuclear and heteronuclear 2D NMR spectra of the alkaloid strychnine.

Journal of Magnetic Resonance 266 (2016) 16–22

Contents lists available at ScienceDirect

Journal of Magnetic Resonance

journal homepage: www.elsevier.com/locate/jmr

Exploring the use of Generalized Indirect Covariance to reconstruct pure shift NMR spectra: Current *Pros* and *Cons*

André Fredi [a], Pau Nolis [a], Carlos Cobas [b], Gary E. Martin [c], Teodor Parella [a,*]

[a] Servei de Ressonància Magnètica Nuclear, Universitat Autònoma de Barcelona, E-08193 Bellaterra, Catalonia, Spain
[b] Mestrelab Research, Santiago de Compostela, E-15706 A Coruña, Spain
[c] NMR Structure Elucidation, Process & Analytical Chemistry, Merck & Co. Inc., 126 E. Lincoln Avenue, Rahway, NJ 07065, United States

ARTICLE INFO

Article history:
Received 15 January 2016
Revised 5 March 2016
Available online 10 March 2016

Keywords:
Pure shift HSQMBC
Pure shift HSQC
Pure shift HSQC-TOCSY
Pure shift NMR
Covariance NMR

ABSTRACT

The current *Pros* and *Cons* of a processing protocol to generate pure chemical shift NMR spectra using Generalized Indirect Covariance are presented and discussed. The transformation of any standard 2D homonuclear and heteronuclear spectrum to its pure shift counterpart by using a reference DIAG spectrum is described. Reconstructed pure shift NMR spectra of NOESY, HSQC, HSQC-TOCSY and HSQMBC experiments are reported for the target molecule strychnine.

1. Introduction

The development of novel experimental strategies to significantly enhance signal resolution by broadband homodecoupling is a current topic of high interest in ^{1}H NMR spectroscopy [1–3]. The original Zangger–Sterk experiment [4,5] has been modified and improved in several ways, highlighting the new PSYCHE pulse scheme as a reference experiment to achieve optimum results without tedious set-up [6]. All of these novel building blocks have been implemented in a number of 1D and 2D homo- and heteronuclear experiments to provide resolution-enhanced pure chemical shift ^{1}H NMR spectra, where signals appear collapsed to singlet resonances. In the heteronuclear case, a pure shift HSQC (psHSQC) spectrum can be obtained without penalty in sensitivity for molecules with C-13 at natural abundance by applying real-time BIRD-based homodecoupling during ^{1}H acquisition [7,8]. However, the BIRD element does not decouple geminal ^{2}J(HH) interactions, and therefore cross peaks from diastereotopic CH_2 protons in psHSQC are not really pure shift because they appear as doublets. In addition, chunked acquisition protocol introduces FID interruption causing undesired relaxation effects, increases in linewidths, and also generates disturbing sidebands along the detected F2 dimension. Real-time BIRD-homodecoupling is based on the selective inversion of ^{1}H–^{13}C vs ^{1}H–^{12}C and hence it partially works in ADEQUATE experiments [9] or definitely not work for other interesting heteronuclear experiments such as HSQC-TOCSY, HMBC/HSQMBC or LR-HSQMBC experiments. Only band-selective pure shift versions of these lasts experiments have been reported using the HOBS scheme [10–13].

On the other hand, covariance processing methods have been used to generate challenging NMR spectral representations from discretely acquired spectra, displaying key features that can be difficult to observe using conventional protocols [14–38]. In particular, indirect covariance has been reported to generate ultra high-resolved pure shift ^{1}H–^{1}H correlation spectra in both F1 and F2 dimensions, by mapping the information extracted from the F1 dimension of F1-homodecoupled COSY, TOCSY and NOESY spectra onto its F2 dimension [39–42].

Following this idea, we present here the first attempts towards a general solution to generate *Pure Shift NMR spectra by using Generalized Indirect Covariance* (psGIC) [14]. The current strategy is based on the calculation of a new 2D psGIC spectrum from the combination of a parent homo- or heteronuclear spectrum and a reference 2D F1-homodecoupled ^{1}H–^{1}H correlation spectrum only showing diagonal cross-peaks (DIAG) which share a common ^{1}H frequency dimension (Fig. 1). Using psGIC, the enhanced signal resolution due to multiplet simplification achieved from the F1 ^{1}H dimension in the DIAG spectrum can be transferred to the F2 dimension of the parent spectrum. It must be emphasized that this approach is not a "real" homodecoupling method; rather, it can be understood as the reduction of the overall multiplet width along

* Corresponding author.
E-mail address: teodor.parella@uab.cat (T. Parella).

http://dx.doi.org/10.1016/j.jmr.2016.03.003
1090-7807/

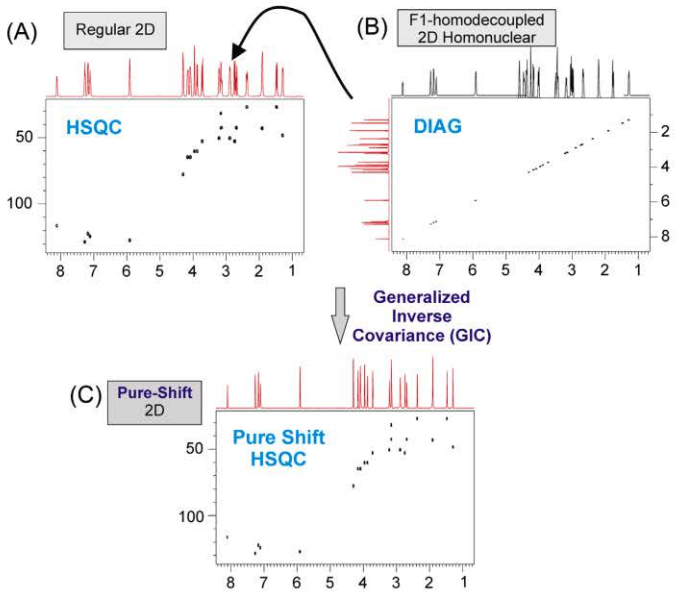

Fig. 1. Processing strategy to generate pure shift NMR spectra using GIC. In the example, the high signal dispersion achieved along the F1-dimension in the F1-homodecoupled DIAG experiment (B) is transferred to the detected F2-dimension of a regular HSQC spectrum (A). Note the resolution enhancement observed in the internal F2 projection of the psGIC-HSQC spectrum (C) or in the expanded area and slices shown in Fig. 2.

the F2 dimension by using a chemical shift selective filter. This method can mean a simple approach to obtain equivalent pure shift NMR spectral representations of otherwise impractical or very time consuming experiments without introducing novel acquisition methods in existing pulse sequences and also without sacrificing sensitivity.

2. Results and discussion

The key point of this proposal is a highly resolved DIAG spectrum that can be obtained by two methods. The results presented here use an experimental DIAG spectrum collected from a modification of the recent PSYCHE-TOCSY pulse sequence [42] with omission of the DIPSI-2 pulse train, in a similar way as reported for the nemoDIAG experiment (Fig. S1A) [43]. An alternative and faster method reconstruct a synthetic 2D DIAG spectrum from an experimental 1D broadband homodecoupled ^{1}H spectrum using the *make2D* reconstruction program (Fig. S4). As proof of concept, conventional 2D HSQC (Fig. 1A) and 2D DIAG (Fig. 1B) experiments of the alkaloid strychnine, **1**, were quickly acquired with a moderate resolution of 2K(F2) * 256(F1) and processed using zero-filling and linear prediction along the F1 dimension to get a final matrix of 2K (F2) * 2K(F1). Then, the processed HSQC and DIAG datasets were combined following the GIC formalism as implemented into the Mnova software (λ = 1). Importantly, these spectra need to be digitally equivalent in their combined F1/F2 dimensions. This co-processing directly provides a reconstructed pure shift HSQC (psGIC-HSQC) spectrum showing well defined singlet signals for all cross-peaks, even for all diastereotopic CH_2 protons (Fig. 2). Experimentally, perfect-BIRD and constant-time BIRD elements have been implemented in time-consuming pure shift pseudo-3D HSQC pulse schemes to achieve efficient ^{2}J(HH) homodecoupling in the measurement of RDC in methylene systems [44,45]. The complete resonance simplification for all cross-peaks allows routine tasks such as spectral analysis, fast extraction of chemical shifts, and automatic peak picking that can facilitate computer-assisted structural elucidation (CASE) program data input.

All potential sources that can generate false correlations have been carefully evaluated. Off-diagonal cross-peaks resulting of *J* transfer during the zero-quantum filter (ZQF) element in the experimental DIAG spectrum have been efficiently removed by using the *cleanDIAG* script that add zeroes outside the diagonal (Fig. S1B). If required, the lack of digital and/or signal resolution in the F1 dimension of the DIAG spectrum can be enhanced using non-uniform sampling NUS [46,47] or applying linear prediction whereas the potentially imperfect homodecoupling due to strong coupling effects only depends on the PSYCHE performance. In the current example, the 1D PSYCHE spectrum of **1** at 600 MHz shows efficient broadband homodecoupling for all signals, except for some distortions observed in the AB spin system corresponding to the H23a/H23b methylene protons (^{2}J(HH) is 13.7 Hz) that appear separated by only 50 Hz and the degenerated H17a/H17b protons (Fig. S3). Finally, artefacts generated during covariance processing due to ^{1}H signal overlap along the F2 dimension are the more critical issue and, at this point, remains to be resolved. As reported previously [18], evaluating reconstructed spectra with different matrix powers (λ) values during GIC calculations (Fig. S5) or the direct comparison between the experimental and the reconstructed psGIC spectra provide two helpful ways to detect such potential artefact responses [22–24]. This problem of signal overlap is clearly observed in psGIC spectra of estradiol (**2**) that presents challenging a crowded area in the aliphatic 1.2–1.4 ppm region, including several diastereotopic CH_2 protons with different degrees of strong coupling effects (Figs. S17–S19). Among the imperfections that need to be addressed, the generation of psGIC datasets offers some *Pros* over the experimental acquisition of real pure shift datasets: (i) it's a simple and fast processing tool that

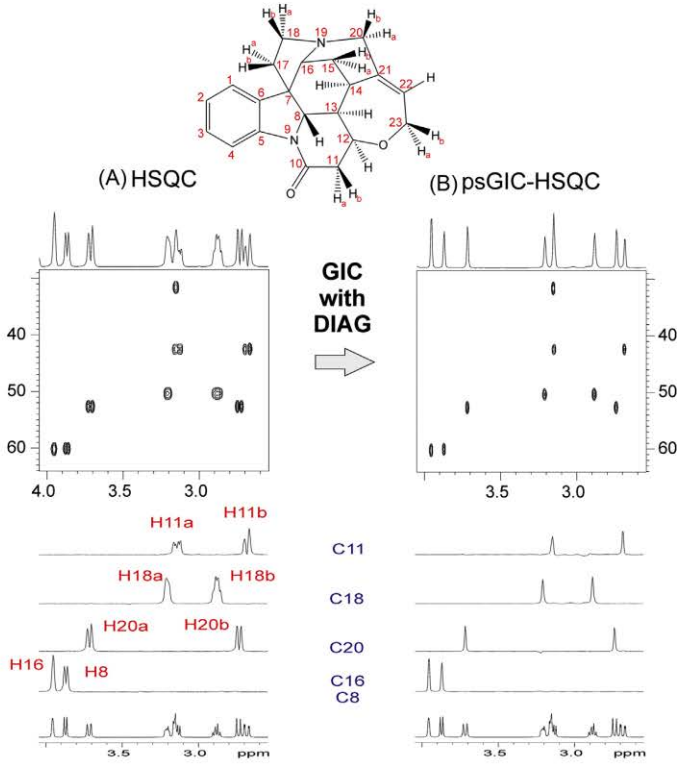

Fig. 2. Expanded area and internal F1 projections of (A) the regular HSQC and (B) the resulting psGIC-HSQC spectra of strychnine, **1**, in $CDCl_3$ after applying GIC. Below are 1D slices extracted at the chemical shifts of some CH and CH_2 carbons. Note how all cross-peaks appear as singlet signals, independent of their carbon multiplicities.

does not require spectrometer time; (ii) no sophisticated pulse sequences need to be developed and the technique can afford results when no available solutions exist to obtain certain experimental pure shift spectra; (iii) it can be applied to a broad range of proton-detected homo- and heteronuclear NMR experiments; (iv) it is important to remember that experimental homodecoupled spectra are not free of spectral artefacts in the form of sidebands, they can suffer from incomplete homodecoupling as well as to the effects of imperfect pulses, mismatch between BIRD optimization and ^1J(CH) values, increases in linewidth and, in many cases, important sensitivity penalties and long acquisition times.

As GIC retains the relative phase of cross-peak, multiplicity-edited psGIC-HSQC is also feasible. Additionally, the combined effects of multiplet simplicity and excellent linewidths helps to improve the spectral quality in experiments like ASAP-HSQC experiment [48] where fast acquisition imposes limited resolution in the acquisition dimension or even transform the experimental psHSQC [7,8] into a true pure shift representation, by removing the ^2J(HH) splitting (Figs. S7 and S8). In analogy, GIC co-processing between a standard 2D HSQC-TOCSY (Fig. 3A) and the reference 2D DIAG dataset affords psGIC-HSQC-TOCSY representation (Fig. 3B) which is not possible to obtain experimentally by real-time BIRD homodecoupling. The evaluation of sensitivity levels in reconstructed NMR spectra is somewhat critical because the noise is not real and therefore the usual measurement of SNR should not be appropriate in such cases. However, a discussion about the noise in covariance spectra has been carefully addressed previously [14,21,38] where it was concluded that GIC processing has limited consequences for the sensitivity. It is important to note that the relative intensities of correlations in all psGIC spectra shown in our work are in excellent agreement with the corresponding resonances from the original experiments (for instance, check the perfect distinction of tiny correlations in Fig. 3C), confirming the excellent reproducibility of GIC.

In a similar fashion, the GIC co-processing also works for long-range correlations as demonstrated by combining the pure in-phase version of the HSQMBC [49] and the reference DIAG spectra to yield the equivalent pure shift correlation map of the HSQMBC (psGIC-HSQMBC) (Fig. 4). The psGIC strategy is not limited to the transformation of any spectra to its pure shift version. It can also be extended to generate a third new spectrum as reported previously for some hyphenated experiments such as inverted direct-responses (IDR) versions of HSQC-TOCSY [22], HSQC-COSY [19,20] and HSQC-NOESY [21]. For instance, psGIC-HSQC-TOCSY or psGIC-HSQMBC-TOCSY spectra could be generated combining the regular HSQC or HSQMBC, respectively, with a F1-homodecoupled PSYCHE-TOCSY [42] as a reference spectrum (Fig. S13).

Another interesting feature of psGIC is its multiple-purpose and universal functionality. The reconstruction of psGIC maps from 2D homonuclear experiments like TOCSY or NOESY would follow a similar approach as described for heteronuclear experiments. As an example, the GIC processing using DIAG and the regular NOESY introduces pure shift to the F2 dimension and subsequent direct covariance allows an exclusive transfer of the chemical shift information to the F1 dimension (Fig. 5). Chemical shifts are magnetic

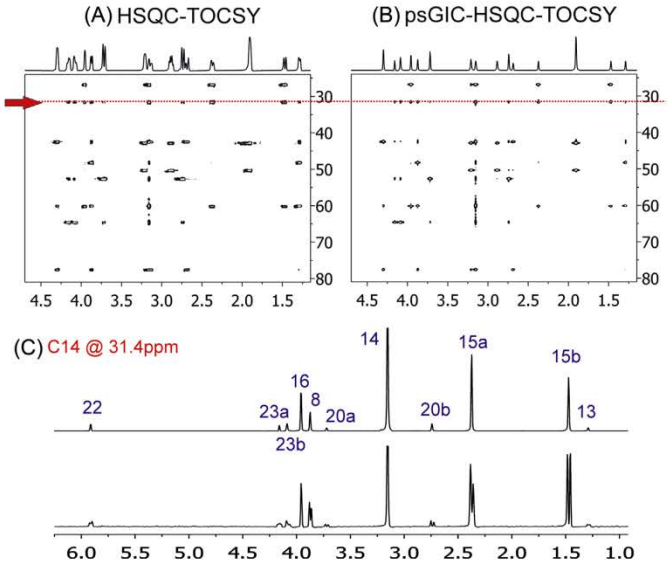

Fig. 3. Aliphatic region corresponding to (A) the regular 2D HSQC-TOCSY and (B) the psGIC-HSQC-TOCSY spectra of **1** generated by GIC with the reference DIAG spectrum. A comparison of the internal F2 projections at the top of each 2D spectrum and the selected C14 rows in (C) shows the absence of *J* multiplicity for all cross-peaks.

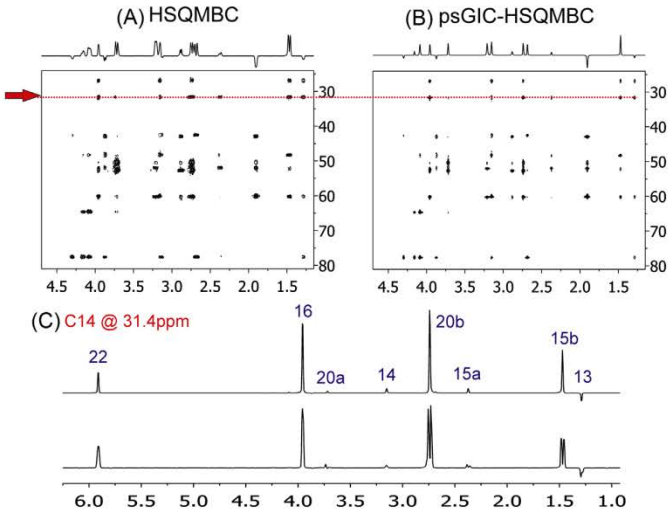

Fig. 4. Aliphatic region corresponding to (A) the regular pure in-phase HSQMBC [49] and (B) the psGIC-HSQMBC spectra of **1** generated by GIC using the reference DIAG spectrum. A comparison of the internal F2 projections at the top of each 2D spectrum and the selected C14 rows in (C) shows the absence of *J* coupling pattern and the excellent reproducibility of singal intensities for all cross-peaks. Note the perfect complementarity with spectra of Fig. 3.

field independent parameters and therefore the pure shift nature of the internal F1 projection of DIAG could also allow GIC processing with datasets acquired in different magnetic field strengths (Fig. S14). In addition, the psGIC methodology is fully compatible with the use of NUS techniques in order to enhance digital resolution along the indirect dimensions of the DIAG and the reconstructed psGIC spectra. For instance, considerable NUS compression percentages (between 3% and 15%) have been successfully applied in regular 2D TOCSY and 2D HSQC experiments, achieving high levels of spectral resolution in optimum acquisition times as reported in the analysis of mixtures [50]. The positive impact that NUS can play in covariance NMR processing could be also demonstrated generating high-resolved ^{1}H–^{1}H and ^{13}C–^{13}C correlations representations [14,22,26] subjecting NUS-enhanced HSQC-TOCSY, HSQMBC and ADEQUATE spectra, or combination of them, to some type of covariance processing (Fig. S15).

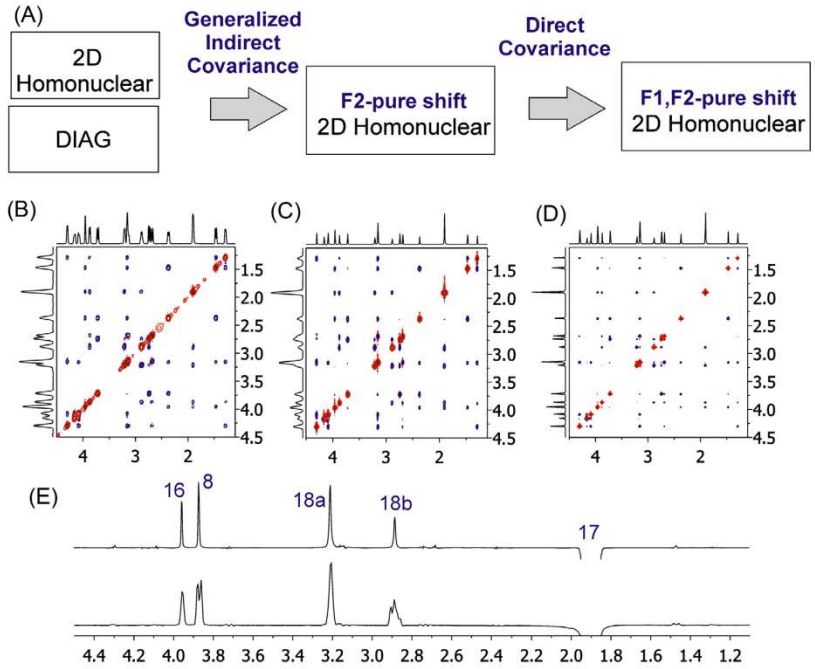

Fig. 5. (A) General strategy to convert a regular homonuclear 2D spectrum to the corresponding pure shift spectrum. GIC processing using the reference 2D DIAG generates singlets in F2 and subsequent direct covariance transfer internally this feature to the F1 dimension; (B) regular NOESY; (C) F2-pure shift NOESY and (D) F1, F2-pure shift NOESY spectra of **1**; (E) 1D slices extracted at the degenerate methylene H17a/b frequency (1.9 ppm).

3. Conclusions

In summary, so far attempts to obtain broadband homodecoupled ^{1}H NMR spectra have been mainly concentrated in the development of experimental pulse sequences. However, most of these reported approaches become time-consuming in terms of spectrometer time, usually suffer of important sensitivity losses and also are not free of the presence of spectral artefacts and anomalies when compared to the regular experiments. Here, the basic principles to generate synthetic pure shift NMR spectra of the most common experiments using a fast GIC processing have been explored. The selective transfer of the chemical shift information from the F1 ^{1}H dimension of a reference DIAG spectrum to the F2 ^{1}H dimension of any standard experiment can provide pure shift NMR spectral representations that are difficult or impossible to obtain experimentally using established pulse sequences. For instance, it has been shown that ^{2}J(HH) splitting in diastereotopic methylene protons are eliminated in psGIC-HSQC spectra or broadband pure shift spectra of experiments like psGIC-HSQC-TOCSY or psGIC-HSQMBC spectra can be reconstructed after some seconds of calculation. Definitively, further developments in the design of pulse schemes to improve the sensitivity and strong coupling effects in homodecoupled experiments and also enhancements in novel NUS schedules, covariance or deconvolution processing algorithms could be incorporated into psGIC to design more efficient strategies to generate such perfect NMR spectra. The use of pure chemical shift data also opens new possibilities in CASE programs for the automated analysis and verification of molecular structures. Further work is currently in progress exploring additional applications as well as new schemes aimed at detecting and removing artifacts due to signal overlap characteristics of covariance processing [22–24].

4. Methods and materials

All NMR experiments were recorded at 298 K on a BRUKER DRX-600 spectrometer equipped with a 3-channel 5-mm TXI probe incorporating a z-gradient coil. The test sample was 20 mg of Strychnine (**1**) in 0.6 ml of $CDCl_3$.

Two-dimensional DIAG, TOCSY, NOESY, HSQC, HSQC-TOCSY, HSQMBC and HSQMBC-TOCSY experiments use a recycle delay of 1 s. ^{1}H and ^{13}C spectral widths were of 6009 Hz (10.01 ppm) and 28,673 Hz (190.0 ppm), respectively. 256 t_1 increments were collected, with 2048 data points in each t_1 increment. Prior to Fourier-transformation, zero-filling and linear prediction in the F1 dimension and a squared sine-square apodization phase-shifted 90° in both dimensions were applied to obtain a 2K * 2K resolution matrix.

The 2D ^{1}H–^{13}C HSQC spectrum of Figs. 1 and 2A was collected using the pulse program hsqcetgpsp (Bruker library) with an interpulse INEPT delay optimized to 140 Hz. 4 scans were collected per t_1 increment and the total experimental time was of 20 min.

The 2D ^{1}H–^{13}C HSQC-TOCSY spectrum of Fig. 3A was collected using the pulse program hsqcdietgpsisp (Bruker library) with an interpulse INEPT delay optimized to 140 Hz and a TOCSY mixing time of 60 ms. 8 scans were collected per t_1 increment and the total experimental time was of 43 min.

The 2D ^{1}H–^{13}C HSQMBC spectrum of Fig. 4A was collected using the PIP-HSQMBC pulse scheme reported in Ref. [49]. The interpulse delay was optimized to 8 Hz. The ZQF element includes a chirped

adiabatic 180° ^{1}H pulse of 30 ms of duration applied simultaneously with a purging G0 gradient of 1.6 G cm^{-1} to remove undesired transverse and ZQ contributions. 16 scans were collected per t_1 increment and the total experimental time was of 1 h 31 m.

The 2D ^{1}H–^{1}H NOESY spectrum of Fig. 5A was collected using the pulse program noesygpph (Bruker library) with a mixing time was set to 500 ms. 8 scans were collected per t_1 increment and the total experimental time was of 55 min.

The homonuclear 2D DIAG experiment was recorded using the 2D PSYCHE-TOCSY pulse scheme reported in Ref. [42], except the use of the DIPSI-2 pulse train (see Fig. S1A). In these experiments, a double frequency-swept chirp pulse length of 30 ms applied simultaneously to a weak gradient of 1.5 G cm^{-1} and with a flip-angle of 20° was used. All other parameters were set as described in the original publication.

Different datasets using NUS of 25% were recorded for some experiments using the standard protocols incorporated into the TOPSPIN 3.1 software package. These datasets were processed using the compressed sensing (cs) algorithm for reconstructing the final NMR spectra.

Generalized Indirect Covariance processing ($\lambda = 1$) was performed using the module implemented into Mnova. The *make2D* macro generates a symmetric diagonal spectrum (DIAG) by first deconvolving the 1D-pure shift ^{1}HNMR spectrum via GSD followed by the synthesis of the DIAG spectrum using 2D-Gaussian lineshapes. These 2D diagonal peaks have identical line widths along both dimensions based on the values derived from the deconvolution of the 1D spectrum. In order to keep memory requirements and computation times manageable, a maximum size of 4K × 4K DIAG matrix is employed. The *cleanDIAG* macro sets all the values in the experimental DIAG spectrum to zero except in a diagonal band with a user defined width (e.g. 35 Hz). A smooth Gaussian function was also used to avoid abrupt jumps from the diagonal band but no differences were found when such function was no used. Both *make2D* and *cleanDIAG* macros are available for Mnova.

Acknowledgments

Financial support for this research provided by MINECO – Spain (project CTQ2012-32436) is gratefully acknowledged. A.F. thanks CNPq-Brazil for a scholarship. We also thank the Servei de Ressonància Magnètica Nuclear, Universitat Autònoma de Barcelona, for allocating instrument time to this project.

Appendix A. Supplementary material

Supplementary data associated with this article can be found, in the online version, at http://dx.doi.org/10.1016/j.jmr.2016.03.003.

References

[1] K. Zangger, Pure shift NMR, Prog. Nucl. Magn. Reson. Spectrosc. 86–87 (2015) 1–20, http://dx.doi.org/10.1016/j.pnmrs.2015.02.002.
[2] L. Castañar, T. Parella, Broadband ^{1}H homodecoupled NMR experiments: recent developments, methods and applications, Magn. Reson. Chem. 53 (2015) 399–426, http://dx.doi.org/10.1002/mrc.4238.
[3] R.W. Adams, Pure shift NMR spectroscopy, eMagRes 3 (2014) 295–310, http://dx.doi.org/10.1002/9780470034590.
[4] K. Zangger, H. Sterk, Homonuclear broadband-decoupled NMR spectra, J. Magn. Reson. 489 (1997) 486–489.
[5] J.A. Aguilar, S. Faulkner, M. Nilsson, G.A. Morris, Pure shift ^{1}H NMR: a resolution of the resolution problem?, Angew Chem., Int. Ed. 49 (2010) 3901–3903, http://dx.doi.org/10.1002/anie.201001107.
[6] M. Foroozandeh, R.W. Adams, N.J. Meharry, D. Jeannerat, M. Nilsson, G.A. Morris, Ultrahigh-resolution NMR spectroscopy, Angew. Chem., Int. Ed. 53 (2014) 6990–6992, http://dx.doi.org/10.1002/anie.201404111.
[7] L. Paudel, R.W. Adams, P. Király, J.A. Aguilar, M. Foroozandeh, M.J. Cliff, M. Nilsson, P. Sándor, G.A. Morris, Simultaneously enhancing spectral resolution and sensitivity in heteronuclear correlation NMR spectroscopy, Angew. Chem., Int. Ed. 52 (2013) 11616–11619, http://dx.doi.org/10.1002/anie.201305709.
[8] M. Pérez-Trujillo, L. Castañar, E. Monteagudo, L.T. Kuhn, P. Nolis, A. Virgili, R.T. Williamson, T. Parella, Simultaneous ^{1}H and ^{13}C NMR enantiodifferentiation from highly-resolved pure shift HSQC spectra, Chem. Commun. 50 (2014) 10214–10217, http://dx.doi.org/10.1039/c4cc04077e.
[9] J. Saurí, W. Bermel, A.V. Buevich, E.C. Sherer, L.A. Joyce, M.H.M. Sharaf, P.L. Schiff, T. Parella, R.T. Williamson, G.E. Martin, Homodecoupled 1,1- and 1,n-ADEQUATE: pivotal NMR experiments for the structure revision of cryptospirolepine, Angew. Chem., Int. Ed. 54 (2015) 10160–10164, http://dx.doi.org/10.1002/anie.201502540.
[10] L. Castañar, P. Nolis, A. Virgili, T. Parella, Full sensitivity and enhanced resolution in homodecoupled band-selective NMR experiments, Chem. Eur. J. 19 (2013) 17283–17286, http://dx.doi.org/10.1002/chem.201303235.
[11] J. Ying, J. Roche, A. Bax, Homonuclear decoupling for enhancing resolution and sensitivity in NOE and RDC measurements of peptides and proteins, J. Magn. Reson. 241 (2014) 97–102, http://dx.doi.org/10.1016/j.jmr.2013.11.006.
[12] L. Castañar, R. Roldán, P. Clapés, A. Virgili, T. Parella, Disentangling complex mixtures of compounds with near-identical (1) H and (13) C NMR spectra using pure shift NMR spectroscopy, Chem. Eur. J. 21 (2015) 7682–7685, http://dx.doi.org/10.1002/chem.201500521.
[13] J. Saurí, E. Sistaré, R. Thomas Williamson, G.E. Martin, T. Parella, Implementing multiplicity editing in selective HSQMBC experiments, J. Magn. Reson. 252 (2015) 170–175, http://dx.doi.org/10.1016/j.jmr.2015.01.006.
[14] F. Zhang, R. Brüschweiler, Indirect covariance NMR spectroscopy, J. Am. Chem. Soc. 126 (2004) 13180–13181, http://dx.doi.org/10.1021/ja047241h.
[15] M. Jaeger, R.L.E.G. Aspers, Covariance NMR and small molecule applications, Annu. Rep. NMR Spectrosc. 83 (2014) 272–360, http://dx.doi.org/10.1016/B978-0-12-800183-7.00005-8.
[16] Y. Chen, F. Zhang, W. Bermel, R. Brüschweiler, Enhanced covariance spectroscopy from minimal datasets, J. Am. Chem. Soc. 128 (2006) 15564–15565, http://dx.doi.org/10.1021/ja065522e.
[17] N. Trbovic, S. Smirnov, F. Zhang, R. Brüschweiler, Covariance NMR spectroscopy by singular value decomposition, J. Magn. Reson. 171 (2004) 277–283, http://dx.doi.org/10.1016/j.jmr.2004.08.007.
[18] D.A. Snyder, R. Brüschweiler, Generalized indirect covariance NMR formalism for establishment of multidimensional spin correlations, J. Phys. Chem. A 113 (2009) 12898–12903, http://dx.doi.org/10.1021/jp9070168.
[19] K.A. Blinov, N.I. Larin, A.J. Williams, K.A. Mills, G.E. Martin, Unsymmetrical covariance processing of COSY or TOCSY and HSQC NMR data to obtain the equivalent of HSQC-COSY or HSQC-TOCSY spectra, J. Heterocycl. Chem. 43 (2006) 163–166, http://dx.doi.org/10.1002/jhet.5570430124.
[20] G.E. Martin, B.D. Hilton, P.A. Irish, K.A. Blinov, A.J. Williams, Using unsymmetrical indirect covariance processing to calculate GHSQC-COSY spectra, J. Nat. Prod. 70 (2007) 1393–1396, http://dx.doi.org/10.1021/np070221j.
[21] K.A. Blinov, A.J. Williams, B.D. Hilton, P.A. Irish, G.E. Martin, The use of unsymmetrical indirect covariance NMR methods to obtain the equivalent of HSQC-NOESY data, Magn. Reson. Chem. 45 (2007) 544–546, http://dx.doi.org/10.1002/mrc.1998.
[22] K.A. Blinov, N.I. Larin, M.P. Kvasha, A. Moser, A.J. Williams, G.E. Martin, Analysis and elimination of artifacts in indirect covariance NMR spectra via unsymmetrical processing, Magn. Reson. Chem. 43 (2005) 999–1007, http://dx.doi.org/10.1002/mrc.1674.
[23] G.E. Martin, B.D. Hilton, K.A. Blinov, A.J. Williams, Using indirect covariance spectra to identify artifact responses in unsymmetrical indirect covariance calculated spectra, Magn. Reson. Chem. 46 (2008) 138–143, http://dx.doi.org/10.1002/mrc.2141.
[24] R.L.E.G. Aspers, P.E.T.J. Geutjes, M. Honing, M. Jaeger, Using indirect covariance processing for structure elucidation of small molecules in cases of spectral crowding, Magn. Reson. Chem. 49 (2011) 425–436, http://dx.doi.org/10.1002/mrc.2766.
[25] K.A. Blinov, N.I. Larin, A.J. Williams, M. Zell, G.E. Martin, Long-range carbon–carbon connectivity via unsymmetrical indirect covariance processing of HSQC and HMBC NMR data, Magn. Reson. Chem. 44 (2006) 107–109, http://dx.doi.org/10.1002/mrc.1766.
[26] G.E. Martin, B.D. Hilton, M.R. Willcott, K.A. Blinov, HSQC-ADEQUATE: an investigation of data requirements, Magn. Reson. Chem. 49 (2011) 350–357, http://dx.doi.org/10.1002/mrc.2757.
[27] G.E. Martin, B.D. Hilton, K.A. Blinov, HSQC-1,1-ADEQUATE and HSQC-1, n-ADEQUATE: enhanced methods for establishing adjacent and long-range ^{13}C–^{13}C connectivity networks, J. Nat. Prod. 74 (2011) 2400–2407, http://dx.doi.org/10.1021/np200540q.
[28] G.E. Martin, B.D. Hilton, M.R. Willcott, K.A. Blinov, HSQC-1, n-ADEQUATE: a new approach to long-range ^{13}C–^{13}C correlation by covariance processing, Magn. Reson. Chem. 49 (2011) 641–647, http://dx.doi.org/10.1002/mrc.2793.
[29] G.E. Martin, K.A. Blinov, M. Reibarkh, R.T. Williamson, ^{1}J(CC)-edited HSQC-1, n-ADEQUATE: a new paradigm for simultaneous direct and long-range carbon–carbon correlation, Magn. Reson. Chem. 50 (2012) 722–728, http://dx.doi.org/10.1002/mrc.3870.
[30] G.E. Martin, R.T. Williamson, K.A. Blinov, C.G. Anklin, W. Bermel, HMBC-1,1-ADEQUATE via generalized indirect covariance: a high sensitivity alternative to n,1-ADEQUATE, Magn. Reson. Chem. 50 (2012) 691–695, http://dx.doi.org/10.1002/mrc.3863.
[31] G.E. Martin, K.A. Blinov, R.T. Williamson, HMBC-1,n-ADEQUATE spectra calculated from HMBC and 1,n-ADEQUATE spectra, Magn. Reson. Chem. 51 (2013) 299–307, http://dx.doi.org/10.1002/mrc.3946.

[32] W. Schoefberger, V. Smrecki, D. Vikic-Topic, N. Mueller, Homonuclear long-range correlation spectra from HMBC experiments by covariance processing, Magn. Reson. Chem. 45 (2007) 583–589, http://dx.doi.org/10.1002/mrc.2013.
[33] G.E. Martin, B.D. Hilton, K.A. Blinov, HSQC-ADEQUATE correlation: a new paradigm for establishing a molecular skeleton, Magn. Reson. Chem. 49 (2011) 248–252, http://dx.doi.org/10.1002/mrc.2743.
[34] G.E. Martin, B.D. Hilton, K.A. Blinov, A.J. Williams, Unsymmetrical indirect covariance processing of hyphenated and long-range heteronuclear 2D NMR spectra – enhanced visualization of ^{2}JCH and ^{4}JCH correlation responses, J. Heterocycl. Chem. 45 (2008) 1109–1113, http://dx.doi.org/10.1002/jhet.5570450426.
[35] G.E. Martin, B.D. Hilton, K.A. Blinov, A.J. Williams, ^{13}C–^{15}N correlation via unsymmetrical indirect covariance NMR: application to vinblastine, J. Nat. Prod. 70 (2007) 1966–1970, http://dx.doi.org/10.1021/np070361t.
[36] G.E. Martin, P.A. Irish, B.D. Hilton, K.A. Blinov, A.J. Williams, Utilizing unsymmetrical indirect covariance processing to define ^{15}N–^{13}C connectivity networks, Magn. Reson. Chem. 45 (2007) 624–627, http://dx.doi.org/10.1002/mrc.2029.
[37] G.E. Martin, B.D. Hilton, P.A. Irish, K.A. Blinov, A.J. Williams, Application of unsymmetrical indirect covariance NMR methods to the computation of the ^{13}C–^{15}N HSQC-IMPEACH and ^{13}C–^{15}N HMBC-IMPEACH correlation spectra, Magn. Reson. Chem. 45 (2007) 883–888, http://dx.doi.org/10.1002/mrc.2064.
[38] D.A. Snyder, A. Ghosh, F. Zhang, T. Szyperski, R. Brüschweiler, Z-matrix formalism for quantitative noise assessment of covariance nuclear magnetic resonance spectra, J. Chem. Phys 45 (2008) 104511–104518, http://dx.doi.org/10.1063/1.2975206.
[39] Y. Xia, G. Legge, K.Y. Jun, Y. Qi, H. Lee, X. Gao, IP-COSY, a totally in-phase and sensitive COSY experiment, Magn. Reson. Chem. 43 (2005) 372–379, http://dx.doi.org/10.1002/mrc.1558.
[40] J.A. Aguilar, A.A. Colbourne, J. Cassani, M. Nilsson, G.A. Morris, Decoupling two-dimensional NMR spectroscopy in both dimensions: pure shift NOESY and COSY, Angew. Chem., Int. Ed. 51 (2012) 6460–6463, http://dx.doi.org/10.1002/anie.201108888.
[41] J.A. Aguilar, J. Cassani, M. Delbianco, R.W. Adams, M. Nilsson, G.A. Morris, Minimising research bottlenecks by decluttering NMR spectra, Chem. Eur. J. 21 (2015) 6623–6630, http://dx.doi.org/10.1002/chem.201406283.
[42] M. Foroozandeh, R.W. Adams, M. Nilsson, G.A. Morris, Ultrahigh-resolution total correlation NMR spectroscopy, J. Am. Chem. Soc. 136 (2014) 11867–11869, http://dx.doi.org/10.1021/ja507201t.
[43] A. Cotte, D. Jeannerat, 1D NMR homodecoupled ^{1}H spectra with scalar coupling constants from 2D NemoZS-DIAG experiments, Angew. Chem., Int. Ed. 54 (2015) 6016–6018, http://dx.doi.org/10.1002/anie.201500831.
[44] T. Reinsperger, B. Luy, Homonuclear BIRD-decoupled spectra for measuring one-bond couplings with highest resolution: CLIP/CLAP-RESET and constant-time-CLIP/CLAP-RESET, J. Magn. Reson. 239 (2014) 110–120, http://dx.doi.org/10.1016/j.jmr.2013.11.015.
[45] L. Kaltschnee, A. Kolmer, I. Timári, V. Schmidts, R.W. Adams, M. Nilsson, K.E. Kövér, G.A. Morris, C.M. Thiele, Perfecting pure shift HSQC: full homodecoupling for accurate and precise determination of heteronuclear couplings, Chem. Commun. 50 (2014) 15702–15705, http://dx.doi.org/10.1039/C4CC04217D.
[46] K. Kazimierczuk, V.Y. Orekhov, Accelerated NMR spectroscopy by using compressed sensing, Angew. Chem., Int. Ed. 50 (2011) 5556–5559, http://dx.doi.org/10.1002/anie.201100370.
[47] V.Y. Orekhov, V.A. Jaravine, Analysis of non-uniformly sampled spectra with multi-dimensional decomposition, Prog. Nucl. Magn. Reson. Spectrosc. 59 (2011) 271–292, http://dx.doi.org/10.1016/j.pnmrs.2011.02.002.
[48] D. Schulze-Sünninghausen, J. Becker, B. Luy, Rapid heteronuclear single quantum correlation NMR spectra at natural abundance, J. Am. Chem. Soc. 136 (2014) 1242–1245, http://dx.doi.org/10.1021/ja411588d.
[49] L. Castañar, J. Saurí, R.T. Williamson, A. Virgili, T. Parella, Pure in-phase heteronuclear correlation NMR experiments, Angew. Chem., Int. Ed. 53 (2014) 8379–8382, http://dx.doi.org/10.1002/anie.201404136.
[50] A. Le Guennec, J.-N. Dumez, P. Giraudeau, S. Caldarelli, Resolution-enhanced 2D NMR of complex mixtures by non-uniform sampling, Magn. Reson. Chem. 53 (2015) 913–920, http://dx.doi.org/10.1002/mrc.4258.

Supporting Information

Exploring the use of Generalized Indirect Covariance to Reconstruct Pure Shift NMR Spectra: Current Pros and Cons

*André Fredi, Pau Nolis, Carlos Cobas, Gary E. Martin and Teodor Parella**

Table of Contents:

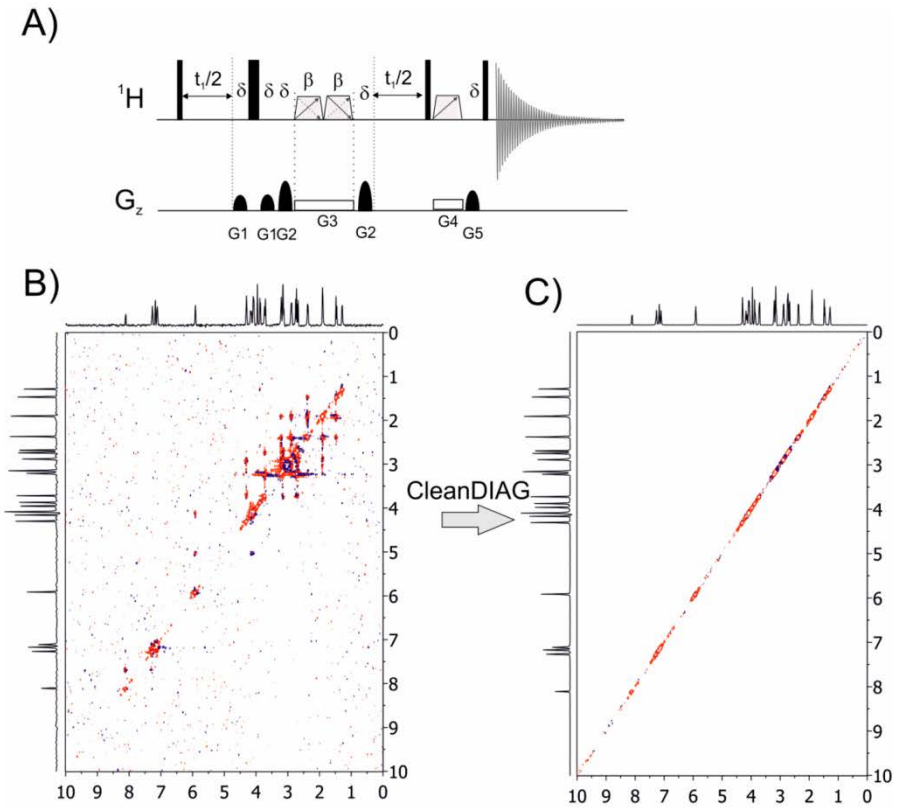

Figure S1: A) Pulse sequence used for the DIAG experiment; B-C) Experimental results showing the removal of any off-diagonal signals in the experimental DIAG spectrum by the *Clean2D* script implemented in Mnova. The script is executed with a customized multiplet width factor. The experimental DIAG spectrum in B) was recorded using a double frequency-swept chirp pulse length of 30 ms applied simultaneously to a weak gradient of 1.5 G/cm and with a flip-angle of β=20°. More details are described in the experimental section.

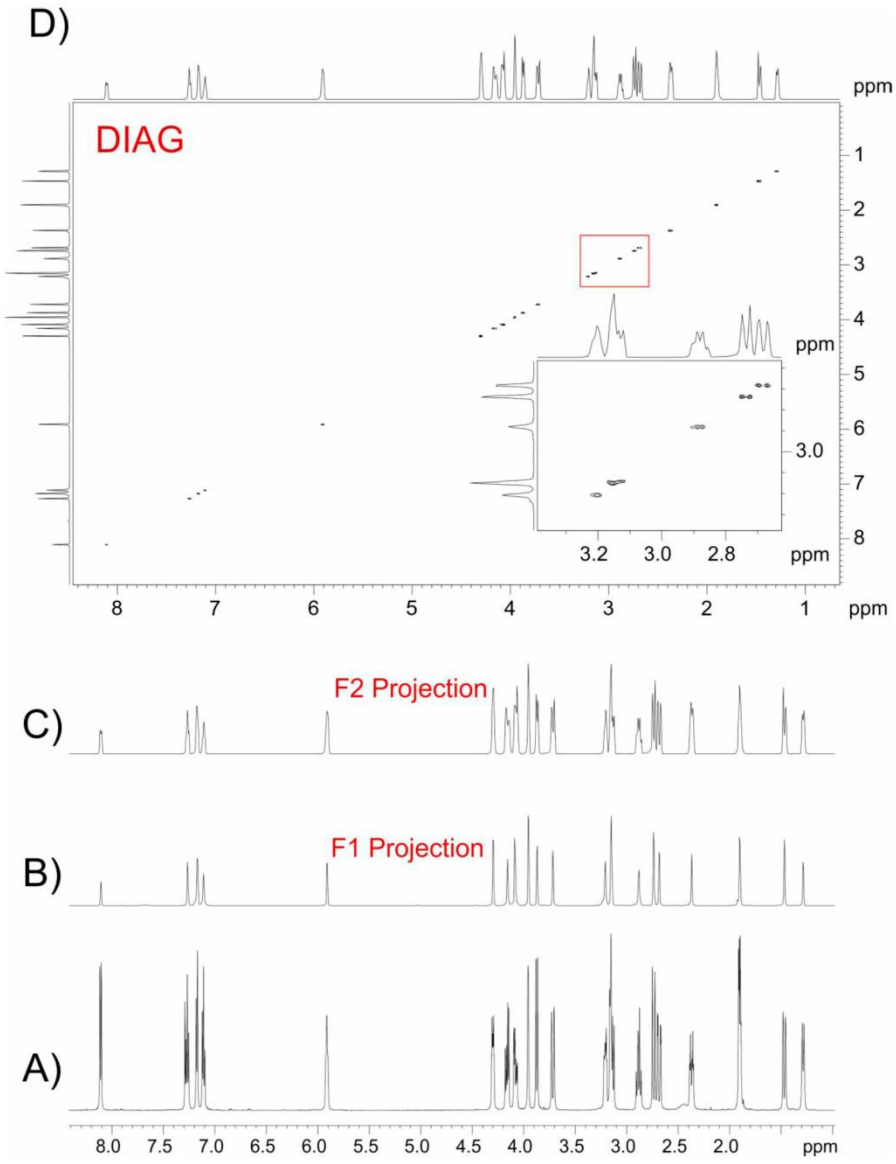

Figure S2: Comparison between the B) internal F1 and C) internal F2 projections in the D) 2D cleanDIAG spectrum of strychnine (see details in Figure S1). The enhanced high resolution obtained along the F1 dimension in DIAG will be projected along the detected F2 dimension of regular homo- and heteronuclear NMR spectra.

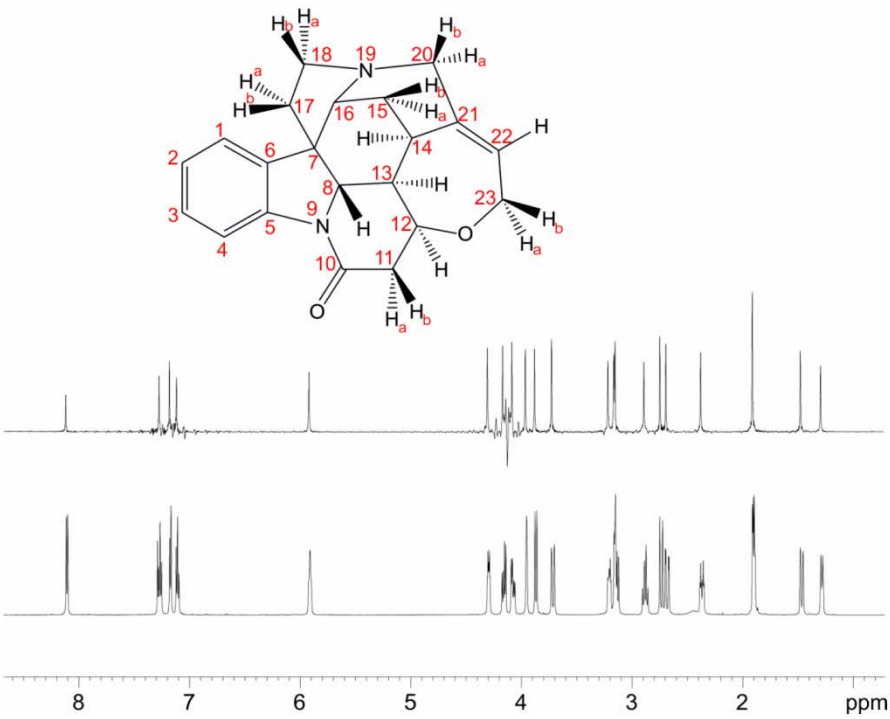

Figure S3: (bottom) 600 MHz ^{1}H NMR spectrum of strychnine in $CDCl_3$; (top) 1D PSYCHE spectrum obtained as described in ref. 6, using the same experimental conditions as for the DIAG experiment (see experimental section). Note that all peaks are simplified to collapsed singlets but strong coupling effects can be observed for H23a and H23b protons (AB spin system at ca. 4.1-4.2 ppm). This imperfect homodecoupling is also observed in the DIAG spectrum and this type of artifacts could generate distorted peaks in 2D pure shift NMR spectra generated by GIC.

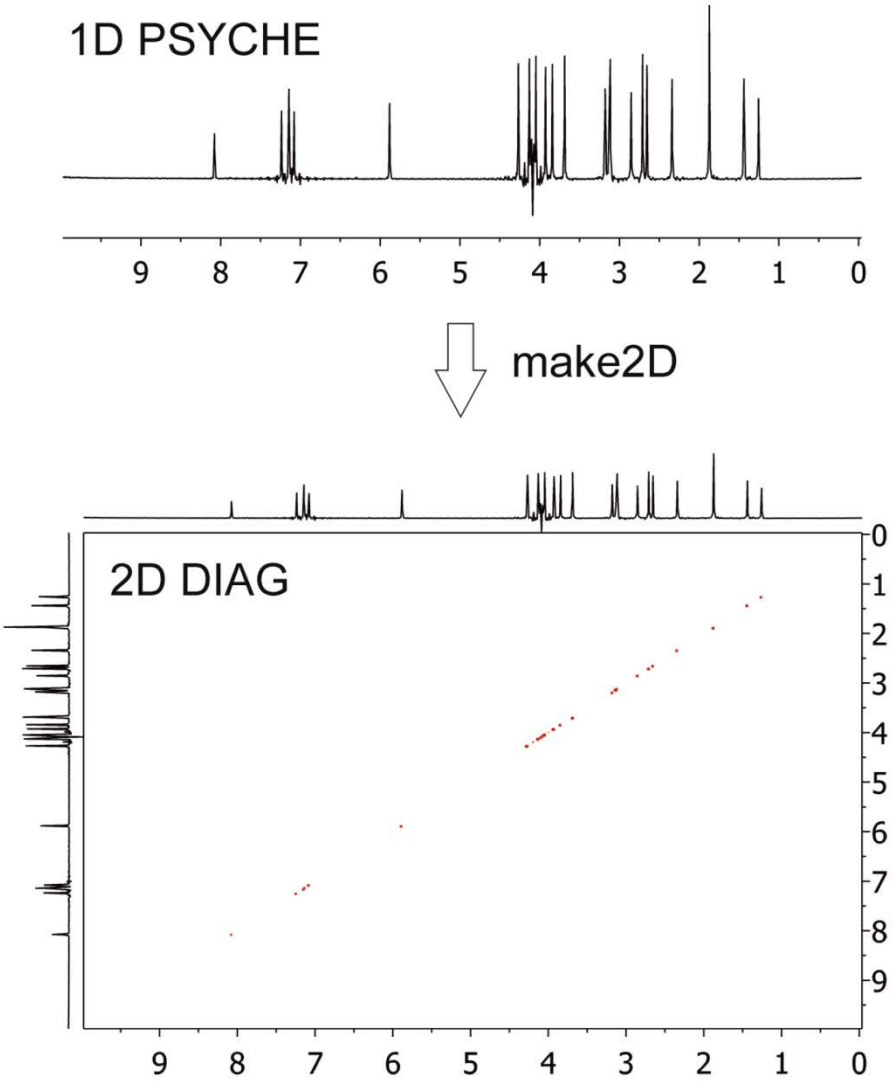

Figure S4: Automatic generation of a synthetic 2D DIAG spectrum from the 1D PSYCHE experiment, using the *make2D* script from Mnova.

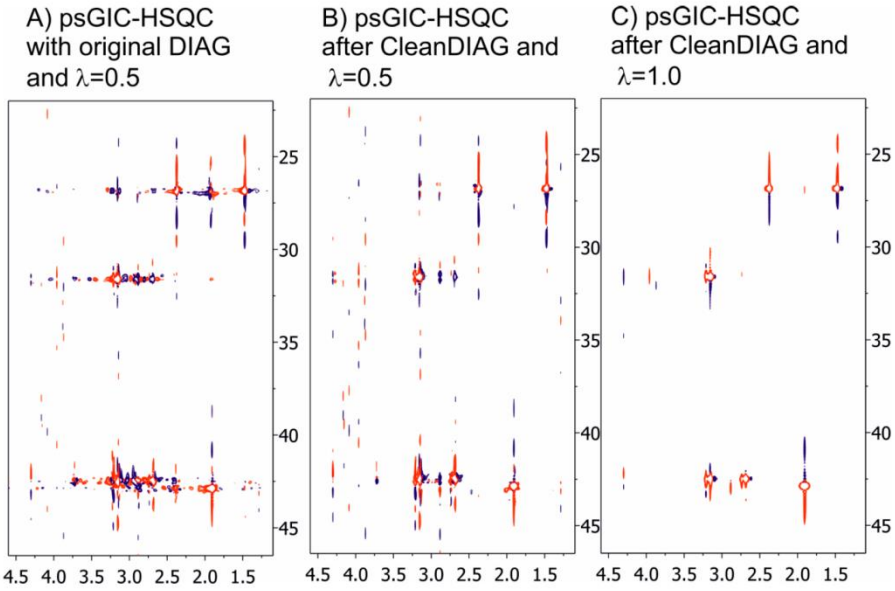

Figure S5: Artifacts observed in 2D psGIC-HSQC spectra of strychnine: A) Using the experimental DIAG spectrum and λ=0.5; B) After applying *CleanDIAG* and λ =0.5; C) as B but λ =1.0. All spectra have been displayed using the same contour plane to show the level of noise and artifacts.

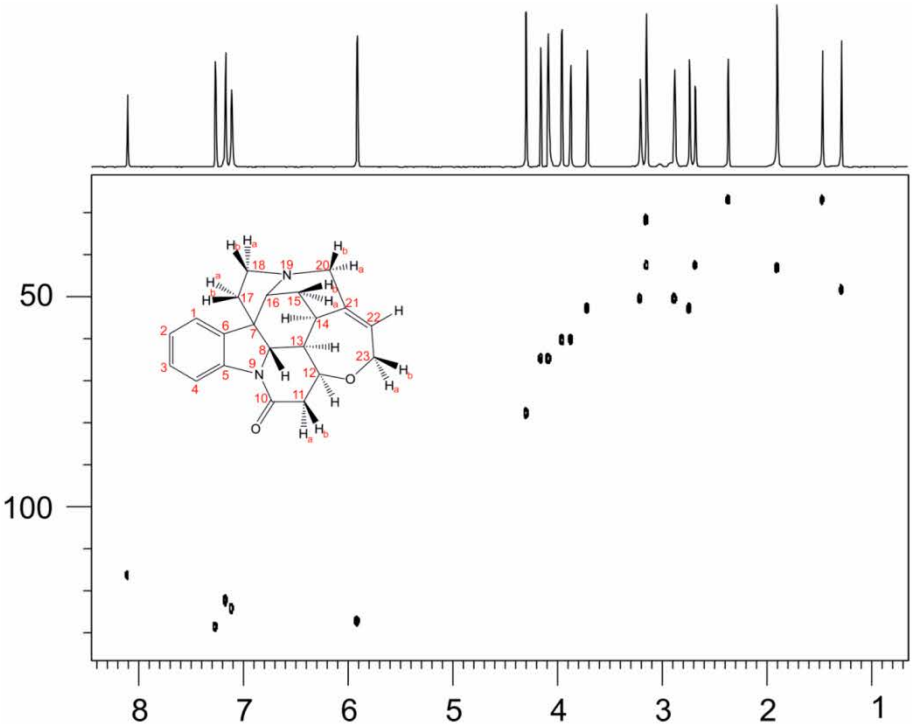

Figure S6: psGIC-HSQC spectrum of strychnine in $CDCl_3$ after combining a regular 2D HSQC and the experimental DIAG spectrum.

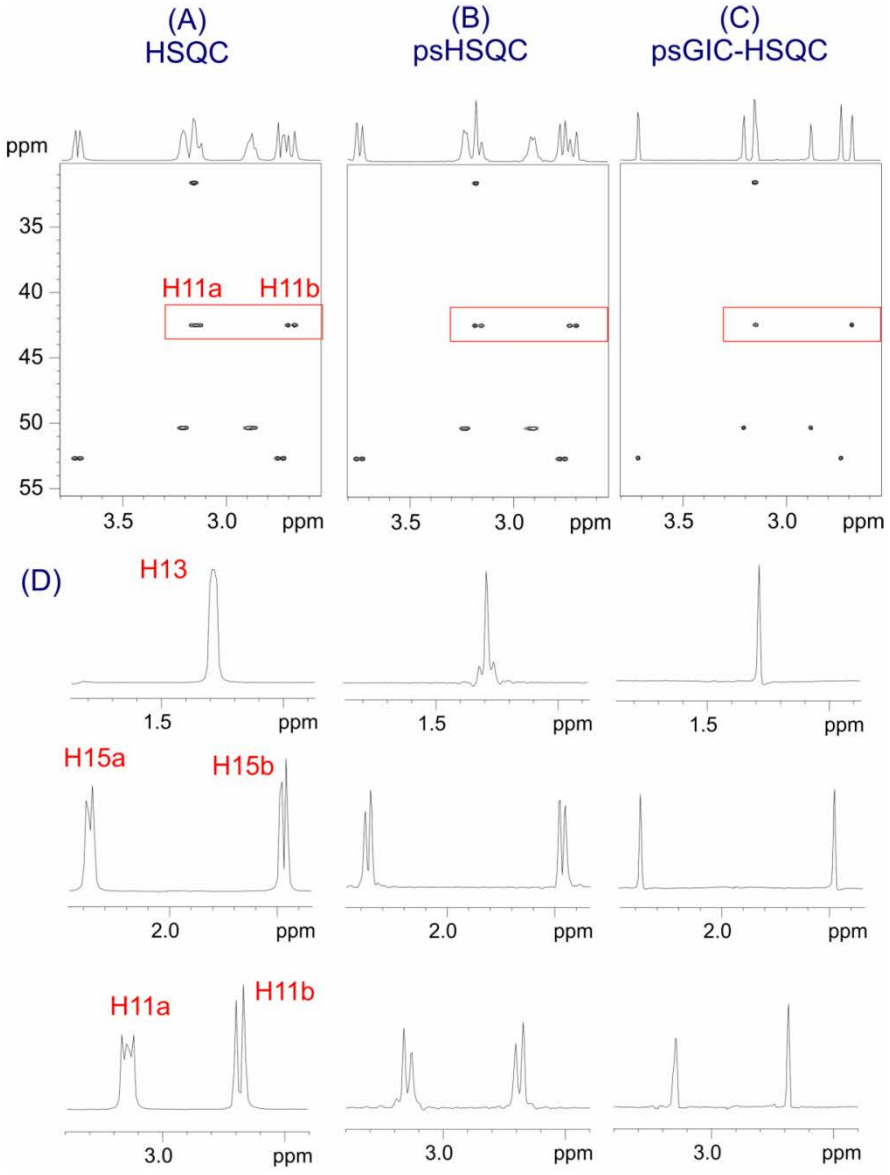

Figure S7: Comparison between the A) regular HSQC, B) experimental pure-shift HSQC (psHSQC) and C) psGIC-HSQC spectra of strychnine. Expanded cross peaks in D) correspond to several CH_2 and CH groups. Note that in psHSQC, CH protons are collapsed to singlets but diastereotopic CH_2 protons show their mutual $^2J(HH)$ coupling. In the psGIC-HSQC spectrum, both CH and CH_2 cross peaks are converted to singlets, providing a complete pure chemical shift representation.

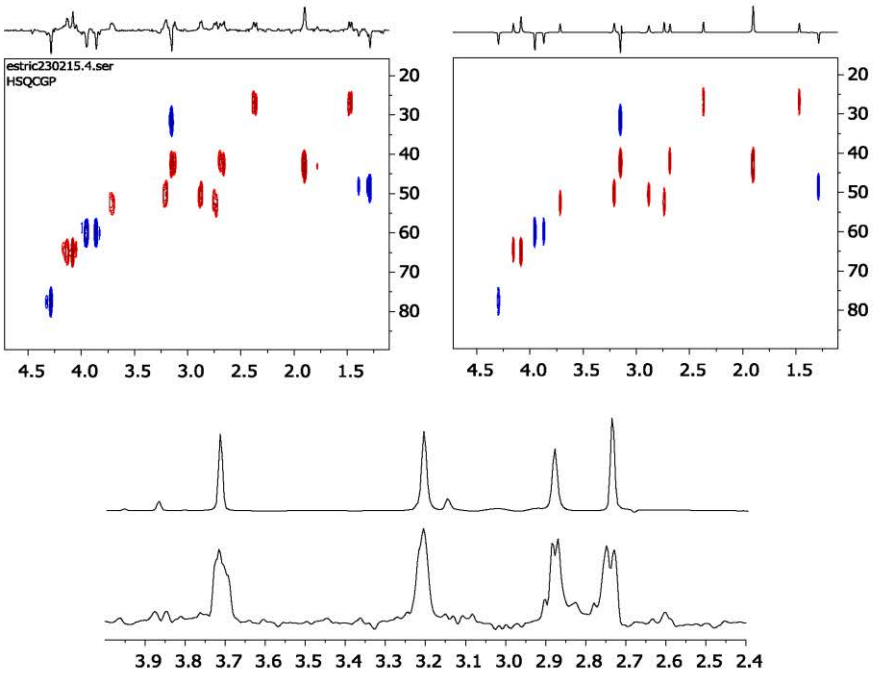

Figure S8: Quick transformation of an experimental multiplicity-edited pure shift HSQC to GICps-ME-HSQC spectra of strychnine using GIC.

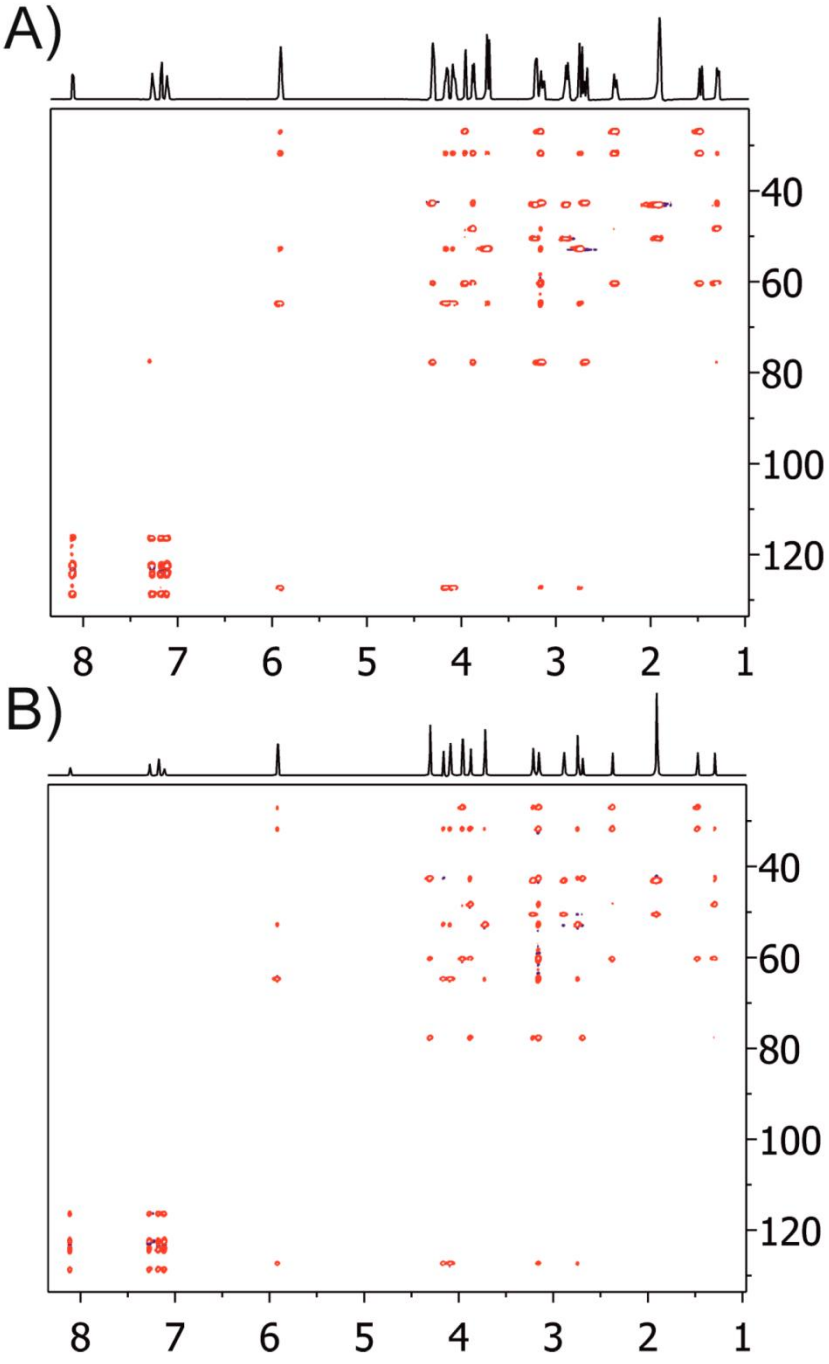

Figure S9: HSQC-TOCSY and psGIC-HSQC-TOCSY of strychnine

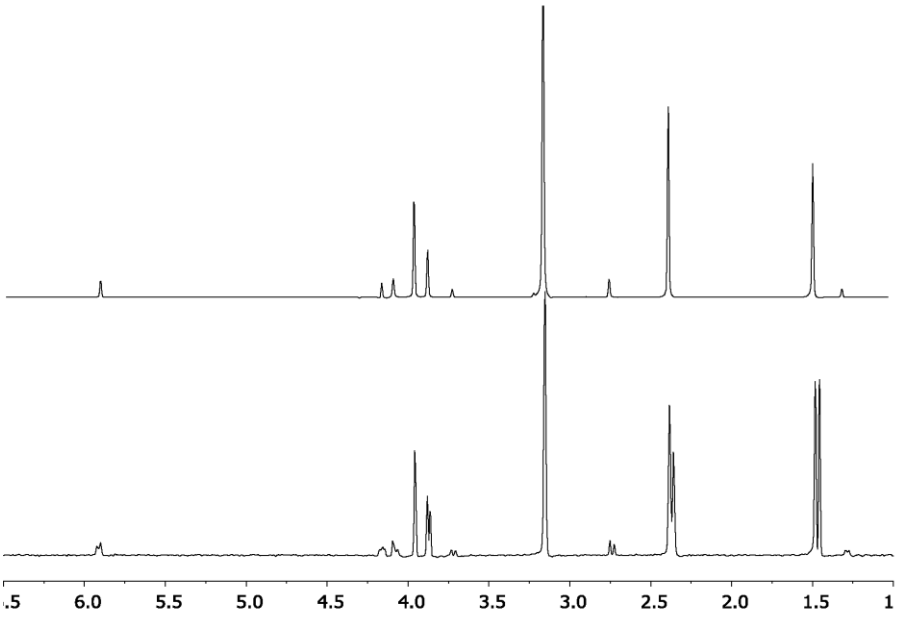

Figure S10: 1D rows extracted from the C14 frequency in (bottom) conventional HSQC-TOCSY and (top) GIC-psHSQC-TOCSY spectra shown in Fig. S9.

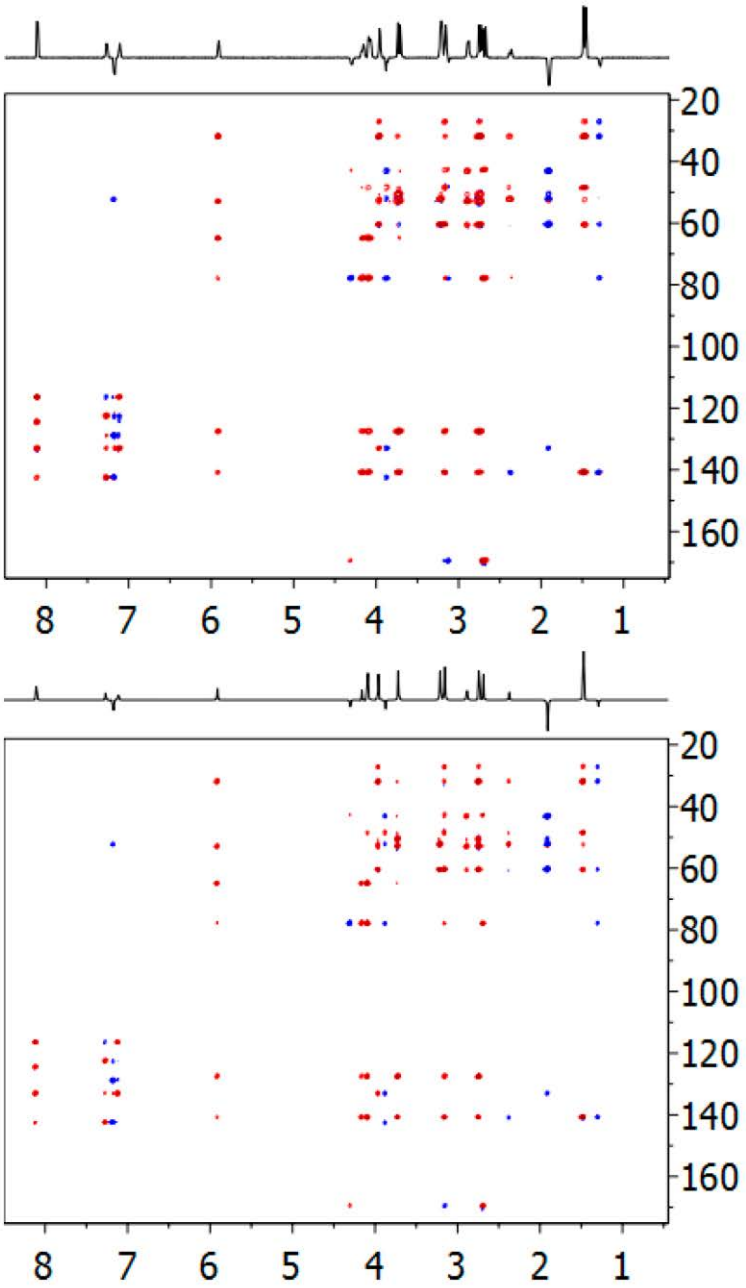

Figure S11: A) 2D HSQMBC and) 2D psGIC-HSQMBC spectra of strychnine.

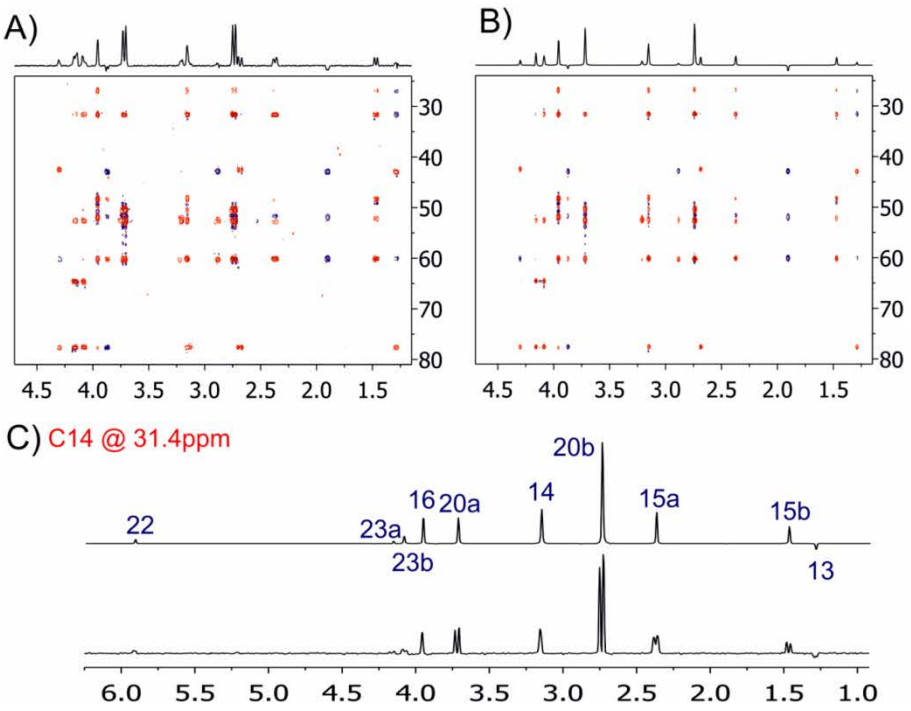

Figure S12: A) 2D HSQMBC-TOCSY and B) 2D psGIC-HSQMBC-TOCSY spectra of strychnine.

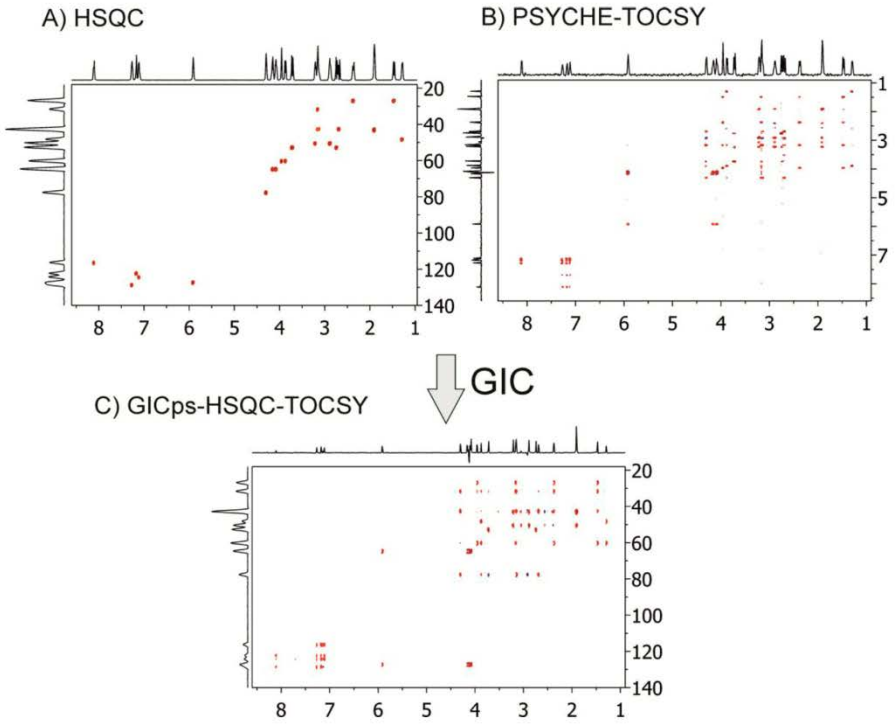

Figure S13: Alternative scheme to generate psGIC-HSC-TOCSY spectrum by combining a regular HSQC and a F1-homodecoupled TOCSY spectrum (PSYCHE-TOCSY).

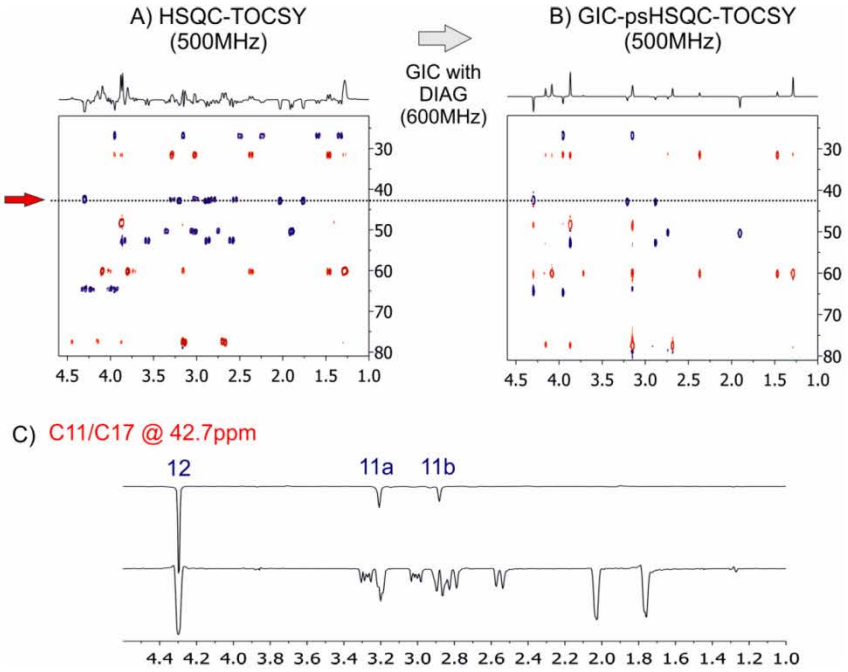

Figure S14. Universality of the psGIC approach. A) multiplicity-edited HSQC-TOCSY spectrum of **1** acquired in a 500 MHz spectrometer; B) pure shift version of the ME-HSQC-TOCSY after GIC processing with the DIAG spectrum of Fig. 1B recorded at a different magnetic field, at 600 MHz. Note that the chemical shift information is retained irrespective of the magnetic field strength and direct responses appearing as large doublets are removed

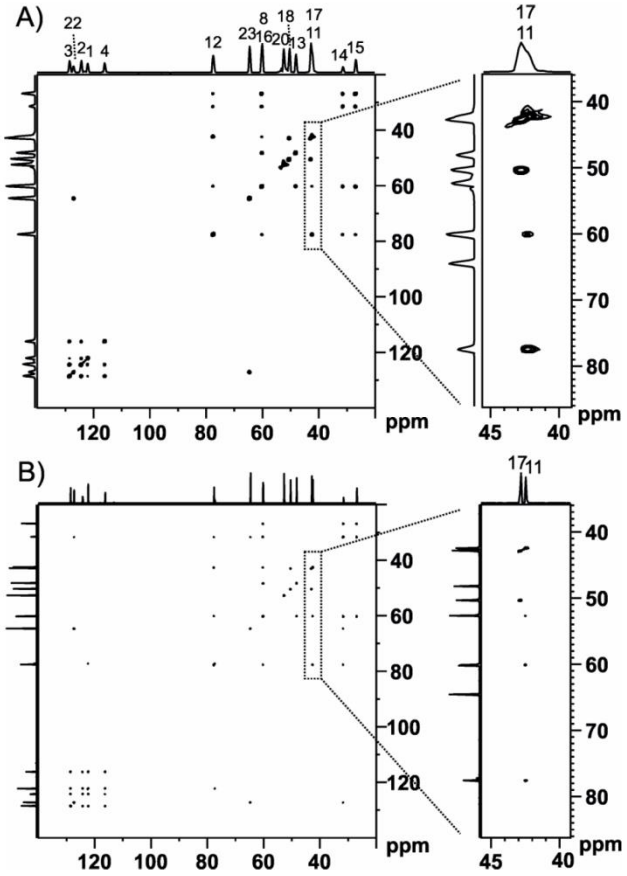

Figure S15. Effect of NUS acquisition in covariance NMR. ^{13}C-^{13}C correlation spectra of strychnine obtained after indirect covariance processing of A) a conventional 2D HSQC-TOCSY and B) a 25% NUS-enhanced HSQC-TOCSY spectrum.

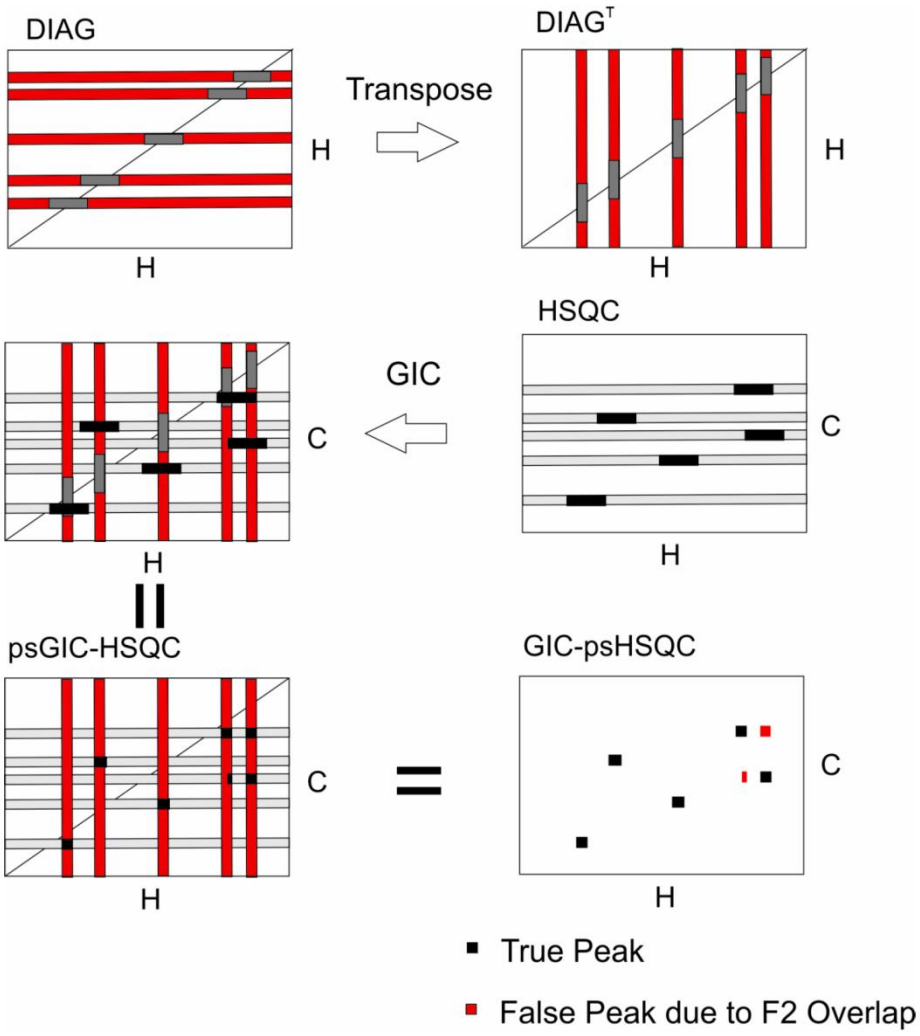

Figure S16: Graphical explanation on the generation of false correlations in psGIC spectra by signal overlap in the F2 dimension.

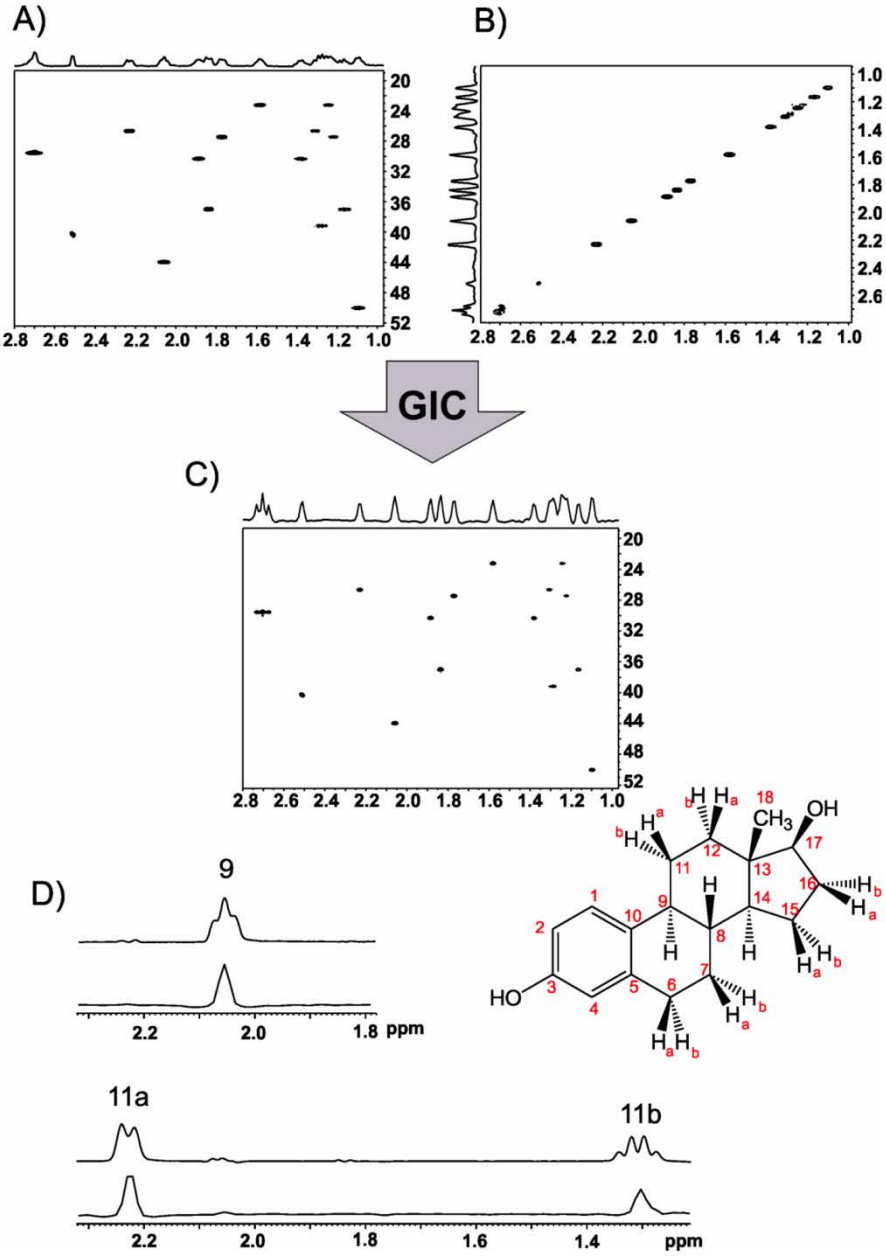

Figure S17: General scheme to obtain the psGIC-HSQC spectrum of estradiol (in C) is obtained after applying generalized unsymmetrical inverse covariance processing of non-uniform sampled (25%) A) conventional 2D HSQC-TOCSY and B) 2D F1-homodecoupled DIAG datasets. D) Comparison of selected 1D rows.

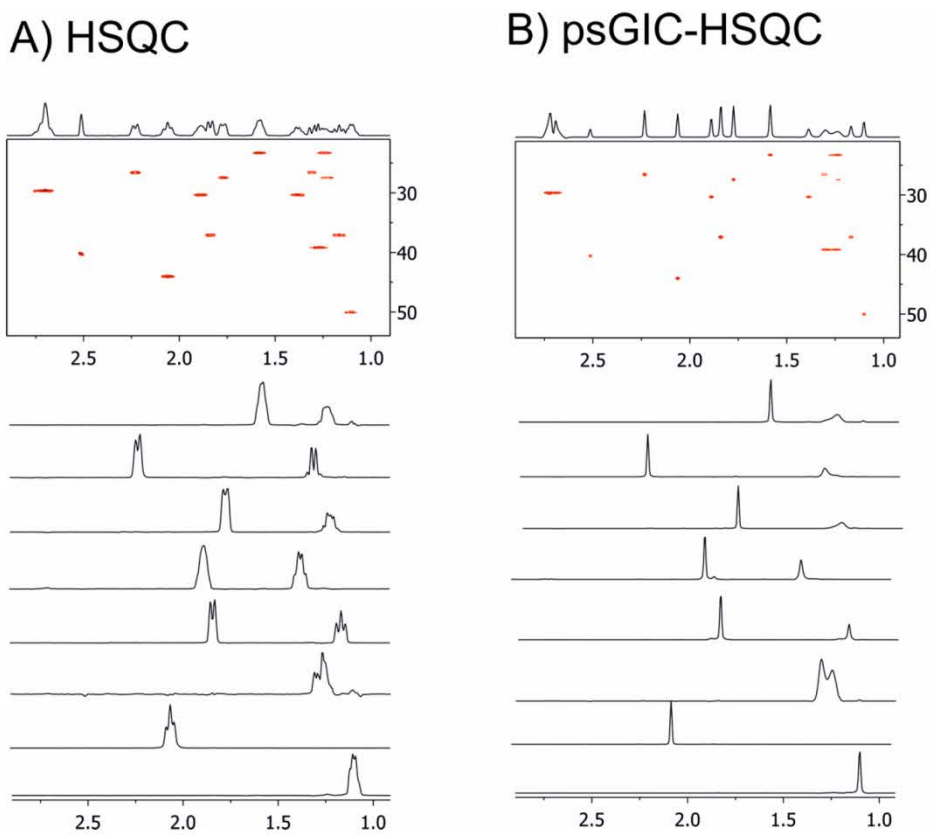

Figure S18: Practical visualization of the generation of false correlations in psGIC-HSQC spectrum of estradiol by signal overlap in the F2 dimension. B) psGIC-HSQC spectrum of estradiol generated from A) a regular HSQC and B) a cleanDIAG spectrum acquired with 256 t_1 increments and processed to 2K in F1.

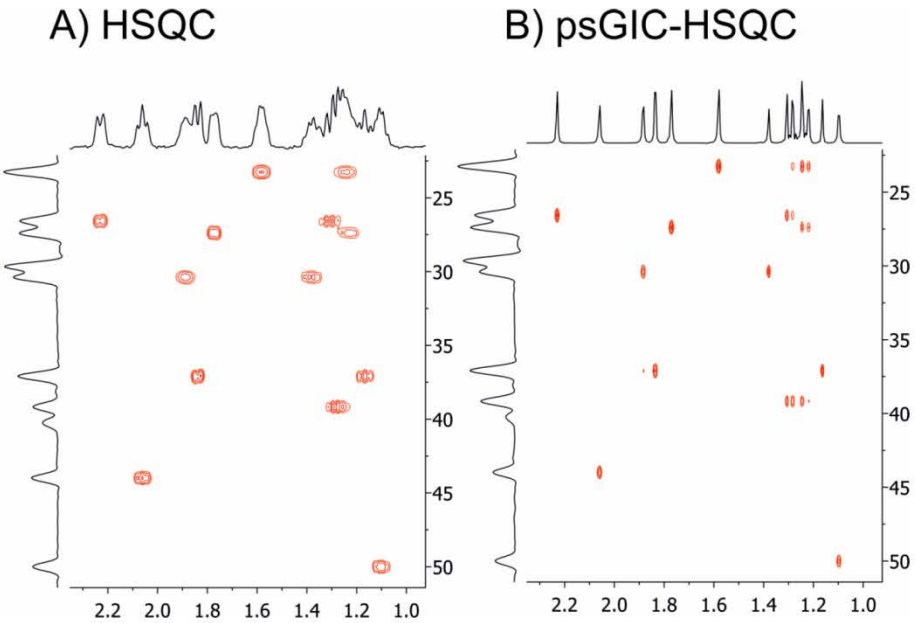

Figure S19: High-resolved psGIC-HSQC spectrum of estradiol generated from a regular HSQC and a 25% NUS-enhanced cleanDIAG spectrum acquired with 512 t1 increments.

PUBLICATION 2

Access to experimentally infeasible spectra by pure shift NMR covariance

André Fredi[a], Pau Nolis[a], Carlos Cobas[b], TeodorParella[a]

[a]Servei de RessonànciaMagnètica Nuclear, UniversitatAutònoma de Barcelona, Catalonia,

[b]MestrelabResearch, Santiago de Compostela, E-15706 A Coruña, Spain

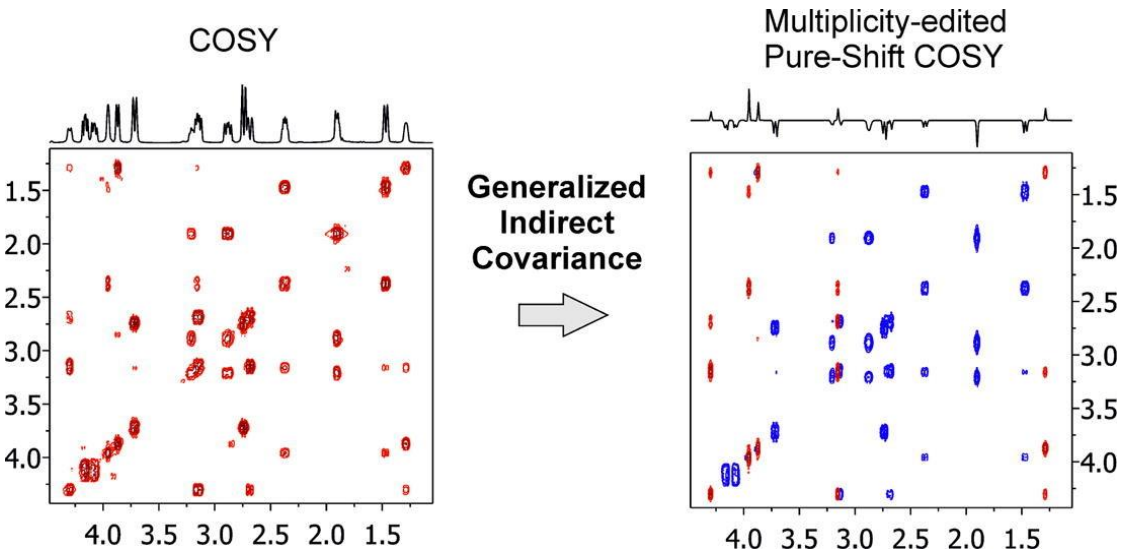

Introduction

The (ME) information is a valuable parameter because it allows the differentiation among CH/CH_3 and CH_2 groups from its relative signal phase. Therefore, this editing strategy reveals essential information for characterisation purposes. The experimental 2D ME-HSQC experiment is an excellent example showing how multiple NMR information in the form of direct $^{1}H–^{13}C$ connectivities and ME can be simultaneously extracted from a single NMR spectrum, simplifying spectral analysis and reducing the overall experimental time which should be needed to record separately the equivalent 2D HSQC and 1D DEPT135 spectra. ME is usually encoded along the F1 dimension, and the nature of cross-peaks are quickly identified as a function of their opposite up/down relative phases (CH/CH_3 peaks are phased up whereas CH_2 appear down).[80–83] Experimentally, ME encoding has also been integrated with alternative formats into different heteronuclear experiments such as ME-HSQC-TOCSY,[84] ME-HMBC,[85] ME-selHSQMBC[86] or ME-ADEQUATE[87] but, unfortunately, it can not be incorporated in other class of NMR experiments.

As a continuation of our psNMR Covariance strategy described above,[88] we report here the insertion of ME by GIC into some 2D spectra that are either impractical to acquire or cannot be acquired at all by available experimental pulses schemes. These principles are demonstrated by generating several reconstructed multiplicity-edited psNMR spectra of some very popular homonuclear and heteronuclear experiments.

Journal of Magnetic Resonance 270 (2016) 161–168

Contents lists available at ScienceDirect

Journal of Magnetic Resonance

journal homepage: www.elsevier.com/locate/jmr

Access to experimentally infeasible spectra by pure-shift NMR covariance

André Fredi [a], Pau Nolis [a], Carlos Cobas [b], Teodor Parella [a,*]

[a] Servei de Ressonància Magnètica Nuclear, Universitat Autònoma de Barcelona, E-08193 Bellaterra, Catalonia, Spain
[b] Mestrelab Research, Santiago de Compostela, E-15706 A Coruña, Spain

ARTICLE INFO

Article history:
Received 27 May 2016
Revised 14 July 2016
Accepted 21 July 2016
Available online 22 July 2016

Keywords:
Pure shift NMR
Covariance NMR
Multiplicity-edited COSY
Multiplicity-edited TOCSY
Multiplicity-edited HMBC

ABSTRACT

Covariance processing is a versatile processing tool to generate synthetic NMR spectral representations without the need to acquire time-consuming experimental datasets. Here we show that even experimentally prohibited NMR spectra can be reconstructed by introducing key features of a reference 1D CH_n-edited spectrum into standard 2D spectra. This general procedure is illustrated with the calculation of experimentally infeasible multiplicity-edited pure-shift NMR spectra of some very popular homonuclear (ME-psCOSY and ME-psTOCSY) and heteronuclear (ME-psHSQC-TOCSY and ME-psHMBC) experiments.

1. Introduction

The power of the NMR spectroscopy strongly relies on its versatility to design NMR pulse sequences that provide useful structural information in a wide variety of molecules and sample conditions. Nowadays, a large number of different NMR experiments are available to be used in a routine and fully automated mode. Besides the increased difficulty of continually creating new pulse schemes, the development and application of all these tools in real samples always involves time-consuming data acquisition and therefore the use of expensive NMR spectrometer time. Data processing is another important area in NMR spectroscopy that is strongly correlated with data analysis. In particular, covariance processing has proven to be a fascinating mathematic treatment to generate novel synthetic NMR spectral representations of small molecules by combining together the features of different spectra in a fast, versatile and cheap spectrometer-free way [1–3], as recently reviewed by Jaeger and Aspers in a very comprehensive manner [4]. As an example, an hyphenated 2D HSQC-COSY spectrum can be synthetically generated by *Generalized Indirect Covariance* (GIC) coprocessing between standard HSQC and COSY spectra [5–6]. Similar economized strategies have also been reported for equivalent HSQC-TOCSY [1,5,7–9], HMBC-TOCSY [10] or HSQC-NOESY [9,11] spectra, avoiding the need for additional acquisition times. Much more interesting, GIC also allows the reconstruction of spectra that should be very time-consuming or even impossible for molecules at natural abundance, as reported for 2D ^{13}C–^{13}C correlation spectra achieved by combining the ^{13}C chemical information contained in two different heteronuclear experiments (HSQC + HMBC [12], HSQC + ADEQUATE [13–17] or HMBC-ADEQUATE [18,19]) or for extremely challenging ^{13}C–^{15}N correlations generated from ^{1}H–^{13}C and ^{1}H–^{15}N HMBC spectra [20–22]. Indeed, these latter ^{13}C–^{15}N experiments have been probed experimentally at natural abundance [23,24].

In the last years, important advances has been made in the field of pure shift NMR of small molecules that use modern broadband homodecoupled NMR pulses schemes [25–27]. The main limitations to design new experimental pure shift experiments with the current knowledge are well established and covariance processing has appeared as an effective complement to obtain pure shift NMR spectra without involving long acquisition times. Thus, indirect covariance has been reported to generate ultra high-resolved pure shift ^{1}H–^{1}H correlation spectra in both indirect F1 and direct F2 dimensions, by internally mapping the information extracted from the F1 dimension of F1-homodecoupled 2D COSY, TOCSY and NOESY spectra onto its F2 dimension [28–31]. In an extension of this *pure shift NMR covariance* concept, a novel general processing strategy has been developed to transfer exclusively the pure chemical shift information from an external reference spectrum to any 2D spectrum [32]. In this case, a reference F1-homodecoupled ^{1}H–^{1}H DIAG spectrum only showing diagonal

* Corresponding author.
E-mail address: teodor.parella@uab.cat (T. Parella).

http://dx.doi.org/10.1016/j.jmr.2016.07.010
1090-7807/

cross-peaks is experimentally recorded as a first step or, in a more efficient way, it can be reconstructed from a 1D pure shift NMR spectrum. Then, for instance, a pure shift HSQC (psHSQC) spectrum [33] can be synthetically generated from its conventional 2D HSQC counterpart and the pure shift DIAG spectrum using GIC. Similar reconstructions have been shown for other spectra that cannot be collected experimentally, such as psHSQC-TOCSY or psHSQMBC [32].

On the other hand, the $^{13}CH_n$ (n = 1–3) multiplicity-edited (ME) information is a valuable parameter that expedites both spectral analysis and assignments. 2D ME-HSQC is a nice example showing how multiple NMR information in form of direct $^{1}H–^{13}C$ connectivities and ME can be simultaneously extracted from a single NMR spectrum, simplifying spectral analysis and reducing the overall acquisition time which should be needed to record separately the equivalent 2D HSQC and 1D DEPT135 spectra. ME is implemented along the indirect F1(^{13}C) dimension and cross-peaks are quickly identified as a function of their opposite up/down relative phases (CH/CH_3 peaks are phased up whereas CH_2 appear down) [34–37]. ME encoding has also been integrated with alternative formats in other heteronuclear experiments such as ME-HSQC-TOCSY [38], ME-HMBC [39,40], ME-selHSQMBC [41] or ME-ADEQUATE [42] but, unfortunately, it has not been incorporated in other class of NMR experiments.

As a continuation of our pure shift NMR covariance strategy described recently [32], we report here the insertion of ME by GIC into a number of 2D spectra that are either impractical to acquire or cannot be acquired at all by available experimental pulses schemes. These principles are demonstrated by generating several reconstructed multiplicity-edited pure-shift NMR spectra of some very popular homonuclear and heteronuclear experiments.

2. Results and discussion

Fig. 1 summarizes the proposed strategy designed to achieve experimentally unfeasible ME pure shift NMR spectra using GIC. The first step is the quick generation of a reference 2D DIAG spectrum using an automatic algorithm implemented in Mnova v11.0 (make2D script) that will be used for GIC co-processing with a number of standard 2D spectra. The $^{1}H–^{1}H$ 2D pure shift ME-DIAG (ME-psDIAG) spectrum (Fig. 1B) is synthetically generated from the internal F2-projection 1D spectrum (Fig. 1A) of an experimental 2D ME-psHSQC spectrum recorded with BIRD-based homodecoupling during acquisition [33]. The main feature of this 1D ^{1}H spectrum is the removal of J(HH) splittings by collapsing coupling patterns to singlets (full homodecoupling), except for ^{2}J(HH) in diastereotopic CH_2 signals that will exhibit a doublet splitting (partial homodecoupling). These simplified multiplet patterns will be transferred together with the ME information to the final covariance calculated 2D spectra, referred to as pure shift throughout the manuscript (Fig. 1C and D). Tables 1 and 2 summarize types of novel homonuclear and heteronuclear spectra that could be generated with the suggested proposal.

GIC represents a valuable tool to incorporate ME in standard homonuclear 2D spectra, providing novel spectral representations that have never been realized experimentally. The results after applying GIC with two standard spectra such as a magnitude-mode 2D COSY and a phase-sensitive 2D TOCSY are presented. It is very interesting that ME encoding represented with the characteristic up/down relative phase can be incorporated in spectra that it is normally mandatory to magnitude calculate because due to their mixed phase properties, as is the case of standard COSY-like spectra. The calculated ME-psCOSY spectrum (Fig. 2C) would seem

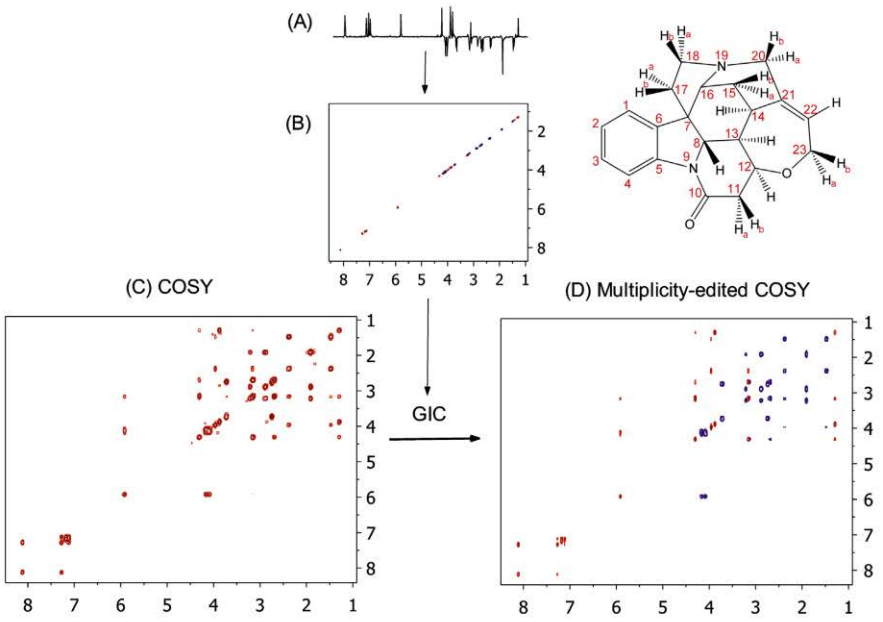

Fig. 1. Experimental procedure to simultaneously incorporate multiplicity editing (ME) and pure shift attributes into a conventional 2D spectrum using Generalized Indirect Covariance (GIC). (A) 1D ME-ps ^{1}H spectrum of strychnine (**1**) in $CDCl_3$; (B) synthetic 2D $^{1}H–^{1}H$ ME-psDIAG spectrum generated from (A) using the make2D program; (C) experimental magnitude-mode 2D COSY spectrum acquired under routine conditions; (D) reconstructed 2D ME-psCOSY spectrum after GIC co-processing between spectra B and C. In practical terms the process can be understood as the transmission of the features contained in spectrum A or in the F1 dimension of spectrum B into the F2 dimension of spectrum C.

Table 1
Reconstructed homonuclear NMR spectra obtained after indirect covariance processing.

1st component spectrum	2nd component spectrum	Spectrum resulting from the component spectra after covariance processing	Observations
COSY	DIAG	**psCOSY**	[32]
TOCSY	DIAG	**psTOCSY**	[32]
NOESY	DIAG	**psNOESY**	[32]
COSY	ME-psDIAG	**ME-psCOSY**	
TOCSY	ME-psDIAG	**ME-psTOCSY**	

Table 2
Reconstructed heteronuclear NMR spectra obtained after indirect covariance processing.

1st component spectrum	2nd component spectrum	Spectrum resulting from the component spectra after covariance processing	Observations
HSQC-COSY	DIAG	**psHSQC-COSY**	[32]
HSQC-TOCSY	DIAG	**psHSQC-TOCSY**	[32]
HSQMBC	DIAG	**psHSQMBC**	[32]
HSQMBC-COSY	DIAG	**psHSQMBC-COSY**	[32]
HSQMBC-TOCSY	DIAG	**psHSQMBC-TOCSY**	[32]
ADEQUATE	DIAG	**psADEQUATE**	[32]
HSQC-COSY	ME-psDIAG	**ME-psHSQC-COSY**	ME in ^{1}H dimension
HSQC-TOCSY	ME-psDIAG	**ME-psHSQC-TOCSY**	ME in ^{1}H dimension
HMBC	ME-psDIAG	**ME-psHMBC**	ME in ^{1}H dimension
HMBC-COSY	ME-psDIAG	**ME-psHMBC-COSY**	ME in ^{1}H dimension
HMBC-TOCSY	ME-psDIAG	**ME-psHMBC-TOCSY**	ME in ^{1}H dimension
ADEQUATE	ME-psDIAG	**ME-psADEQUATE**	ME in ^{1}H dimension
HSQC	ME-psCOSY^T	**ME-psHSQC-COSY**	Also TOCSY versions
ME-HSQC	psCOSY^T	**ME-psHSQC-COSY**	Also TOCSY versions
ME-psHSQC	COSY	**ME-psHSQC-COSY**	Also TOCSY versions

T is the transposed matrix.

to be a hypothetical pure in-phase COSY spectrum represented in a phase-sensitive mode with the added bonus of both ME and pure-shift. Experimentally, a spectrum like this is highly challenging and currently it is unreachable. It is worth noting that all GIC processing described in this manuscript could also be performed from the non pure shift version of the ME-HSQC experiment, retaining only the ME information (Fig. 2B). As a novel feature of the reconstructed 2D ME-psCOSY vs the conventional COSY (Fig. 2C vs A), it is obvious that the simultaneous determination of ^{1}H–^{1}H J connectivities and CH_n multiplicity by simple visual inspection considerably simplifies both the direct analysis and interpretation. The recognition of spin subsystems can be quickly established from the analysis of F1 rows, as shown for the protons resonating at 1.28 ppm (H13 - Fig. 2D) and 2.37 ppm (H15a - Fig. 2E). The positive diagonal peak at 1.28 ppm (assigned as CH) shows three different cross peaks at 3.15 ppm (positive peak; CH), 3.87 ppm (positive peak; CH) and 4.30 ppm (positive peak; CH). This quickly assigns it as a CH (H13) proton surrounded by other three CH (H14, H8 and H12 respectively) groups. It might be worth noting for the instructional value that the intensity of the H8 correlation reflects the trans-diaxial relationship between H8 and H13. On the other hand, the diagonal H15a negative signal shows a negative cross-peak with its geminal H15b proton at 1.47 ppm as well as with the positive signals at 3.15 ppm (H14) and 3.95 ppm (H16), identifying a CH–CH_2–CH subspin system. In addition, the phase asymmetry between cross peaks also allows the identification of pairs of neighboring carbons. For instance, the above diagonal H22 (5.91 ppm)/H23a–b (4.17–4.07 ppm) cross peaks are negative whereas the opposite upper diagonal H23a–b/H22 cross peaks are positive, instantly confirming a CH–CH_2 spin group. The expansions shown in Fig. 2B and C also serve to discuss a fundamental aspect in the current GIC implementation, as already been described and detected as the current cons of the method in our previous work: the generation of artifacts by proton signal overlap, as clearly visualized with the two overlapped signals resonating at 3.15 ppm (H14) and 3.14 ppm (H11a). The cross-peak between 3.14(F2) ppm and 2.71(F1) ppm corresponding to the geminal H11a–H11b connectivity should be a negative doublet but appears as a mixed positive/negative phase due to the collapsing of the singlet corresponding to H14 with the left component of the doublet corresponding to H11a. Although the pure shift approach greatly improves signal resolution along the detected F2 dimension, this type of artefacts due to the unavoidable signal overlap remains to be solved [7–9,32]. Methods to detect and remove them are out of the scope of this work and will be presented elsewhere. Some interesting features of covariance processing is that the calculated GIC spectra are free in terms of spectrometer time, they are quickly generated after some seconds of calculation in a conventional personal computer and it might be analyzed together with the experimental spectrum in case of doubts.

The same features and conclusions could be extrapolated to any other homonuclear spectra. Thus, the complementary multiplicity-edited pure shift 2D TOCSY (ME-psTOCSY) spectrum of (**1**) (Fig. 3B) is readily available from the experimental phase-sensitive 2D TOCSY dataset (Fig. 3A). The analysis of the row corresponding to H15a (equivalent to Fig. 2E) affords new correlations with the positive H13 and H22 protons as well as with the negative H23a/b protons. For pulse sequence developers, designing pulse sequences capable of generating experimental spectra similar to ME-psCOSY and ME-psTOCSY would likely be quite difficult if not impossible. Further, even if such pulse sequences could be designed, they would probably be hampered by sensitivity losses due to ^{13}C editing and T_2 relaxation as well as of difficulties to have a careful control of J(HH) evolution to provide pure in–phase ^{1}H multiplets and pure chemical shift representation at the same time. Optionally, the high resolution available along the F2 dimension can be internally transferred

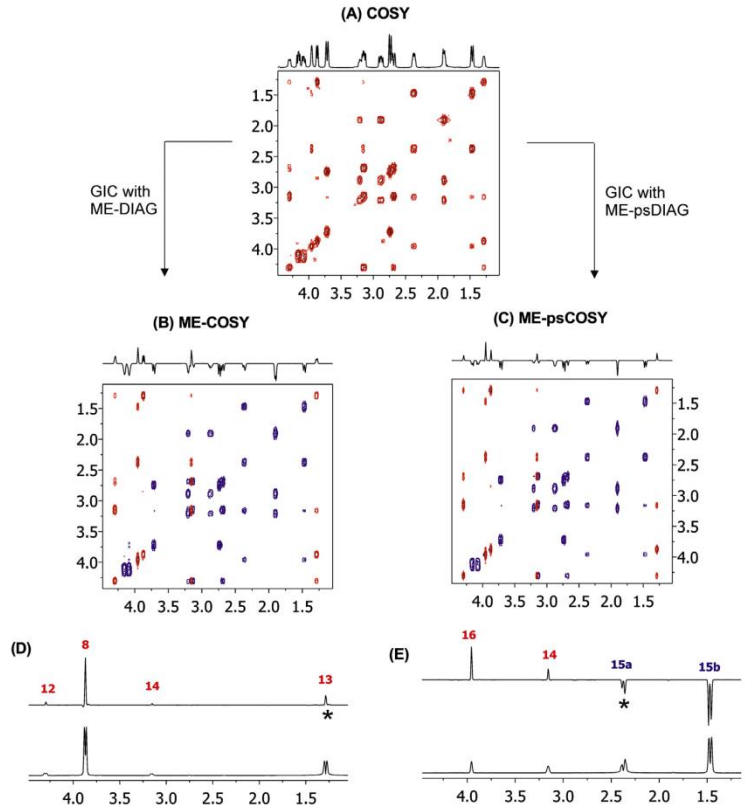

Fig. 2. Expanded areas of the (A) conventional magnitude-mode COSY and (B-C) reconstructed ME-COSY and ME-psCOSY spectra of strychnine, respectively, after GIC processing with the corresponding non pure shift and pure shift DIAG spectra. (D-E) Selected 1D rows extracted from spectra A (bottom) and C (top), respectively. The asterisk marks the diagonal peak. Positive phased resonances are plotted in red and negative phased in blue. (For interpretation of the references to color in this figure legend, the reader is referred to the web version of this article.)

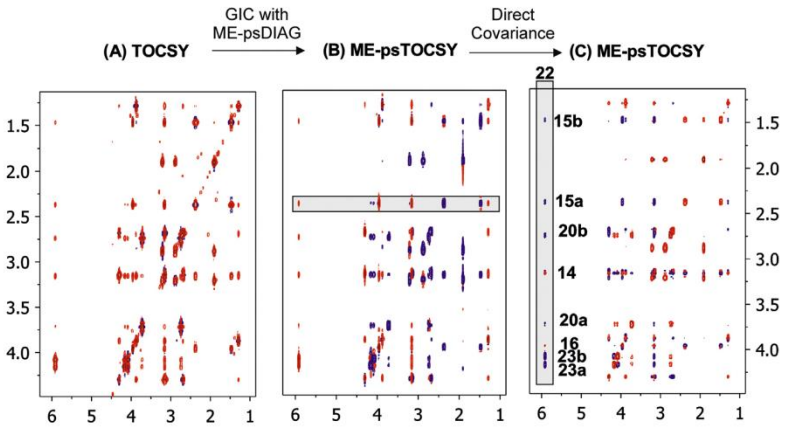

Fig. 3. (A) Conventional phase-sensitive TOCSY; (B) reconstructed ME-TOCSY spectra with pure shift character along F2 after GIC processing between spectrum (A) and the ME-psDIAG spectrum; (C) reconstructed ME-TOCSY spectra with pure shift features in both dimensions after applying direct covariance in (B).

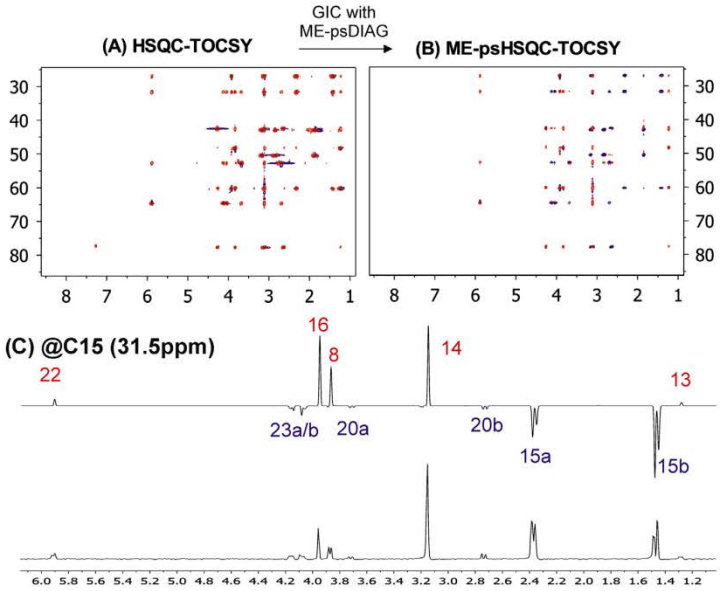

Fig. 4. (A) Conventional 2D HSQC-TOCSY and (B) reconstructed 2D ME-psHSQC-TOCSY spectra of strychnine obtained after GIC processing with the ME-psDIAG spectrum. (C) Comparison between the conventional vs the edited row extracted at the C15 chemical shift. Note that all CH appear up as singlets whereas negative CH_2 are doublets.

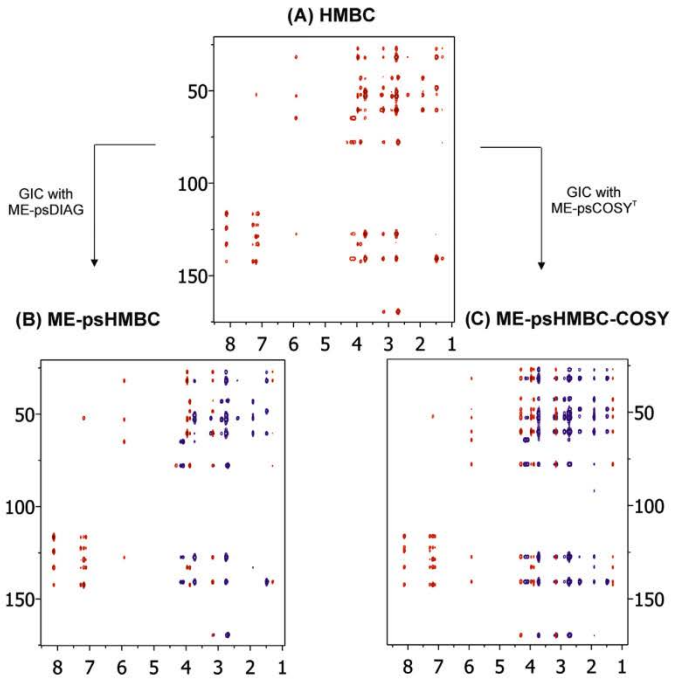

Fig. 5. (A) Magnitude-mode HMBC of strychnine; (B) MEpsHMBC reconstructed from the HME-DIAG; (C) reconstructed MEpsHMBC-COSY spectrum from the standard HMBC and the MEpsCOSY spectrum.

to the F1 dimension by a further direct covariance processing to achieve pure shift signals in both dimensions (Fig. 3C). Due to the peak phase asymmetry, the rows corresponding to diagonal CH signals are unaffected but those from CH_2 are re-inverted again and therefore column analysis should be more informative. Both reconstructed ME-psCOSY and ME-psTOCSY spectra are amenable for further GIC processing in order to generate new hyphenated experiments, similarly as previously described for conventional HSQC/COSY, HSQC/TOCSY, HSQC/NOESY, HMBC/TOCSY pairs... (see further discussion of Fig. 5C). On the other hand, although ME could be incorporated in 2D NOESY/ROESY spectra by GIC, the importance of the phase properties of cross-peaks in these spectra could render further analysis difficult and thus is not considered here.

Covariance processing not only shows great potential to generate some ME ^{1}H–^{13}C spectra that could be available experimentally but also to rebuild ME spectra that have never reported or are really complicated to be designed with current techniques. One reported example of unrealistic NMR is the reconstruction of a ME-HSQC-COSY spectrum from the standard ME-HSQC and COSY spectra [6]. An equivalent ME-HSQC-COSY showing clean up/down phase pattern for COSY cross-peaks would be difficult to achieve experimentally due to their resulting mixed phases. On the other hand, ME-psHSQC is currently the only existing experiment that can include ME and pure shift features in a unique spectrum [33], but we use here it as a reference spectrum for GIC processing and therefore it will not be discussed how to get it synthetically. Pulse sequences to record multiplicity-edited versions of other heteronuclear experiments like HSQC-TOCSY [38], HMBC/HSQMBC [39–41] or ADEQUATE [42] have also been reported, where ME was always incorporated along the indirect F1(^{13}C) dimension, although pure shift versions have never been elaborated.

Fig. 4 shows the ME-psHSQC-TOCSY spectrum obtained from GIC processing between the standard HSQC-TOCSY and ME-psDIAG spectra. As a difference with the experimental ME-HSQC-TOCSY spectrum, ME is implemented along the F2(^{1}H) dimension and therefore the useful ME information is extracted from row analysis instead of column analysis. Alternatively, ME could also be incorporated along the F1(^{13}C) dimension combining the transpose spectrum of the standard HSQC-TOCSY and a ^{13}C–^{13}C ME-DIAG (CME-DIAG) spectrum generated from a 1D DEPT-135 spectrum or the F1 internal projection of a 2D ME-HSQC spectrum (data not shown). Both methods would afford complementary spectra but with different phase properties and this could be used to detect artifacts or signal phase distortions due to severe signal overlap. In addition to the useful mixing between HSQC-TOCSY + DIAG, comparable ME-psHSQC-TOCSY spectra could also be obtained by other feasible GIC combinations: (i) HSQC and ME-psTOCSY^{T} (T is the transposed matrix); (ii) psHSQC and ME-TOCSY^{T}, (iii) ME-HSQC with psTOCSY^{T} or (iv) ME-psHSQC and TOCSY.

Similarly to the above COSY description, the standard HMBC experiment is usually processed in a magnitude mode due to the unavoidable JHH evolution during the involved long delays that generates complex mixed phases in all cross-peaks. Recently, a pure in-phase version of the HSQMBC experiment (PIP-HSQMBC) has been proposed,[43] but the different in-phase positive/negative character in cross-peak phases due to J(HH) evolution during INEPT periods precludes the experimental implementation of ME. On the other hand, ME has been implemented in two versions of the HMBC experiment: (i) using differential spectroscopy to generate two separate C/CH_2 vs CH/CH_3 subspectra [39,40] and (ii) by the up/down approach in ^{1}H-selective HSQMBC versions [41]. Fig. 5B shows the exciting ME-psHMBC spectrum reconstructed by GIC from the standard magnitude-mode HMBC and ME-psDIAG spectra. Row analysis allows trace out simultaneously long-range ^{1}H–^{13}C connectivities and the CH_n multiplicity of a selected ^{1}H signal. Comparable results should be obtained in other heteronuclear experiments, like the 1,1-ADEQUATE experiment where the resulting ME-psADEQUATE spectrum would display instantly two-bond ^{1}H–^{13}C connectivities and ME (data not shown). In this case, pure shift [44] and ME [42] have been individually introduced on experimental sequences but not together. Pure-shift ADEQUATE experiments have recently been reported demonstrating its usefulness for structural characterization of proton-deficient natural products [44,45], showing partial homodecoupling between neighboring protonated carbons but offering full homodecoupling for non-protonated carbons in 1,1-version and for all cross-peaks in 1,*n*-versions.

The proposed covariance method is amenable to future improvements and it can be easily adapted to novel experiments and developments. For instance, ME-ps ^{1}H–^{1}H [46] and ^{13}C–^{13}C [12–19] correlations can be generated by direct and indirect covariance, respectively, of any reported heteronuclear spectrum. On the other hand, the reconstructed ME-psCOSY and ME-psTOCSY spectra can be considered for further covariance processing to generate interesting hyphenated correlations. As an example, a ME-psHMBC-COSY spectrum can be reconstructed by GIC between the standard HMBC and the transposed ME-psCOSY spectra (Fig. 5C), giving a major number of correlations that can be useful to observe missing two-bond correlations in the original HMBC spectrum or to detect very long-range correlations up to four- and five bonds away. Similar strategies should be applicable for HMBC-TOCSY like experiments [47] or for experiments not yet described such as ADEQUATE-COSY or ADEQUATE-TOCSY spectra.

As discussed in Ref. [32], signal overlap remains the key problem to solve in order to minimize/avoid the number of possible artifacts generated by covariance co-processing [7–9]. The number of artifacts strongly depends on the levels of signal resolution along the F2/F1 dimensions. In the near future, the concerted use of non-uniform sampling (NUS) [48] and homodecoupling techniques to acquire ultra high-resolution experimental datasets will offer optimum conditions to maximize both signal and digital resolution per spectrometer time and this will contribute to minimize the presence of artifacts or phase distortions in the reconstructed spectra.

3. Conclusions

In summary, a simple and efficient covariance processing task opens new perspectives to reconstruct novel NMR spectra from standard experimental datasets. It has been shown that GIC processing (i) can convert an existing 2D spectrum to its pure shift version, (ii) can introduce new information ($^{13}CH_n$ multiplicity) in standard spectra in the form of up/down relative phase, and (iii) can generate new "synthetic" spectra, even for currently impossible experiments, incorporating pure-shift and ME features. Examples have been provided for a wide range of high-rich content NMR spectra as demonstrated for multiplicity-edited pure shift versions of some relevant experiments like COSY, TOCSY, HSQC-TOCSY and HMBC. These reconstructed GIC spectra can offer a significant added value in spectral analysis and structural characterization of small molecules, and they must be used as complements to experimental spectra in cases of doubts or, as a major current challenge, to identify accidental artefacts due to ^{1}H signal overlap. We are working on further refinements of the reported GIC processes to automatically detect and remove such artefacts as well as on improved developments that will expand the utilization of GIC.

4. Methods and materials

Generalized Indirect Covariance processing ($\lambda = 1$) was performed using the module implemented into Mnova. The *make2D*

macro creates a symmetric diagonal spectrum (DIAG) by first deconvolving the 1D ME-ps ^{1}H NMR spectrum via GSD followed by the synthesis of the 2D ME-psDIAG spectrum using 2D-Gaussian lineshapes. These 2D diagonal peaks have identical line widths along both dimensions based on the values derived from the deconvolution of the 1D spectrum. In order to keep memory requirements and computation times manageable, a maximum size of 4 K × 4 K DIAG matrix is employed. The *make2D* macro is available for Mnova (http://mestrelab.com).

All experimental NMR datasets were recorded at 298 K on a BRUKER DRX-600 spectrometer equipped with a 3-channel 5-mm TXI probe incorporating a z-gradient coil. The test sample was 20 mg of strychnine (**1**) in 0.6 ml of $CDCl_3$. Two-dimensional COSY, TOCSY, HSQC, HSQC-TOCSY and HMBC experiments were acquired and processed under conventional routine conditions, and no special requirements were needed for GIC processing. The 1D ME-ps ^{1}H NMR spectrum was obtained from the internal F2 projection of a 2D ^{1}H–^{13}C pure shift ME-HSQC spectrum, as described in Ref. [33]. The only important requirement was a good resolution in the acquisition ^{1}H dimension because the number of t_1 increments is not critical. We used a recycle delay of 1 s interpulse INEPT delay optimized to 140 Hz. 2 scans were collected per t_1 increment and the total experimental time was of 20 min. ^{1}H and ^{13}C spectral widths were of 6009 Hz (10.01 ppm) and 28,673 Hz (190.0 ppm), respectively. 256 t_1 increments were collected, with 2048 data points in each t_1 increment. Prior to Fourier-transformation, zero-filling and linear prediction in the F1 dimension and a squared sine-square apodization phase-shifted 90° in both dimensions were applied to obtain a 2 K ∗ 2 K resolution matrix.

Acknowledgments

Financial support for this research provided by MINECO – Spain (project CTQ2015-64436-P) is gratefully acknowledged. A.F. thanks CNPq-Brazil for a scholarship. We also thank the Servei de Ressonància Magnètica Nuclear, Universitat Autònoma de Barcelona, for allocating instrument time to this project.

References

[1] F. Zhang, R. Brüschweiler, Indirect covariance NMR spectroscopy, J. Am. Chem. Soc. 126 (2004) 13180–13181, http://dx.doi.org/10.1021/ja047241h.
[2] N. Trbovic, S. Smirnov, F. Zhang, R. Brüschweiler, Covariance NMR spectroscopy by singular value decomposition, J. Magn. Reson. 171 (2004) 277–283, http://dx.doi.org/10.1016/j.jmr.2004.08.007.
[3] Y. Chen, F. Zhang, W. Bermel, R. Brüschweiler, Enhanced covariance spectroscopy from minimal datasets, J. Am. Chem. Soc. 128 (2006) 15564–15565, http://dx.doi.org/10.1021/ja065522e.
[4] M. Jaeger, R.L.E.G. Aspers, Covariance NMR and small molecule applications, Ann. Rep. NMR Spectrosc. 83 (2014) 272–360, http://dx.doi.org/10.1016/B978-0-12-800183-7.00005-8.
[5] K.A. Blinov, N.I. Larin, A.J. Williams, K.A. Mills, G.E. Martin, Unsymmetrical covariance processing of COSY or TOCSY and HSQC NMR data to obtain the equivalent of HSQC-COSY or HSQC-TOCSY spectra, J. Heterocycl. Chem. 43 (2006) 163–166, http://dx.doi.org/10.1002/jhet.5570430124.
[6] G.E. Martin, B.D. Hilton, P.A. Irish, K.A. Blinov, A.J. Williams, Using unsymmetrical indirect covariance processing to calculate GHSQC-COSY spectra, J. Nat. Prod. 70 (2007) 1393–1396, http://dx.doi.org/10.1021/np070221j.
[7] K.A. Blinov, N.I. Larin, M.P. Kvasha, A. Moser, A.J. Williams, G.E. Martin, Analysis and elimination of artifacts in indirect covariance NMR spectra via unsymmetrical processing, Magn. Reson. Chem. 43 (2005) 999–1007, http://dx.doi.org/10.1002/mrc.1674.
[8] G.E. Martin, B.D. Hilton, K.A. Blinov, A.J. Williams, Using indirect covariance spectra to identify artifact responses in unsymmetrical indirect covariance calculated spectra, Magn. Reson. Chem. 46 (2008) 138–143, http://dx.doi.org/10.1002/mrc.2141.
[9] R.L.E.G. Aspers, P.E.T.J. Geutjes, M. Honing, M. Jaeger, Using indirect covariance processing for structure elucidation of small molecules in cases of spectral crowding, Magn. Reson. Chem. 49 (2011) 425–436, http://dx.doi.org/10.1002/mrc.2766.
[10] D.A. Snyder, R. Brüschweiler, Generalized indirect covariance NMR formalism for establishment of multidimensional spin correlations, J. Phys. Chem. A 113 (2009) 12898–12903, http://dx.doi.org/10.1021/jp9070168.
[11] K.A. Blinov, A.J. Williams, B.D. Hilton, P.A. Irish, G.E. Martin, The use of unsymmetrical indirect covariance NMR methods to obtain the equivalent of HSQC-NOESY data, Magn. Reson. Chem. 45 (2007) 544–546, http://dx.doi.org/10.1002/mrc.1998.
[12] K.A. Blinov, N.I. Larin, A.J. Williams, M. Zell, G.E. Martin, Long-range carbon-carbon connectivity via unsymmetrical indirect covariance processing of HSQC and HMBC NMR data, Magn. Reson. Chem. 44 (2006) 107–109, http://dx.doi.org/10.1002/mrc.1766.
[13] G.E. Martin, B.D. Hilton, M.R. Willcott, K.A. Blinov, HSQC-ADEQUATE: an investigation of data requirements, Magn. Reson. Chem. 49 (2011) 350–357, http://dx.doi.org/10.1002/mrc.2757.
[14] G.E. Martin, B.D. Hilton, K.A. Blinov, HSQC-1,1-ADEQUATE and HSQC-1, n-ADEQUATE: enhanced methods for establishing adjacent and long-range 13C–13C connectivity networks, J. Nat. Prod. 74 (2011) 2400–2407, http://dx.doi.org/10.1021/np200540q.
[15] G.E. Martin, B.D. Hilton, M. Robert Willcott, K.A. Blinov, HSQC-1, n-ADEQUATE: a new approach to long-range 13C–13C correlation by covariance processing, Magn. Reson. Chem. 49 (2011) 641–647, http://dx.doi.org/10.1002/mrc.2793.
[16] G.E. Martin, K.A. Blinov, M. Reibarkh, R.T. Williamson, 1J(CC)-edited HSQC-1, n-ADEQUATE: a new paradigm for simultaneous direct and long-range carbon-carbon correlation, Magn. Reson. Chem. 50 (2012) 722–728, http://dx.doi.org/10.1002/mrc.3870.
[17] G.E. Martin, B.D. Hilton, K.A. Blinov, HSQC-ADEQUATE correlation: a new paradigm for establishing a molecular skeleton, Magn. Reson. Chem. 49 (2011) 248–252, http://dx.doi.org/10.1002/mrc.2743.
[18] G.E. Martin, R.T. Williamson, K.A. Blinov, C.G. Anklin, W. Bermel, HMBC-1,1-ADEQUATE via generalized indirect covariance: a high sensitivity alternative to n,1-ADEQUATE, Magn. Reson. Chem. 50 (2012) 691–695, http://dx.doi.org/10.1002/mrc.3863.
[19] G.E. Martin, K.A. Blinov, R.T. Williamson, HMBC-1, n-ADEQUATE spectra calculated from HMBC and 1, n-ADEQUATE spectra, Magn. Reson. Chem. 51 (2013) 299–307, http://dx.doi.org/10.1002/mrc.3946.
[20] G.E. Martin, B.D. Hilton, K.A. Blinov, A.J. Williams, (13)C-(15)N correlation via unsymmetrical indirect covariance NMR: application to vinblastine, J. Nat. Prod. 70 (2007) 1966–1970, http://dx.doi.org/10.1021/np070361t.
[21] G.E. Martin, P.A. Irish, B.D. Hilton, K.A. Blinov, A.J. Williams, Utilizing unsymmetrical indirect covariance processing to define (15)N-(13)C connectivity networks, Magn. Reson. Chem. 45 (2007) 624–627, http://dx.doi.org/10.1002/mrc.2029.
[22] G.E. Martin, B.D. Hilton, P.A. Irish, K.A. Blinov, A.J. Williams, Application of unsymmetrical indirect covariance NMR methods to the computation of the 13C-15 N HSQC-IMPEACH and 13C–15N HMBC-IMPEACH correlation spectra, Magn. Reson. Chem. 45 (2007) 883–888, http://dx.doi.org/10.1002/mrc.
[23] S. Cheatham, P. Gierth, W. Bermel, Ē. Kupče, HCNMBC – a pulse sequence for H–(C)–N Multiple Bond Correlations at natural isotopic abundance, J. Magn. Reson. 247 (2014) 38–41, http://dx.doi.org/10.1016/j.jmr.2014.07.011.
[24] S. Cheatham, M. Kline, Ē. Kupče, Exploiting natural abundance 13C–15N coupling as a method for identification of nitrogen heterocycles: practical use of the HCNMBC sequence, Magn. Reson. Chem. 53 (2015) 363–368, http://dx.doi.org/10.1002/mrc.4205.
[25] K. Zangger, Pure shift NMR, Prog. Nucl. Magn. Reson. Spectrosc. 86–87 (2015) 1–20, http://dx.doi.org/10.1016/j.pnmrs.2015.02.002.
[26] L. Castañar, T. Parella, Broadband (1) H homodecoupled NMR experiments: recent developments, methods and applications, Magn. Reson. Chem. 53 (2015) 399–426, http://dx.doi.org/10.1002/mrc.4238.
[27] R.W. Adams, Pure shift NMR spectroscopy, eMagRes 3 (2007) 295–310, http://dx.doi.org/10.1002/9780470034590.
[28] Y. Xia, G. Legge, K.Y. Jun, Y. Qi, H. Lee, X. Gao, IP-COSY, a totally in-phase and sensitive COSY experiment, Magn. Reson. Chem. 43 (2005) 372–379, http://dx.doi.org/10.1002/mrc.1558.
[29] J.A. Aguilar, A.A. Colbourne, J. Cassani, M. Nilsson, G.A. Morris, Decoupling two-dimensional NMR spectroscopy in both dimensions: pure shift NOESY and COSY, Angew. Chem. – Int. Ed. 51 (2012) 6460–6463, http://dx.doi.org/10.1002/anie.201108888.
[30] J.A. Aguilar, J. Cassani, M. Delbianco, R.W. Adams, M. Nilsson, G.A. Morris, Minimising research bottlenecks by decluttering NMR spectra, Chemistry 21 (2015) 6623–6630, http://dx.doi.org/10.1002/chem.201406283.
[31] M. Foroozandeh, R.W. Adams, M. Nilsson, G.A. Morris, Ultrahigh-resolution total correlation NMR spectroscopy, J. Am. Chem. Soc. 136 (2014) 11867–11869, http://dx.doi.org/10.1021/ja507201t.
[32] A. Fredi, P. Nolis, C. Cobas, G.E. Martin, T. Parella, Exploring the use of generalized indirect covariance to reconstruct pure shift NMR spectra: current pros and cons, J. Magn. Reson. 266 (2016) 16–22, http://dx.doi.org/10.1016/j.jmr.2016.03.003.
[33] L. Paudel, R.W. Adams, P. Király, J.A. Aguilar, M. Foroozandeh, M.J. Cliff, M. Nilsson, P. Sándor, G.A. Morris, Simultaneously enhancing spectral resolution and sensitivity in heteronuclear correlation NMR spectroscopy, Angew. Chem. – Int. Ed. 52 (2013) 11616–11619, http://dx.doi.org/10.1002/anie.201305709.
[34] A. Virgili, T. Parella, F. Sánchez-Ferrando, Improved sensitivity in gradient-based 1D and 2D multiplicity-edited HSQC experiments, J. Magn. Reson. 277 (1997) 274–277.
[35] R.D. Boyer, R. Johnson, K. Krishnamurthy, Compensation of refocusing inefficiency with synchronized inversion sweep (CRISIS) in multiplicity-edited HSQC, J. Magn. Reson. 165 (2003) 253–259, http://dx.doi.org/10.1016/j.jmr.2003.08.009.

[36] H. Hu, K. Krishnamurthy, Doubly compensated multiplicity-edited HSQC experiments utilizing broadband inversion pulses, Magn. Reson. Chem. 46 (2008) 683–689, http://dx.doi.org/10.1002/mrc.2221.
[37] P. Sakhaii, W. Bermel, A different approach to multiplicity-edited heteronuclear single quantum correlation spectroscopy, J. Magn. Reson. 259 (2015) 82–86, http://dx.doi.org/10.1016/j.jmr.2015.07.006.
[38] T. Parella, J. Belloc, F. Sánchez-Ferrando, A. Virgili, A general building block to introduce carbon multiplicity information into multi-dimensional HSQC-type experiments, J. Magn. Reson. 719 (1998) 715–719, http://dx.doi.org/10.1002/(SICI)1097-458X(199810)36:10<715::AID-OMR355>3.0.CO;2-T.
[39] N.T. Nyberg, O.W. Sørensen, Multiplicity-edited broadband HMBC NMR spectra, Magn. Reson. Chem. 44 (2006) 451–454, http://dx.doi.org/10.1002/mrc.1776.
[40] A.J. Benie, O.W. Sørensen, Improved multiplicity-editing of HMBC NMR spectra, Magn. Reson. Chem. 44 (2006) 739–743, http://dx.doi.org/10.1002/mrc.
[41] J. Saurí, E. Sistaré, R. Thomas Williamson, G.E. Martin, T. Parella, Implementing multiplicity editing in selective HSQMBC experiments, J. Magn. Reson. 252 (2015) 170–175, http://dx.doi.org/10.1016/j.jmr.2015.01.006.
[42] T. Parella, F. Sánchez-Ferrando, Improved multiplicity-edited ADEQUATE experiments, J. Magn. Reson. 166 (2004) 123–128, http://dx.doi.org/10.1016/j.jmr.2003.10.010.
[43] L. Castañar, J. Saurí, R.T. Williamson, A. Virgili, T. Parella, Pure in-phase heteronuclear correlation NMR experiments, Angew. Chem. Int. Ed. Engl. 53 (2014) 8379–8382, http://dx.doi.org/10.1002/anie.201404136.
[44] J. Saurí, W. Bermel, A.V. Buevich, E.C. Sherer, L.A. Joyce, M.H.M. Sharaf, P.L. Schiff Jr., T. Parella, R.T. Williamson, G.E. Martin, Homodecoupled 1,1- and 1, n-ADEQUATE: pivotal NMR experiments for the structure revision of cryptospirolepine, Angew. Chem. Int. Ed. 54 (2015) 10160–10164, http://dx.doi.org/10.1002/anie.201502540.
[45] C. Lorenc, J. Saurí, A. Moser, A.V. Buevich, A.J. Williams, R.T. Williamson, G.E. Martin, M.W. Peczuh, Turning spiroketals inside out: a rearrangement triggered by an enol ether epoxidation, Chem. Open 4 (2015) 577–580, http://dx.doi.org/10.1002/open.201500122.
[46] W. Schoefberger, V. Smrecki, D. Vikic-Topic, N. Mueller, Homonuclear long-range correlation spectra from HMBC experiments by covariance processing, Magn. Reson. Chem. 45 (2007) 583–589, http://dx.doi.org/10.1002/mrc.2013.
[47] J. Saurí, N. Marcó, R.T. Williamson, G.E. Martin, T. Parella, Extending long-range heteronuclear NMR connectivities by HSQMBC-COSY and HSQMBC-TOCSY experiment, J. Magn. Reson. 258 (2015) 25–32, http://dx.doi.org/10.1016/j.jmr.2015.06.004.
[48] V.Y. Orekhov, V.A. Jaravine, Analysis of non-uniformly sampled spectra with multi-dimensional decomposition, Prog. Nucl. Magn. Reson. Spectrosc. 59 (2011) 271–292, http://dx.doi.org/10.1016/j.pnmrs.2011.02.002.

PUBLICATION 3

Accurate measurement of J_{HH} in overlapped signals by TOCSY–edited SERF Experiment

André Fredi, Pau Nolis, Teodor Parella

Servei de RessonànciaMagnètica Nuclear, UniversitatAutònoma de Barcelona, Catalonia,

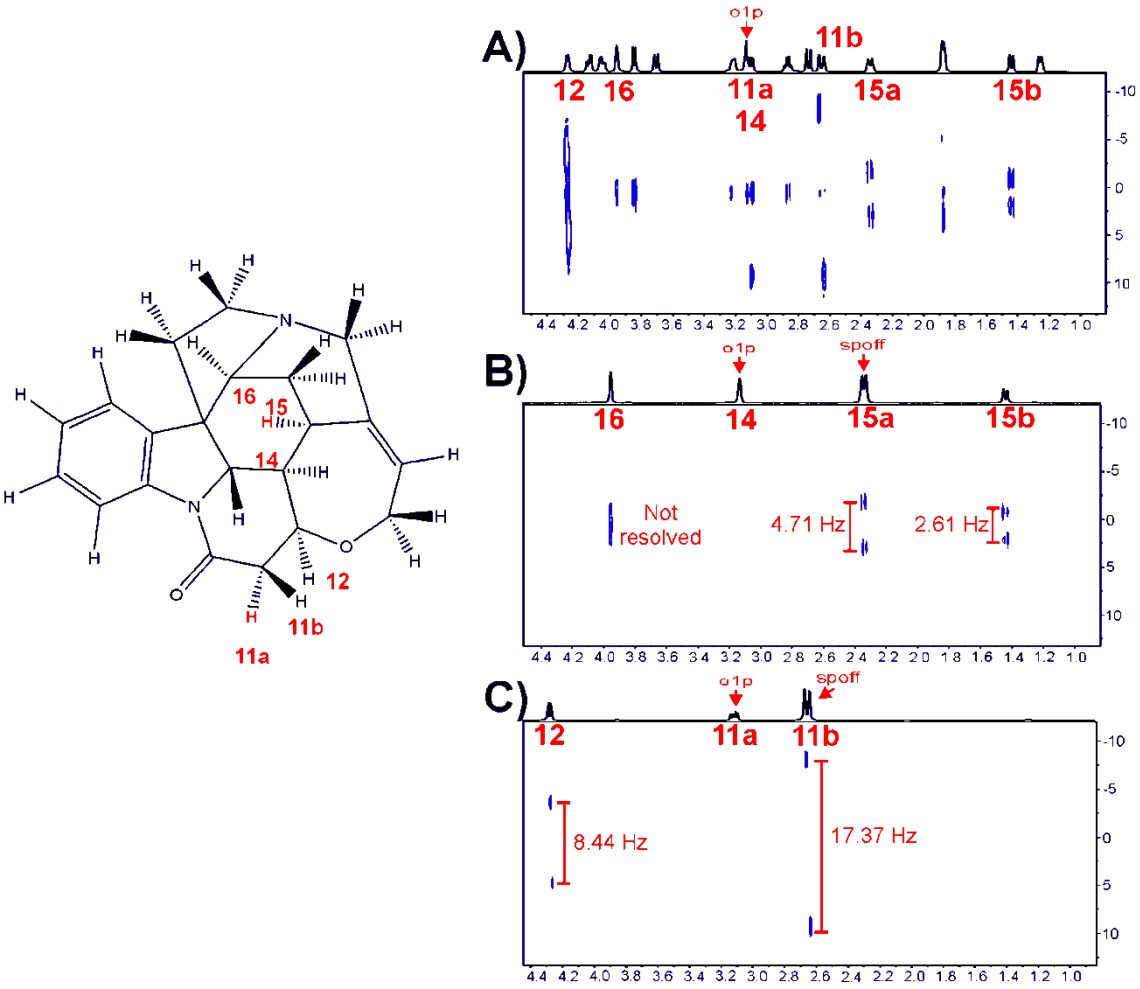

Introduction

The analysis of multiplet *J* patterns in ^{1}H NMR spectra usually affords the extraction of J_{HH} values. However, such determinations are often limited by the presence of overlapped signals hidden in overcrowded areas. A typical strategy is to record alternative NMR experiments that simplify the appearance of ^{1}H multiplets in a different format. For instance, the 2D *J*-res experiment[38] offers a user-friendly representation where *J* multiplets are spread out along the F1 dimension, independent of their chemical shifts.

The SERF pulse scheme is based on the excitation of a passive spin followed by a doubly-selective echo where the two selected protons (the same passive spin and a second active spin) are both selectively inverted at the middle of a variable echo period. The result is a characteristic *J*-res spectrum displaying only the J_{HH} coupling between the active and the passive protons in the form of a clean doublet along F1 and at the chemical shift of the passive spin in F2. The SERF experiment was improved with an improved gradient-encoded version (the G-SERF experiment)[75] that allows the measurement of all J_{HH} for a selected proton in a single *J*-res spectrum.

On the other hand, the TOCSY experiment[3,89] is a very efficient editing tool to select exclusively those proton signals belonging to the same *J* spin network. In small molecules, from a practical point of view and when possible, TOCSY is best performed in a selective 1D mode (referred to as selTOCSY), affording high-quality and clean 1D spectra of specific spin systems in short experimental times.[90]

Selective G-SERF or the new PSYCHEDELIC experiments only work for isolated signals on which frequency-selective excitation can be successfully applied. These experiments were initially designed to determine all J_{HH} for a selected proton resonance. However, they fail for overlapped signals. A doubly-selective TOCSY-GSERF scheme is here developed for the measurement of J_{HH} in protons resonating in crowded regions. This new experiment takes advantage of the editing features of an initial TOCSY transfer to uncover hidden resonances that become accessible to perform the subsequent frequency-selective refocusing.

Research article

MRC

Received: 29 November 2016 Revised: 22 December 2016 Accepted: 23 December 2016 Published online in Wiley Online Library: 20 February 2017

(wileyonlinelibrary.com) DOI 10.1002/mrc.4572

Accurate measurement of J_{HH} in overlapped signals by a TOCSY-edited SERF Experiment

André Fredi, Pau Nolis* and Teodor Parella*

Selective refocusing (GSERF or the recent PSYCHEDELIC) experiments were originally designed to determine all proton–proton coupling constants (J_{HH}) for a selected proton resonance. They work for isolated signals on which selective excitation can be successfully applied but, as it happens in other selective experiments, fail for overlapped signals. To circumvent this limitation, a doubly-selective TOCSY-GSERF scheme is presented for the measurement of J_{HH} in protons resonating in crowded regions. This new experiment takes advantage of the editing features of an initial TOCSY transfer to uncover hidden resonances that become accessible to perform the subsequent frequency-selective refocusing.

Keywords: proton–proton coupling constants; *J*-resolved; GSERF; selective TOCSY; PSYCHE; PSYCHEDELIC

Introduction

The measurement of proton–proton coupling constants J_{HH} is usually performed by a simple analysis of multiplet *J* patterns in conventional ^{1}H NMR spectra. However, such determinations are often limited by the presence of overlapped signals hidden in overcrowded areas. A typical strategy is to record alternative NMR experiments that simplify the appearance of ^{1}H multiplets in a different format. For instance, the popular 2D *J*-resolved experiment[1] offers a user-friendly representation where *J* multiplets are spread out along the indirect dimension, independent of their chemical shifts. On the other hand, the TOCSY experiment[2] is a very efficient editing tool to select exclusively those proton signals belonging to the same *J* spin network. In small molecules, from a practical point of view and when possible, TOCSY is best performed in a selective 1D mode (referred to as selTOCSY), affording high-quality and clean 1D spectra of specific spin systems in short acquisition times.[3] Nowadays, the selTOCSY experiment is an essential and indispensable NMR tool for chemists to disentangling and assign ^{1}H multiplets typically found in overcrowded areas. The only practical requirement for the success of selTOCSY is to have an isolated proton signal to be initially selected and from which the magnetization will be transferred to other neighboring protons within the same *J* network.

These methods afford clean multiplets for an efficient analysis but not assign specific J_{HH} values. Other NMR methods are available to determine and assign J_{HH} in an unambiguous way, of which we should highlight the selective refocusing (SERF) experiment,[4] which was originally designed to obtain exclusively the J_{HH} between two specific *J*-coupled protons. The SERF pulse scheme is based on the excitation of a passive spin followed by a doubly-selective echo where the two selected protons (the same passive spin and a second active spin) are both selectively inverted at the middle of a variable echo period. The result is a characteristic *J*-resolved spectrum displaying only the J_{HH} coupling between the active and the passive protons in the form of a clean doublet along F1 and at the chemical shift of the passive spin in F2. The SERF experiment was improved with a more complete gradient-encoded version (the GSERF experiment)[5] that allows the measurement of all J_{HH} for a selected proton in a single *J*-resolved spectrum. GSERF incorporates the concept of spatially-encoded slice-selective (SS) excitation/refocusing, when each proton signal in the ^{1}H spectrum is selectively excited and/or refocused in a particular z-slice of the NMR tube. Experimentally, this is performed by applying simultaneously a selective 90° or 180° ^{1}H pulse together with a weak pulsed field gradient. Obviously, the major drawback of GSERF is the severe penalty in sensitivity due to the slice selection procedure but the interest lies in the obtention of a nice spectral *J*-resolved representation where the extraction of J_{HH} is simply and accurately performed by measuring doublets along the high-resolved F1 dimension. In the last years, a number of new GSERF variants have been developed,[6–9] including approaches to improve its low sensitivity,[6] the incorporation of broadband homodecoupling capabilities in the F2 dimension to simplify multiplet patterns to singlets,[6] the design of related 1D versions using real-time homodecoupling techniques,[7,6] the determination of J_{HH} between equivalent protons in symmetrical molecules,[8] or the extension in the measurement of heteronuclear ^{1}H–^{19}F couplings.[9]

Another serious inconvenience of GSERF is the need that the active proton to be monitored must be sufficiently isolated in the ^{1}H spectrum for a reliable frequency-selective perturbation. Here, we propose a modification of the most sensitive version of the GSERF experiment, the recent PSYCHEDELIC experiment,[6d] to extend its applicability for overlapped ^{1}H signals. The new experiment uses the improved sensitivity properties of the PSYCHE scheme[10] for broadband inversion instead to the SS element and also the advantage to apply the echo/anti-echo approach to provide pure absorption lineshapes and therefore improved resolution. Our

* *Correspondence to: Pau Nolis and Teodor Parella, Servei de Ressonància Magnètica Nuclear, Facultat de Ciències, Universitat Autònoma de Barcelona, E-08193 Bellaterra (Barcelona), Catalonia, Spain. E-mail: pau.nolis@uab.cat; teodor.parella@uab.cat*

Servei de Ressonància Magnètica Nuclear, Facultat de Ciències, Universitat Autònoma de Barcelona, E-08193 Bellaterra (Barcelona), Catalonia, Spain

proposal relies on a known strategy already implemented in other NMR experiments, which incorporates a selective TOCSY scheme as a preparation period.[11] The resulting doubly-selective TOCSY-GSERF experiment takes advantage of the editing features of TOCSY to uncover hidden resonances that become accessible to perform the required selective refocusing. The potential of this new method is demonstrated for two target molecules with different spectral complexity.

Results and Discussion

The pulse scheme of the two-dimensional TOCSY-GSERF experiment (Fig. 1) consists of two sequential steps. The first part is a conventional selTOCSY block applied on a well-isolated ^{1}H resonance (site A) in order to simplify the apearance of overlapped regions. The TOCSY mixing consists of a regular DIPSI-2 pulse train with zero-quantum (ZQ) filtration to afford pure in-phase multiplets. The second part is a GSERF block based on the PSYCHEDELIC scheme which has been originally proposed to be run in a 3D acquisition mode. We have simplified the original pulse timing by suppressing the broadband homodecoupling features in order to perform a faster data acquisition in a more suitable 2D mode. The echo/anti-echo data combination approach is followed to provide pure absorption lineshapes and improved resolution that allows a much more accurate measurement of J_{HH}. A detailed description of this echo/anti-echo procedure can be found in Sinnaeve *et al.*[6] and will not be repeated here. In addition, the impact of strong coupling effects remains exactly the same as the original experiment and therefore will not be discussed either. The GSERF module is designed to refocus only protons selected by the TOCSY mixing and by the selective refocusing element to be applied on a relayed proton (site B). In practice, the two unique requirements for optimal experiment execution are the definition of the experimental conditions for selective excitation of the starting proton and for the selective refocusing of the relayed proton of interest. In contrast to conventional GSERF spectra, TOCSY-GSERF affords clean 2D *J*-resolved spectra only displaying the signals filtered by the TOCSY element as a doublets along the indirect dimension. All irrelevant signals that would appear as singlets in the central F1 = 0 row in GSERF spectra will be missing in TOCSY-GSERF spectra, greatly facilitating the observation and measurement of small doublets in highly congested areas. For instance, the H14 proton of strychnine (**1**) is obscured in the 2D PSYCHEDELIC spectrum obtained after selective refocusing of H15b, precluding the corresponding $J_{H14,H15b}$ measurement by signal overlap (Fig. 2A). However, a clean doublet corresponding to the small value of 1.7 Hz can be accurately determined in the equivalent and cleaner TOCSY-GSERF spectrum after selection of H15b in both TOCSY and GSERF steps (Fig. 2B).

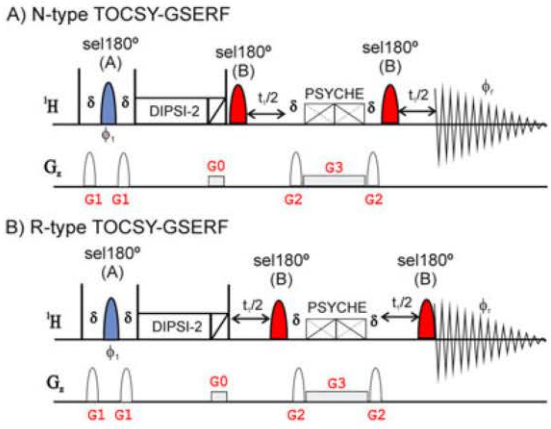

Figure 1. Pulse sequence of the 2D TOCSY-GSERF experiment for the measurement of J_{HH} in overlapped ^{1}H signals. Phase sensitive data showing pure absorption lineshapes are generated by combining (top) N-type and (bottom) R-type datasets acquired in an interleaved mode and processed using the echo/anti-echo procedure. Pulsed Field gradients (PFG) are indicated in the G_z line: Gradients G1 and G2 are used for proper single PFG echo refocusing and G0 is used for zero-quantum filtration. Narrow rectangles are hard 90° ^{1}H pulses, the PSYCHE element is indicated with two low-power chirp β pulses applied simultaneously to a weak rectangle gradient (G3) and shaped pulses represent selective 180° pulses applied to the frequency of an isolated starting proton (site A) for TOCSY propagation and to the relayed proton of interest (site B) for selective refocusing. The basic phase cycle is: ϕ_1 = x, y, −x, −y and ϕ_r = x, −x. More details can be found in the Experimental section.

As a proof of concept, Fig. 3 shows several doubly-selective TOCSY-GSERF spectra obtained for **1**. Three different protons (H18a, H11a and H14) resonate together near 3.15 ppm, precluding the successfully selective perturbation of each individual signal due to overlap. The TOCSY-GSERF spectrum resulting of the indiscriminate perturbation of all three protons at the same time by a 20 ms Gaussian-shaped pulse in both A and B sites (Fig. 3B) affords doublets that cannot be attributed to each individual signal. It is recommended to set-up the optimum conditions of a GSERF-TOCSY experiment by recording previously the equivalent selTOCSY experiment. Thus, Fig. 3C and E shows the preliminary 1D selTOCSY spectra quickly acquired after selective excitation of the isolated H15a and H11b protons, respectively. These experiments were used to determine the optimum conditions for the more efficient TOCSY transfer (mixing time set to 60 ms) to the target H14 and H11a protons, respectively. Figures 3D and F show the corresponding TOCSY-GSERF spectra with double excitation on H15a/H14 and H11b/H11a, respectively, acquired with the experimental conditions established previously using the selTOCSY experiments. The TOCSY-GSERF resulting of the first excitation of H15a and the following refocusing of H14 show J_{HH} for the H14 proton. Note that even in the case where H14 is a non-resolved broad resonance, vicinal J_{HH} values of 4.7 and 1.7 Hz can be accurately measured for H15a and H15b, respectively, whereas the small four-bond $J_{H14,H16}$ splitting is not resolved. The theoretical three-bond coupling with H13 is not observed because signal intensity of TOCSY-GSERF peaks will depend mainly of TOCSY propagation (note that H13 was not observed in the preliminar selTOCSY spectrum). In the second example, two clear doublets corresponding to the couplings of H11b and H12 with the relayed H11a proton are observed. In all cases, in contrast to the original SERF experiments, the resulting TOCSY-GSERF spectrum only display the relevant signals whereas non-coupled resonances do not appear at F1 = 0. All these measured J_{HH} values agree with those reported previously (Table S1) obtained experimentally[12a] and by simulation using the automatic coupling constants analyzer approach[12b] or using optimized DFT calculations via linear scaling of Fermi contacts.[12c]

Figure 4A shows the potential of the TOCSY-GSERF experiment applied to a more challenging example, the steroid methyltestosterone. This molecule presents an overcrowded aliphatic region in the ^{1}H spectrum with a large number of signals between 0.9 and 2.5 ppm. Clearly, selTOCSY experiments applied on the isolated H7a (Fig. 4B) and H16b (Fig. 4D) protons facilitate the observation of cleaner 1D spectra and the efficient deciphering

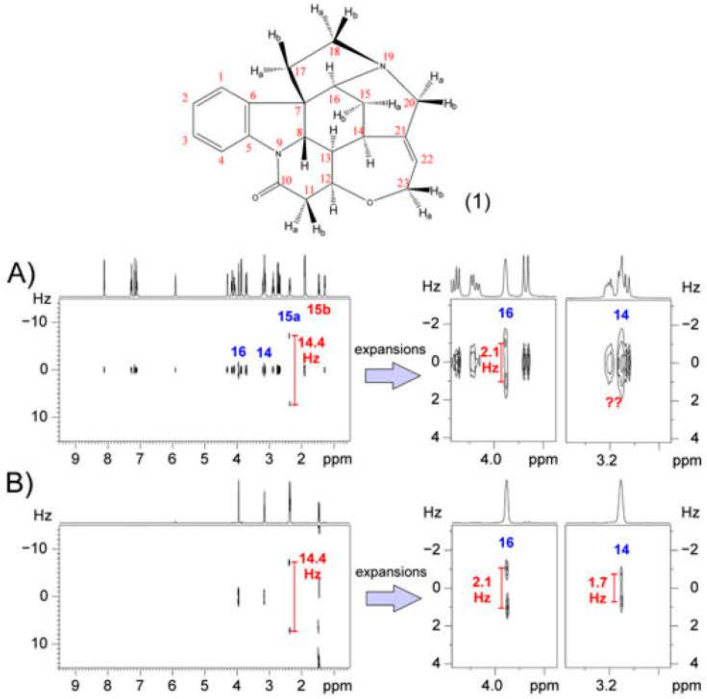

Figure 2. (A) 600.13 MHz 2D GSERF spectrum of strychnine (**1**) in $CDCl_3$ acquired with the PSYCHEDELIC pulse scheme described in Sinnaeve *et al.*[6d] A reduced 2D version without the homodecoupling feature was used. The active H15b proton was selectively refocused by a 20 ms Gaussian 180° ^{1}H pulse; (B) Equivalent TOCSY-GSERF spectrum acquired with the pulse sequence of Fig. 1 under the same experimental conditions as (A). The selective 180° pulses (20 ms) for TOCSY transfer (mixing of 60 ms) and for refocusing were both applied selectively on H15b. On the right, expansions are shown to observe the excellent resolution achieved in F1 to resolve the small splittings corresponding to $^3J_{H15b,H16}$ and $^3J_{H15b,H14}$.

of overlapped ^{1}H multiplets that aids to the identification, analysis and assignment of signals. In particular, we are interested in the two fully overlapped signals resonating at 1.85–1.9 ppm that correspond to the H7b and H16a protons. The corresponding TOCSY-GSERF spectra acquired with the same settings as previously established in their 1D selTOCSY counterparts afford 2D maps where accurate values of J_{HH} for both H7b and H16a can be determined (Fig. 4C and E, respectively). In the case of H7b, its equatorial position can be established accordingly to the moderate vicinal J_{HH} values with H6a (equatorial–equatorial interaction of 2.5 Hz), H6b (equatorial–axial interaction of 5.3 Hz) and H8 (equatorial–axial interaction of 3.5 Hz) protons. On the other hand, the axial position of H16a is established accordingly to the axial–axial interaction with H15b (12.1 Hz) and the axial–equatorial interaction with H15a (3.6 Hz) as well as to the large geminal coupling with H16b ($^2J_{HH}$ = 13.9 Hz). Note that some ultra long-range peaks observed in the selTOCSY spectrum due to the efficient multiple-relay TOCSY transfer are not split along F1 dimension in the TOCSY-GSERF spectrum because of their very small *J* magnitude.

Conclusions

In summary, a novel approach to extend the current limitations of GSERF experiments have been reported. The incorporation of a selTOCSY block for editing allows the obtention of GSERF spectra for overlapped signals. TOCSY-GSERF affords cleaner spectra because only protons resulting of the TOCSY transfer are visualized and retains the same basic features of the original GSERF experiments in terms of nice spectral representation, excellent resolution in F1, great simplicity in the extraction of J_{HH} and unambiguous assignment. The use of the principles described for PSYCHE-type experiments ensures maximum sensitivity levels, improving by one order of magnitude those expected with the original spatially-encoded SS methods.

Methods and Materials

NMR experiments were recorded on a 600 MHz spectrometer equipped with a triple-resonance ^{1}H/^{13}C/^{15}N inverse probe. The temperature for all measurements was set to 298 K. Two test samples containing 20 mg of strychnine (sample 1) and 20 mg of methyltestosterone (sample 2) dissolved in 0.6 ml of $CDCl_3$ were used. The recycle delay and the TOCSY mixing time in all TOCSY-GSERF spectra were set to 1 s and 60 ms, respectively. Gradient amplitudes for G1 and G2 were set to 15 and 40, respectively, measured as percentage of the absolute gradient strength of 53.5 G/cm. Sine bell-shaped gradients had 1 ms of duration and were followed by a recovery delay of 100 μs (overall duration of δ). The TOCSY mixing consisted of a 8.5 KHz DIPSI-2 pulse train followed by a 20 ms Chirp pulse simultaneous applied with a rectangular pulsed-field gradient (G0 = 11%). The selective 180° ^{1}H pulses in the TOCSY preparation periods (site A) were 20 ms for all spectra of sample 1

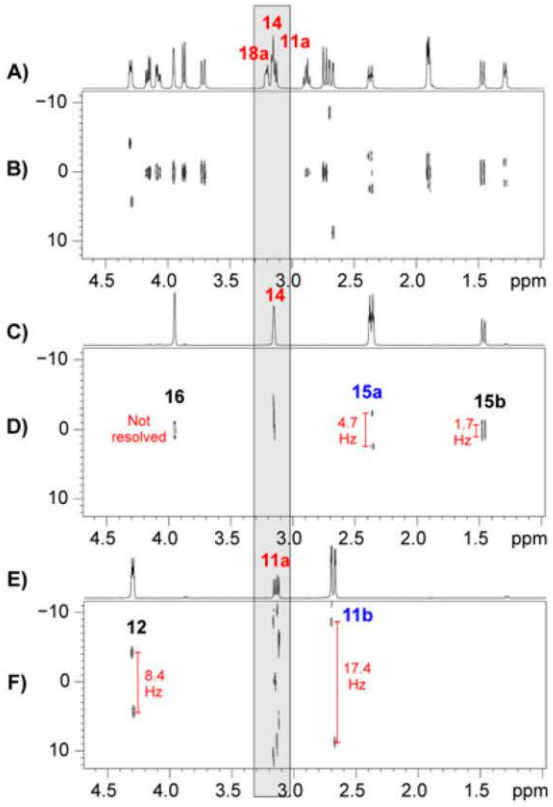

Figure 3. 600.13 NMR spectra of **1** in $CDCl_3$. (A) Conventional ^1H spectrum; (B) TOCSY-GSERF spectrum after selective refocusing at the same offset of 3.15 ppm (H4, H18a and H11a) in both TOCSY and GSERF steps; (C) and (E) 1D selTOCSY spectra after selective excitation of H15a and H12, respectively. The selective pulse was a 20 ms Gaussian-shaped, and the mixing time was set to 60 ms; (D) TOCSY-GSERF spectrum obtained after selective TOCSY at 2.35 ppm (H15a) and GSERF at 3.14 ppm (H14); and (F) TOCSY-GSERF spectrum obtained after selective TOCSY at 2.65 ppm (H11b) and GSERF at 3.14 ppm (H11a). The 2D spectra in (D) and (F) were acquired with the same TOCSY conditions as the 1D selTOCSY spectra in (C) and (E), respectively.

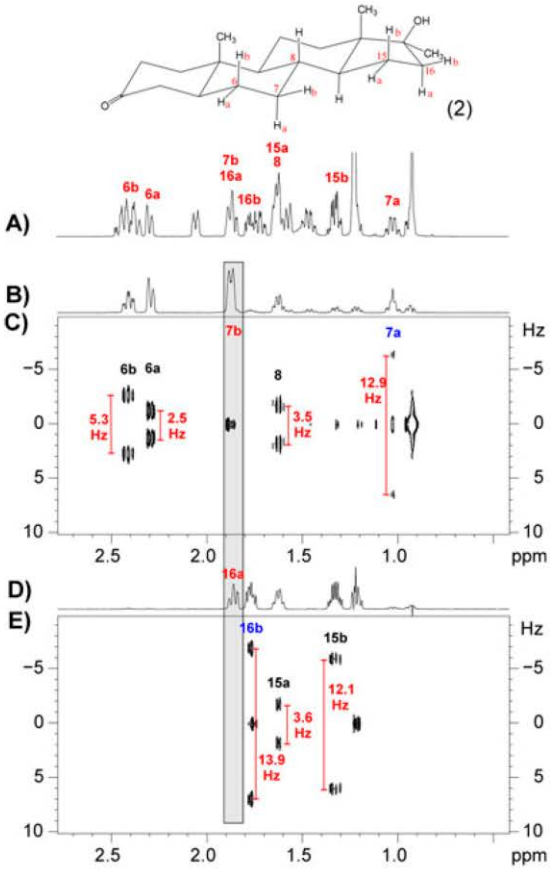

Figure 4. (A) ^1H NMR spectrum of methyltestosterone (**2**) in $CDCl_3$; (B) and (D) 1D selTOCSY spectra after selective excitation of the H7a (1.01 ppm) and H16b (1.78 ppm) protons with a Gaussian-shaped 180° ^1H pulse of 80 ms and a mixing time of 60 ms. (C) and (E) 2D TOCSY-GSERF spectra acquired with the same experimental conditions as described in (B) and (D), respectively, and after selective refocusing at 1.86 ppm (H7b and H16a protons, respectively) with a 20 ms Gaussian pulse.

(Figs 2 and 3) and 80 ms for all spectra of sample 2 (Fig. 4). All selective 180° refocusing pulses in the GSERF blocks (site B) were 20 ms Gaussian shaped pulses. Preliminary fast 1D selTOCSY spectra were recorded to set-up an optimum mixing time for a proper intensity optimization. The PSYCHE element consisted of low-flip-angle double frequency swept chirp pulses of duration 30 ms along with the gradient G3 (1%), as described in the original publication. Spectral widths and number of time-domain points used along F2/F1 dimensions were equal to 6000 Hz/40 Hz and 2048/64 points, respectively (FID resolution 2.93 and 0.65 Hz, respectively). The number of scans was set to 8 (sample 1) or 32 (sample 2). Unshifted sine window functions were applied in both dimensions prior Fourier transformation. All experiments were acquired and processed using the echo/anti-echo protocol. The pulse program for Bruker spectrometers is available in the Supporting Information, where an automated interleaved acquisition of the N-type and R-type data is already included. The experimental time for each 2D spectrum was 20 min (sample 1) and 1 h and 20 min (sample 2).

Acknowledgements

Financial support for this research provided by the Spanish MINECO (project CTQ2015-64436-P) is gratefully acknowledged. A. F. thanks CNPq-Brazil for a scholarship. We also thank to the Servei de Ressonància Magnètica Nuclear, Universitat Autònoma de Barcelona, for allocating instrument time to this project.

References

[1] (a) W. P. Aue, J. Karhan, R. R. Ernst. *J. Chem. Phys.* **1976**, *64*, 4226–4227. B. Luy. *J. Magn. Reson.* **2009**, *201*, 18–24. (b) M. J. Thrippleton, R. A. E. Edden, J. Keeler. *J. Magn. Reson.* **2005**, *174*, 97–109. (c) M. Foroozandeh, R. W. Adams, P. Kiraly, M. Nilsson, G. A. Morris. *Chem. Commun.* **2015**, *51*, 15410–15413.
[2] (a) L. Braunschweiler, R. R. Ernst. *J. Magn. Reson.* **1983**, *53*, 521–528. (b) A. Bax, D. G. Davis. *J. Magn. Reson.* **1985**, *65*, 355–360. (c) A. J. Pell, J. Keeler. *J. Magn. Reson.* **2007**, *189*, 293–299.
[3] (a) T. Facke, S. Berger. *J. Magn. Reson. A* **1995**, *113*, 257–259. (b) C. Dalvit, G. Bovermann. *Magn. Reson. Chem.* **1995**, *33*, 156–159. (c) P. Adell, T.

Parella, F. Sánchez-Ferrando, A. Virgili. *J. Magn. Reson. B* **1995**, *108*, 77–80.
[4] T. Facke, S. Berger. *J. Magn. Reson. A* **1995**, *113*, 114–116.
[5] N. Giraud, L. Beguin, J. Courtieu, D. Merlet. *Angew. Chem. Int. Ed.* **2010**, *49*, 3481–3484.
[6] (a) L. Beguin, N. Giraud, J. M. Ouvrard, J. Courtieu, D. Merlet. *J. Magn. Reson.* **2009**, *199*, 41–47. (b) D. Pitoux, B. Plainchont, D. Merlet, Z. Hu, D. Bonnaff, J. Farjon, N. Giraud. *Chem. A Eur. J.* **2015**, *21*, 9044–9047. (c) J. E. Herbert Pucheta, D. Pitoux, C. M. Grison, S. Robin, D. Merlet, D. J. Aitken, N. Giraud, J. Farjon. *Chem. Commun.* **2015**, *51*, 7939–7942. (d) D. Sinnaeve, M. Foroozandeh, M. Nilsson, G. A. Morris. *Angew. Chem. Intl. Ed.* **2016**, *55*, 1090–1093. (e) L. Lin, Z. Wei, Y. Lin, Z. Chen. *J. Magn. Reson.*, **2016**, *272*, 20–24; (f) Lokesh, N. Suryaprakash. *Chem. Commun.* **2014**, *50*, 8550–8553.
[7] (a) N. Gubensäk, W. M. F. Fabian, K. Zangger. *Chem. Commun.* **2014**, *50*, 12254–12257. (b) N. Lokesh, S. R. Chaudhari, N. Suryaprakash. *Chem. Commun.* **2014**, *50*, 15597–15600. (c) S. R. Chaudhari, N. Suryaprakash. *Chemphyschem* **2015**, *16*, 1079–1082.
[8] P. Nolis, A. Roglans, T. Parella. *J. Magn. Reson.* **2005**, *173*, 305–309.
[9] M. E. Di Pietro, C. Aroulanda, D. Merlet. *J. Magn. Reson.* **2013**, *234*, 101–105.
[10] M. Foroozandeh, R. W. Adams, N. J. Meharry, D. Jeannerat, M. Nilsson, G. A. Morris. *Angew. Chem. Intl. Ed.* **2014**, *53*, 6990–6992.
[11] (a) L. Poppe, H. van Halbeek. *J. Magn. Reson.* **1992**, *96*, 185–190. (b) P. Adell, T. Parella, F. Sanchez-Ferrando, A. Virgili. *J. Magn. Reson. A* **1995**, *113*, 124–127. (c) M. J. Gradwell, H. Kogelberg, T. A. Frenkiel. *J. Magn. Reson.* **1997**, *124*, 267–270. (d) D. Uhrin, P. N. Barlow. *J. Magn. Reson.* **1997**, *126*, 248–255. (e) H. Hu, S. A. Bradley, K. Krishnamurthy. *J. Magn. Reson.* **2004**, *171*, 201–206. (f) H. Sato, Y. Kajihara. *Carbohydr. Res.* **2005**, *340*, 469–479. (g) S. A. Bradley, K. Krishnamurthy, H. Hu. *J. Magn. Reson.* **2005**, *172*, 110–117. (h) S. J. Duncan, R. Lewis, M. A. Bernstein, P. Sandor. *Magn. Reson. Chem.* **2007**, *45*, 283–288.
[12] (a) J. C. Carter, G. W. Luther, T. C. Long. *J. Magn. Reson.* **1974**, *15*, 122–131. (b) J. C. Cobas, V. Constantino-Castillo, M. Martin-Pastor, F. del Rio-Portillo. *Magn. Reson. Chem.* **2005**, *43*, 843–848. (c) A. G. Kutateladze, O. Mukhina. *J. Org. Chem.* **2014**, *79*, 8397–8406.

Supporting information

Additional supporting information may be found online in the supporting information tab for this article.

Supporting Information

Accurate measurement of J_{HH} in overlapped signals by a TOCSY-edited SERF Experiment

André Fredi, Pau Nolis*andTeodor Parella*

Servei de RessonànciaMagnètica Nuclear, UniversitatAutònoma de Barcelona, E-08193 Bellaterra (Barcelona), Catalonia, Spain

Table S1: Comparison of experimental and calculated J(HH) coupling constants (in Hz) of strychnine

	ref. 12b	ref. 12c		thiswork
		expt	calc	
H14-H15a	4.78	4.77	4.70	4.7
H14-H15b	1.86	1.88	1.94	1.7
H15a-H15b	14.27	14.30	14.26	14.4
H15b-H16	2.16	2.16	2.12	2.1
H11a-H11b	17.38	17.39	17.26	17.4
H11a-H12	8.43	8.42	8.74	8.4

```
;TOCSY-GSERF
;SeRMN UAB (http://sermn.uab.cat)
; Selective TOCSY filtered 2D J-resolved experiment using the Pell-Keeler method
; applying PSYCHE and selective pulses to evolve only selected couplings

#include <Avance.incl>
#include <Delay.incl>
#include<Grad.incl>

"d0=0u"
"in0=inf2/2"
"p2 = p1*2"
"l0=1" ; switch for Pell-Keeler

;PSYCHE calculations
"cnst50=(cnst20/360)*sqrt((2*cnst21)/(p40/2000000))"
"p30=1000000.0/(cnst50*4)"
"cnst31= (p30/p1) * (p30/p1)"
"spw40=plw1/cnst31"
"p12=p40"

;shape pulse offset calculations
"cnst3 = cnst1*bf1" ;selto controlled by cnst1
"spoffs22 = cnst3-o1"
"cnst4 = cnst2*bf1" ;selto controlled by cnst2
"spoffs1 = cnst4-o1"

;tocsy mixing time
"FACTOR1=(d9/(p6*115.112))/2"
"l1=FACTOR1*2"

"acqt0=0"
baseopt_echo


1 ze
2 50u
20u LOCKH_OFF
d1
20u pl1:f1
50u UNBLKGRAD
p1 ph1

  3u
  p16:gp1
d16 pl0:f1
p22:sp22:f1 ph22:r     ; sel. 180 pulse on spin A
3u
  p16:gp1
  d16 pl1:f1

  p1 ph3
```

```
;  10u gron0              ;optional z-filter
;  (p32:sp29 ph3):f1
;  20ugroff
  d16 pl10:f1


                                                    ;begin DIPSI2
4 p6*3.556 ph23
   p6*4.556 ph25
   p6*3.222 ph23
   p6*3.167 ph25
   p6*0.333 ph23
   p6*2.722 ph25
   p6*4.167 ph23
   p6*2.944 ph25
   p6*4.111 ph23

   p6*3.556 ph25
   p6*4.556 ph23
   p6*3.222 ph25
   p6*3.167 ph23
   p6*0.333 ph25
   p6*2.722 ph23
   p6*4.167 ph25
   p6*2.944 ph23
   p6*4.111 ph25

  p6*3.556 ph25
  p6*4.556 ph23
  p6*3.222 ph25
  p6*3.167 ph23
  p6*0.333 ph25
  p6*2.722 ph23
  p6*4.167 ph25
  p6*2.944 ph23
p6*4.111 ph25

  p6*3.556 ph23
  p6*4.556 ph25
  p6*3.222 ph23
  p6*3.167 ph25
  p6*0.333 ph23
  p6*2.722 ph25
  p6*4.167 ph23
  p6*2.944 ph25
  p6*4.111 ph23
lo to 4 times l1
                                                    ;end DIPSI2

; p16:gp2                ;optional
 ; d16
10u gron0*1.333
```

```
(p32*0.75:sp29 ph3):f1
  20u groff

d16 pl1:f1
  p1 ph3


if "l0 %2 == 0" ; R-type
{
d0 ;Jcoup evolution 2DJ
}
4u pl0:f1
p11:sp1:f1 ph3:r ; sel. 180 pulse on spin B
4u
if "l0 %2 == 1" ; N-type
{
d0 ;Jcoupevolution 2DJ
}
d16
p16:gp2
d16
( center (p40:sp40 ph3):f1 (p12:gp3 ) ; PSYCHE
d16
p16:gp2
d16
if "l0 %2 == 0" ; R-type
{
d0 ;Jcoupevolution 2DJ
}
4u
p11:sp1:f1 ph4:r ; sel. 180 pulse on spin B
4u
if "l0 %2 == 1" ; N-type
{
d0 ;Jcoup evolution 2DJ
}

go=2 ph31
50u mc #0 to 2 F1EA(calclc(l0,+1), caldel(d0,+in0)) ; 2D Jres
20u LOCKH_OFF
exit

ph1 = 0
ph2 = 0
ph3 = 0
ph4 = 0
ph22 = 0 1 2 3
ph23=3
ph25=1
ph31= 0 2

;pl0: 0 W
```

;pl1 : f1 channel - power level for pulse (default)
;p1 : f1 channel - high power 90 pulse
;p2 : f1 channel - high power 180 pulse
;p11: sel. 180 pulse width for spin S
;p16: CTP gradient pulse duration
;p40: duration of PSYCHE double chirp
;d1 : relaxation delay; 1-5 * T1
;d16: [1ms] delay for homospoil/gradient recovery
;cnst1: Chemical shift of selective pulse for selTOCSY block(in ppm)
;cnst2: Chemical shift of selective pulse for Jres block(in ppm)
;cnst20: desired flip angle for PSYCHE pulse element (degree) (normally 10-25)
;cnst21: bandwidth of each chirp in PSYCHE pulse element (Hz) (normally 10000)
;cnst50: desired PSYCHE RF fiere 99re ld for chirp pulse in Hz
;NS: 4 * n, total number of scans: NS * TD0
;FnMODE: Echo-Antiecho in F2
;sp22: (spin A selective pulse power level
;spoffs22: (spin A) selective pulse offset
;spnam22: (spin A) file name for selective pulse
;sp1: (spin B) selective pulse power level
;spoffs1: (spin B) selective pulse offset
;spnam1: (spin B) file name for selective pulse
;sp40: (PSYCHE) power level of chirp element (calculated from cnst21)
;spoffs40: (PSYCHE) selective pulse offset (0 Hz)
;spnam40: (PSYCHE) file name for selective pulse
; for z-gradients only
;gpz0: 11%
;gpz1: 15%
;gpz2: 40%
;gpz3: 1%
;use gradient files:
;gpnam0: RECT.1
;gpnam1: SMSQ10.100
;gpnam2 SMSQ10.100
;gpnam3: RECT.1

4. CONCLUSIONS

A new processing technique referred to as *psNMR Covariance* has been developed for the synthetic reconstruction of psNMR spectra. Also, it is now possible to insert ME information in NMR spectra that are extremely difficult or impossible to acquire by experimental pulse sequence design. To finish, in the last work an improved GSERF experiment, referred to as selTOCSY-G-SERF, has been developed to analyse and measure J_{HH} couplings with high accuracy in overlapped regions. Detailed conclusions of each work are:

Publication 1:

- A general strategy to generate synthetic psNMR spectra using a fast GIC processing has been explored. This co-processing method, called psNMR covariance, has been applied to the most common homonuclear and heteronuclear NMR experiments.
- psNMR Covariance is a general and cheap alternative for the attempts to obtain broadband homodecoupled 2D NMR spectra without experimental pulse sequence design.
- psNMR Covariance demonstrated to be a fast and efficient processing tool available for the non-experienced user, without in-depth knowledge about the mathematical treatment.
- Some unfeasible NMR spectra can be quickly reconstructed from standard datasets. In particular, it has been shown that $^2J_{HH}$ splitting in diastereotopic methylene systems are removed in psGIC-HSQC. Other reconstructed spectra like, for instance, psGIC-HSQMBC or psGIC-HSQC-TOCSY can be now available after some seconds of calculation.
- psNMR Covariance can be applied to a broad range of NMR experiments, and it is compatible with other mathematical

treatments and data processing algorithms like NUS, different kinds of covariance-derived NMR datasets or deconvolution procedures.

Publication 2:

- psNMR Covariance can reconstruct 2D spectra incorporating simultaneously pure-shift features and ME information ($^{13}CH_n$ multiplicity) in the form of up/down relative phase.
- The proposed strategy can generate new “synthetic” NMR spectra incorporating simultaneously ps and ME features, even for challenging or impossible NMR experiments.
- ME information can be transferred by GIC into different kinds of experimental COSY, TOCSY or HMBC spectra, among others.
- Spectral reconstruction by GIC can offer a significant added value in automated spectra analysis, generating complementary multiplicity-edited psNMR spectra useful to the computer-assisted structural elucidation of small molecules.

Publication 3:

- A new selTOCSY-GSERF experiment solves the overlapping signal limitations existing in conventional G-SERF experiments, allowing the measurement of J_{HH} in challenging crowded regions.
- selTOCSY-GSERF is a potent, general tool to measure *J* couplings with high accuracy. The incorporation of a selTOCSY block into the G-SERF experiment offers cleaner spectra because only the protons selecting by selTOCSY are exclusively visualised.
- selTOCSY-GSERF retains all the features of the original PSYCHEDELIC experiment, maximising sensitivity thanks to the

PSYCHE element and optimising experimental time due to the optimum 2D acquisition mode.

5. ON-GOING RESEARCH

In this section, some ideas and some on-going projects that have not been completed are briefly presented.

Reconstructed Homodecoupled selTOCSY spectra by GSD

The experimental 1D selTOCSY-PSYCHE sequence expends a long time to acquire a single 1D spectrum.[63] The 1D selTOCSY experiment is much faster than its ps version. Our preliminary results show that synthetic ps1D selTOCSY spectra can be quickly generated in seconds, also preserving the original signal intensities. The idea is to acquire the 1D selTOCSY spectrum and reconstruct the ps1D selTOCSY by a special co-processing did by Mestrenova[15]. This co-processing is based on a new script in which it obtains the chemical shift information from the 1D spectrum by Global Spectral Deconvolution (GSD) and rebuilds a new 1D spectrum with only one signal for each chemical shift.

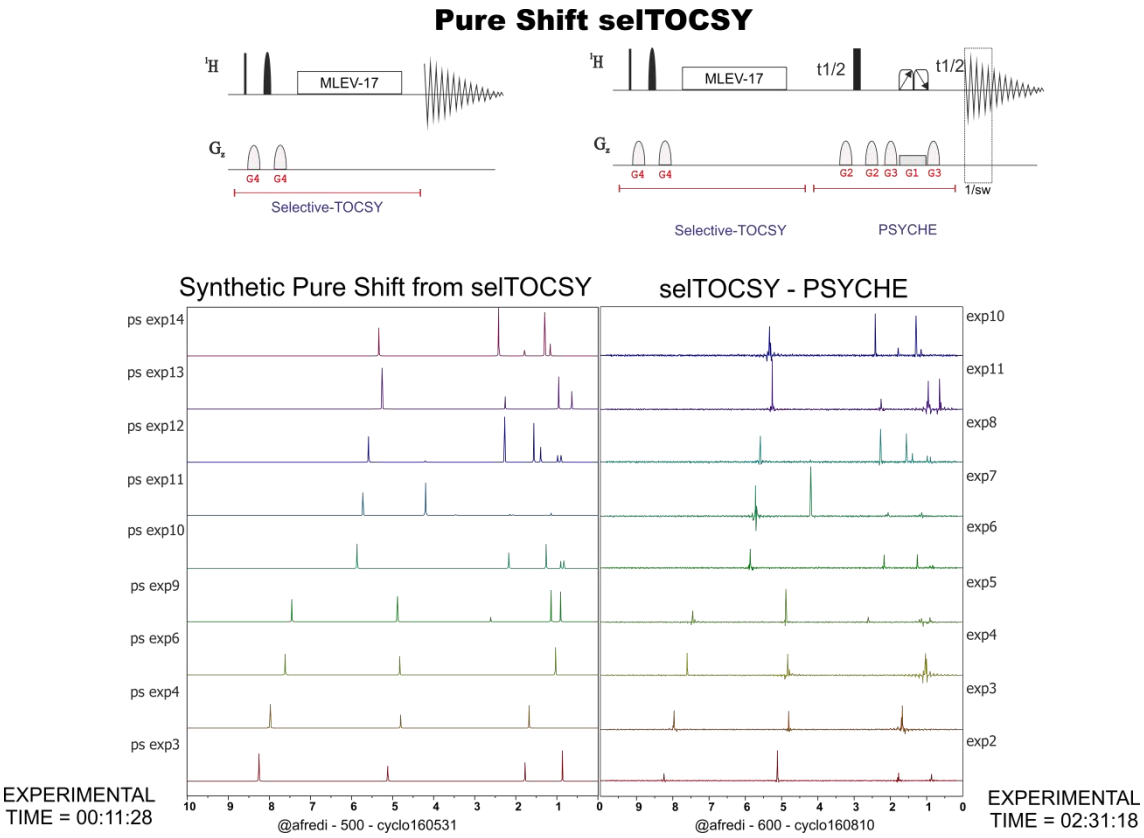

Figure 20: (Left) Synthetic ps selTOCSY after applying GSD and a new script to reconstruct ps spectrum and (Right) conventional selTOCSY spectra. The total experimental time for all Synthetic ps selTOCSY spectra: 11 minutes and 28 seconds; entire experimental time of Experimental ps selTOCSY all spectra: 2 hours, 31 minutes and 18 seconds.

Reconstruction of Diffusion-edited 2D spectra by psNMR Covariance

Experimental diffusion-edited NMR experiments require long acquisition times due to their 3D acquisition mode. It was idealized that 2D diffusion-edited NMR spectra could be synthetically reconstructed by Covariance NMR from original datasets using a selected DOSY row as a target co-processing and combine with an HSQC spectrum. This approach can be applied to any homonuclear or heteronuclear 2D spectrum. Figure 21 shows the schematic strategy to obtain a reconstructed DOSY-HSQC spectrum from an experimental DOSY and HSQC spectra. This idea was not tested experimentally. But it is

known that signals overlapping in the DOSY or HSQC spectra can generate artefacts.

The same idea can be applied by exchanging the DOSY spectrum for a selTOCSY, thus generating this selectivity necessary to follow the idea of creating separate spectra of mixtures of substances under study from some kind of selective experiment and doing the re-construction with NMR Covariance.

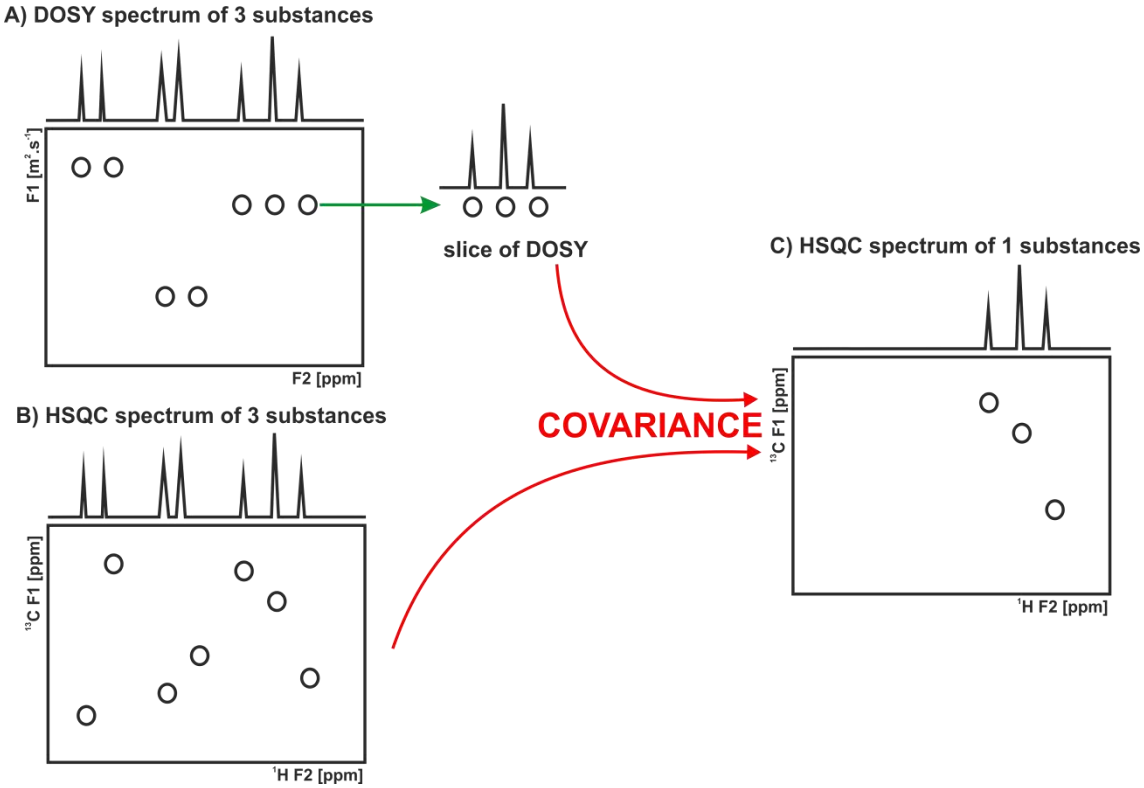

Figure 21: A) Conventional 2D DOSY spectrum. The green arrow indicates the extraction of one line from the DOSY spectrum; B) 2D HSQC spectrum. The red arrows indicate the Covariance processing that is performed combining the selected DOSY row with a standard 2D HSQC spectrum of a mixture sample giving a C) 2D diffusion-edited HSQC spectral representation only of the selected substance.

Measurement of heteronuclear coupling constants from heteronuclear *J*-resolved spectrum for high-abundant ^{19}F or ^{31}P nuclei.

Heteronuclear versions of the PSYCHE-GSERF experiment can be developed for the measurement of the magnitude of J_{HX} coupling constants

(X=^{31}P or ^{19}F). The 2D heteronuclear G-SERF spectrum affords ^{1}H δ in F2 and the selected J_{HX} doublets in F1. The PSYCHE block decoupled the *J* and δ in F1 dimension providing a better intensity compared with other ps building blocks. The sel180º pulse selects the heteronuclear of interest and leaves that its *J* evolves during the t_1 period. Thus, the new experiment proved to be quite efficient for measuring *J* between ^{1}H and ^{31}P or ^{19}F. This new approach combines the benefits of G-SERF and the benefits of PSYCHE block.

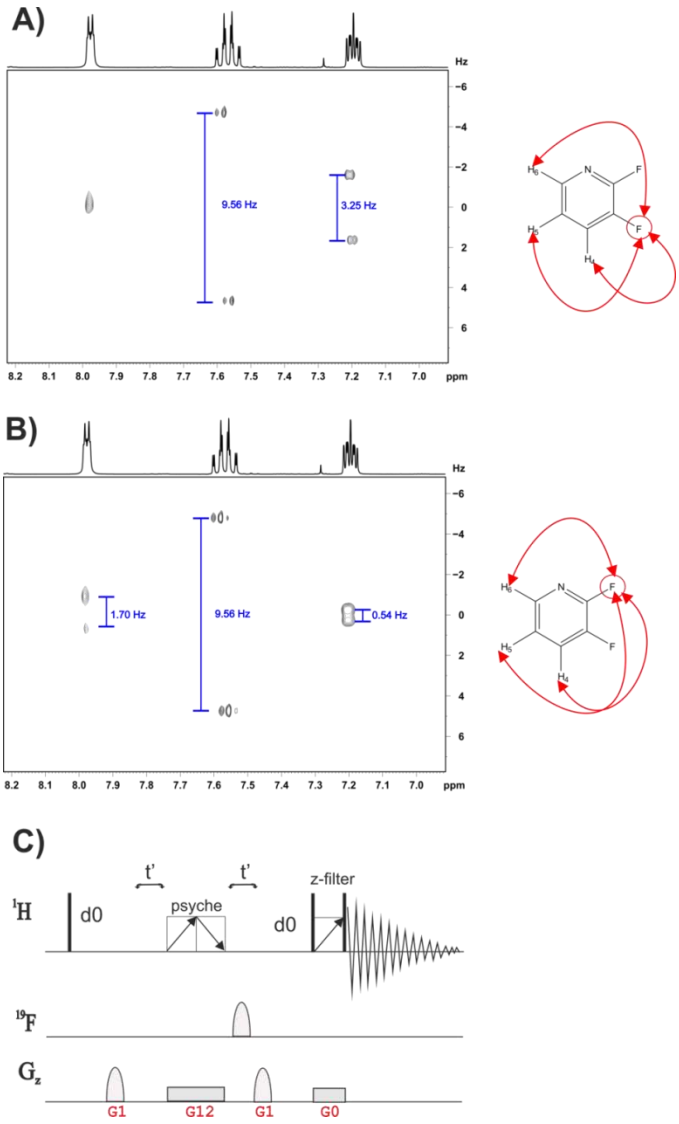

Figure 22: Selective heteronuclear PSYCHE-G-SERF spectra corresponding to the selective excitation of (A) fluorine-1 and (B) fluorine-1 of 2,3 difluoropyridine in $CDCl_3$. Both spectra were acquired in a 400 MHz NMR spectrometer using two scans, 2048 complex points in F2 and 64 t_1 increments.

6. BIBLIOGRAPHY

1. Ernst, R. R. & Anderson, W. A. Application of fourier transform spectroscopy to magnetic resonance. *Rev. Sci. Instrum.* **37,** 93–102 (1966).

2. Aue, W., Bartholdi, E. & Ernst, R. Two-dimensional spectroscopy. Application to nuclear magnetic resonance. *J. Chem. Phys.* **64,** 2229–2246 (1976).

3. Keeler, J. *Understanding NMR spectroscopy*. (2014).

4. Led, J. J. & Gesmar, H. Application of the Linear Prediction Method to NMR Spectroscopy. *Chem. Rev.* **91,** 1413–1426 (1991).

5. Barna, J. C. ., Laue, E. ., Mayger, M. ., Skilling, J. & Worrall, S. J. . Exponential sampling, an alternative method for sampling in two-dimensional NMR experiments. *J. Magn. Reson.* **73,** 69–77 (1987).

6. Kazimierczuk, K. & Orekhov, V. Y. Accelerated NMR spectroscopy by using compressed sensing. *Angew. Chemie - Int. Ed.* **50,** 5556–5559 (2011).

7. Rovnyak, D., Sarcone, M. & Jiang, Z. Sensitivity enhancement for maximally resolved two-dimensional NMR by nonuniform sampling. *Magn. Reson. Chem.* **49,** 483–491 (2011).

8. Watkins, J. C. *An Introduction to the Science of Statistics : Preliminary Edition*. (2014).

9. Aspers, R. L. E. G., Geutjes, P. E. T. J., Honing, M. & Jaeger, M. Using indirect covariance processing for structure elucidation of small molecules in cases of spectral crowding. *Magn. Reson. Chem.* **49,** 425–436 (2011).

10. Chen, Y. *et al.* Quantitative covariance NMR by regularization. *J. Biomol. NMR* **38,** 73–77 (2007).

11. Zhang, F., Robinette, S. L., Bruschweiler-Li, L. & Brüschweiler, R. Web server suite for complex mixture analysis by covariance NMR. *Magn. Reson. Chem.* **47,** S118–S122 (2009).

12. Zhang, F., Bruschweiler-Li, L. & Brüschweiler, R. Simultaneous de novo identification of molecules in chemical mixtures by doubly indirect covariance NMR spectroscopy. *J. Am. Chem. Soc.* **132,** 16922–16927 (2010).

13. Jaeger, M. & Aspers, R. L. E. G. *Covariance NMR and small molecule applications*. *Annual Reports on NMR Spectroscopy* **83,** (2014).

14. Lindon, J. C., Tranter, G. E. & Koppenaal, D. W. *Encyclopedia of Spectroscopy and Spectrometry*. (2017).

15. mestrelab.com.

16. Brüschweiler, R. & Zhang, F. Covariance nuclear magnetic resonance spectroscopy. *J. Chem. Phys.* **120,** 5253–5260 (2004).

17. Cobas, C. NMR Data Evaluation: Review of Covariance Applications. *Stan's Libr. Vol. V, NMR* **V,** 1–8 (2014).

18. Brüschweiler, R. & Zhang, F. Covariance nuclear magnetic resonance spectroscopy. *J. Chem. Phys.* **120,** 5253–5260 (2004).

19. Trbovic, N., Smirnov, S., Zhang, F. & Brüschweiler, R. Covariance NMR spectroscopy by singular value decomposition. *J. Magn. Reson.* **171,** 277–283 (2004).

20. Martin, G. E., Hilton, B. D., Blinov, K. A. & Williams, A. J. Multistep correlations via covariance processing of COSY/GCOSY spectra: Opportunities and artifacts. *Magn. Reson. Chem.* **46,** 997–1002 (2008).

21. Zhang, F., Trbovic, N., Wang, J. & Brüschweiler, R. Double-quantum biased covariance spectroscopy: Application to the 2D INADEQUATE experiment. *J. Magn. Reson.* **174,** 219–222 (2005).

22. Zhang, F. & Bruschweiler, R. Indirect covariance NMR spectroscopy. *J. Am. Chem. Soc.* **126,** 13180–13181 (2004).

23. Williams, A., Martin, G. & Rovnyak, D. *Modern NMR Approaches To The Structure Elucidation of Natural Products Volume 1: Instrumentation and Software*. **1,** (2017).

24. Blinov, K. A. *et al.* Analysis and elimination of artifacts in indirect covariance NMR spectra via unsymmetrical processing. *Magn. Reson. Chem.* **43,** 999–1007 (2005).

25. Schoefberger, W., Smrecki, V., Vikic-Topic, D. & Müller, N. Homonuclear long-range correlation spectra from HMBC experiments by covariance processing. *Magn. Reson. Chem.* **45,** 583–589 (2007).

26. Morris, G. A., Aguilar, J. A., Evans, R., Haiber, S. & Nilsson, M. True chemical shift correlation maps: A TOCSY experiment with pure shifts in both dimensions. *J. Am. Chem. Soc.* **132,** 12770–12772 (2010).

27. Foroozandeh, M., Adams, R. W., Nilsson, M. & Morris, G. A. Ultrahigh-resolution total correlation NMR spectroscopy. *J. Am. Chem. Soc.* **136,** 11867–11869 (2014).

28. Aguilar, J. A., Colbourne, A. A., Cassani, J., Nilsson, M. & Morris, G. A. Decoupling two-dimensional NMR spectroscopy in both dimensions: Pure shift NOESY and COSY. *Angew. Chemie - Int. Ed.* **51,** 6460–6463 (2012).

29. Martin, G. E., Hilton, B. D., Blinov, K. A. & Williams, A. J. ^{13}C-^{15}N Correlation correlation via unsymmetrical indirect covariance NMR: Application to vinblastine. *J. Nat. Prod.* **70,** 1966–1970 (2007).

30. Blinov, K. A., Larin, N. I., Williams, A. J., Mills, K. A. & Martin, G. E. Unsymmetrical covariance processing of COSY or TOCSY and HSQC

NMR data to obtain the equivalent of HSQC-COSY or HSQC-TOCSY spectra. *J. Heterocycl. Chem.* **43,** 163–166 (2006).

31. Martin, G. E., Hilton, B. D. & Blinov, K. A. HSQC-ADEQUATE correlation: A new paradigm for establishing a molecular skeleton. *Magn. Reson. Chem.* **49,** 248–252 (2011).

32. Blinov, K. A., Larin, N. I., Williams, A. J., Zell, M. & Martin, G. E. Long-range carbon-carbon connectivity via unsymmetrical indirect covariance processing of HSQC and HMBC NMR data. *Magn. Reson. Chem.* **44,** 107–109 (2006).

33. Martin, G. E., Hilton, B. D., Blinov, K. A. & Williams, A. J. Unsymmetrical indirect covariance processing of hyphenated and long-range heteronuclear 2D NMR spectra - Enhanced visualization of $^{2}J_{CH}$ and $^{4}J_{CH}$ correlation responses. *J. Heterocycl. Chem.* **45,** 1109–1113 (2008).

34. Martin, G. E., Hilton, B. D., Irish, P. a, Blinov, K. a & Williams, A. J. ^{13}C-^{15}N connectivity networks via unsymmetrical indirect covariance processing of 1H-13C HSQC and 1H-15N IMPEACH spectra. *J. Heterocycl. Chem.* **44,** 1219–1222 (2007).

35. Snyder, D. A. & Brüschweiler, R. Generalized indirect covariance NMR formalism for establishment of multidimensional spin correlations. *J. Phys. Chem. A* **113,** 12898–12903 (2009).

36. Snyder, D. A. & Brüschweiler, R. Generalized Indirect Covariance NMR Formalism for Establishment of Multi-Dimensional Spin Correlations. *J. Phys. Chem.* **113,** 12898–12903 (2009).

37. Martin, G. E., Hilton, B. D., Blinov, K. A. & Williams, A. J. Using indirect covariance spectra to identify artifact responses in unsymmetrical indirect covariance calculated spectra. *Magn. Reson. Chem.* **46,** 138–143 (2008).

38. Aue, W. P., Karhan, J. & Ernst, R. R. Homonuclear broad band decoupling and two-dimensional J-resolved NMR spectroscopy. *J. Chem. Phys.* **64,** 4226–4227 (1976).

39. Adams, R. W. Pure Shift NMR Spectroscopy. *eMagRes* **3,** 295–310 (2014).

40. Meyer, N. H. & Zangger, K. Viva la resolución! Enhancing the resolution of 1H NMR spectra by broadband homonuclear decoupling. *Synlett* **25,** 920–927 (2014).

41. Castañar, L. & Parella, T. Broadband ^{1}H homodecoupled NMR experiments: recent developments, methods and applications. *Magn. Reson. Chem.* **53,** 399–426 (2015).

42. Zangger, K. Pure shift NMR. *Prog. Nucl. Magn. Reson. Spectrosc.* **86–87,** 1–20 (2015).

43. Garbow, J. R., Weitekamp, D. & Pines, A. Bilinear Rotation Decoupling of Homonuclear Scalar Interaction. *Chem. Phys. Lett.* **93,** 504–509 (1982).

44. Aguilar, J. A., Nilsson, M. & Morris, G. A. Simple Pronton Spectra from Complex Spin Systems: Pure Shift NMR Spectroscopy Using BIRD. *Angew. Chemie - Int. Ed.* **50,** 9716–9717 (2011).

45. Paudel, L. *et al.* Simultaneously Enhancing Spectral Resolution and Sensitivity in Heteronuclear Correlation NMR Spectroscopy. *Angew. Chemie - Int. Ed.* **52,** 11616–11619 (2013).

46. Lupulescu, A., Olsen, G. L. & Frydman, L. Toward single-shot pure-shift solution ^{1}H NMR by trains of BIRD-based homonuclear decoupling. *J. Magn. Reson.* **218,** 141–146 (2012).

47. Sakhaii, P., Haase, B. & Bermel, W. Experimental access to HSQC spectra decoupled in all frequency dimensions. *J. Magn. Reson.* **199,** 192–198 (2009).

48. Reinsperger, T. & Luy, B. Homonuclear BIRD-decoupled spectra for measuring one-bond couplings with highest resolution : CLIP / CLAP-RESET and. *J. Magn. Reson.* **239,** 110–120 (2014).

49. Online, V. A. *et al.* '"Perfecting"' pure shift HSQC: full homodecoupling for accurate and precise determination of heteronuclear couplings. *Chem. Commun.* **50,** 15702–15705 (2014).

50. Timári, I. *et al.* Accurate determination of one-bond heteronuclear coupling constants with '" pure shift "' broadband proton-decoupled CLIP / CLAP-HSQC experiments. *RSC Adv.* **4,** 130–138 (2014).

51. Liu, Y. *et al.* Using pure shift HSQC to characterize microgram samples of drug metabolites. *TETRAHEDRON Lett.* **55,** 5450 (2014).

52. Aguilar, J. A., Morris, A. & Kenwright, A. M. 'Pure shift' ^{1}H NMR, a robust method for revealing heteronuclear couplings in complex spectra. *RSC Adv.* **4,** 8278–8282 (2014).

53. Donovan, K. J. & Frydman, L. HyperBIRD : A Sensitivity-Enhanced Approach to Collecting Homonuclear-Decoupled Proton NMR Spectra. *Angew. Chemie - Int. Ed.* **54,** 594–598 (2015).

54. Brüschweiler, R., Griesinger, C., Sørensen, O. W. & Ernst, R. R. Combined use of hard and soft pulses for ω1 decoupling in two-dimensional NMR spectroscopy. *J. Magn. Reson.* **78,** 178–185 (1988).

55. Castañar, L., Nolis, P., Virgili, A. & Parella, T. Full sensitivity and enhanced resolution in homodecoupled band-selective NMR experiments. *Chem. - A Eur. J.* **19,** 17283–17286 (2013).

56. Castañar, L., Nolis, P., Virgili, A. & Parella, T. Measurement of T1/T2 relaxation times in overlapped regions from homodecoupled 1H singlet signals. *J. Magn. Reson.* **244,** 30–35 (2014).

57. Castañar, L., Saurí, J., Nolis, P., Virgili, A. & Parella, T. Implementing homo- and heterodecoupling in region-selective HSQMBC experiments. *J. Magn. Reson.* **238,** 63–69 (2014).

58. Castañar, L., Roldán, R., Clapés, P., Virgili, A. & Parella, T. Disentangling complex mixtures of compounds with near-identical ^{1}H and ^{13}C NMR spectra using pure shift NMR spectroscopy. *Chem. - A Eur. J.* **21,** 7682–7685 (2015).

59. Zangger, K. & Sterk, H. Homonuclear Broadband-Decoupled NMR Spectra. *J. Magn. Reson.* **124,** 486–489 (1997).

60. Lauterbur, P. C. Image formation by induced local interactions. Examples employing nuclear magnetic resonance. *Nat. (London, United Kingdom)* **242,** 190–191 (1973).

61. Foroozandeh, M. *et al.* Ultrahigh-resolution NMR spectroscopy. *Angew. Chemie - Int. Ed.* **53,** 6990–6992 (2014).

62. Bohlen, J. M., Rey, M. & Bodenhausen, G. Refocusing with chirped pulses for broadband excitation without phase dispersion. *J. Magn. Reson.* **84,** 191–197 (1989).

63. Dal Poggetto, G., Castañar, L., Morris, G. A. & Nilsson, M. A new tool for NMR analysis of complex systems: selective pure shift TOCSY. *RSC Adv.* **0,** 1–3 (2013).

64. Foroozandeh, M. *et al.* Ultrahigh-Resolution Diffusion-Ordered Spectroscopy. *Angew. Chemie - Int. Ed.* **55,** 15579–15582 (2016).

65. Hahn, E. L. Spin Echoes. *Phys. Rev.* **80,** 580–594 (1950).

66. Pell, A. J. & Keeler, J. Two-dimensional *J*-spectra with absorption-mode lineshapes. *J. Magn. Reson.* **189,** 293–299 (2007).

67. Luy, B. Adiabatic z-filtered *J*-spectroscopy for absorptive homonuclear decoupled spectra. *J. Magn. Reson.* **201,** 18–24 (2009).

68. Thrippleton, M. J., Edden, R. A. E. & Keeler, J. Suppression of strong coupling artefacts in *J*-spectra. *J. Magn. Reson.* **174,** 97–109 (2005).

69. Mandelshtam, V. A., Van, Q. N. & Shaka, A. J. Obtaining proton chemical shifts and multiplets from several 1D NMR signals. *J. Am. Chem. Soc.* **120,** 12161–12162 (1998).

70. Foroozandeh, M., Adams, R. W., Kiraly, P., Nilsson, M. & Morris, G. A. Measuring couplings in crowded NMR spectra: pure shift NMR with multiplet analysis. *Chem. Commun.* **51,** 15410–15413 (2015).

71. Thrippleton, M. J. & Keeler, J. Elimination of zero-quantum interference in two-dimensional NMR spectra. *Angew. Chemie - Int. Ed.* **42,** 3938–3941 (2003).

72. Facke, T. & Berger, S. SERF, a New Method for H,H Spin-Coupling Measurement in Organic Chemistry. *J. Magn. Reson. Ser. A* **113,** 114–116 (1995).

73. Beguin, L., Giraud, N., Ouvrard, J. M., Courtieu, J. & Merlet, D.

Improvements to selective refocusing phased (SERFph) experiments. *J. Magn. Reson.* **199,** 41–47 (2009).

74. Verma, A. & Baishya, B. Real-time bilinear rotation decoupling in absorptive mode J-spectroscopy: Detecting low-intensity metabolite peak close to high-intensity metabolite peak with convenience. *J. Magn. Reson.* **266,** 51–58 (2016).

75. Giraud, N., Béguin, L., Courtieu, J. & Merlet, D. Nuclear magnetic resonance using a spatial frequency encoding: Application to *J*-edited spectroscopy along the sample. *Angew. Chemie - Int. Ed.* **49,** 3481–3484 (2010).

76. Mishra, S. K., Lokesh, N. & Suryaprakash, N. Clean G-SERF an NMR experiment for the complete eradication of axial peaks and undesired couplings from the complex spectrum. *RSC Adv.* **7,** 735–741 (2017).

77. Sinnaeve, D., Foroozandeh, M., Nilsson, M. & Morris, G. A. A general method for extracting individual coupling constants from crowded ^{1}H NMR spectra. *Angew. Chemie - Int. Ed.* **55,** 1090–1093 (2016).

78. Herbert Pucheta, J. E. *et al.* Pushing the limits of signal resolution to make coupling measurement easier. *Chem. Commun.* **51,** 7939–7942 (2015).

79. Lokesh, N., Chaudhari, S. R. & Suryaprakash, N. Quick re-introduction of selective scalar interactions in a pure-shift NMR spectrum. *Chem. Commun.* **50,** 15597–15600 (2014).

80. Parella, T., Sánchez-Ferrando, F. & Virgili, A. Improved Sensitivity in Gradient-Based 1D and 2D Multiplicity-Edited HSQC Experiments. *J. Magn. Reson.* **126,** 274–277 (1997).

81. Boyer, R. D., Johnson, R. & Krishnamurthy, K. Compensation of refocusing inefficiency with synchronized inversion sweep (CRISIS) in multiplicity-edited HSQC. *J. Magn. Reson.* **165,** 253–259 (2003).

82. Hu, H. & Krishnamurthy, K. Doubly compensated multiplicity-edited HSQC experiments utilizing broadband inversion pulses. *Magn. Reson. Chem.* **46,** 683–689 (2008).

83. Sakhaii, P. & Bermel, W. A different approach to multiplicity-edited heteronuclear single quantum correlation spectroscopy. *J. Magn. Reson.* **259,** 82–86 (2015).

84. Parella, T., Belloc, J., Sanchez-Ferrando, F. & Virgili, A. A general building block to introduce carbon multiplicity information into multi-dimensional HSQC-type experiments. *Magn. Reson. Chem.* **36,** 715–719 (1998).

85. Nyberg, N. T. & Sørensen, O. W. Multiplicity-edited broadband HMBC NMR spectra. *Magn. Reson. Chem.* **44,** 451–454 (2006).

86. Saurí, J., Sistaré, E., Thomas Williamson, R., Martin, G. E. & Parella, T.

Implementing multiplicity editing in selective HSQMBC experiments. *J. Magn. Reson.* **252,** 170–175 (2015).

87. Parella, T. & Sánchez-Ferrando, F. Improved multiplicity-edited ADEQUATE experiments. *J. Magn. Reson.* **166,** 123–128 (2004).

88. Fredi, A., Nolis, P., Cobas, C., Martin, G. E. & Parella, T. Exploring the use of Generalized Indirect Covariance to reconstruct pure shift NMR spectra: Current Pros and Cons. *J. Magn. Reson.* (2016). doi:10.1016/j.jmr.2016.03.003

89. Braunschweiler, L. & Ernst, R. R. Coherence transfer by isotropic mixing: Application to proton correlation spectroscopy. *J. Magn. Reson.* **53,** 521–528 (1983).

90. Dalvit, C. & Bovermann, G. Pulsed Field Gradient One-Dimensional NMR Selective ROE and TOCSY Experiments. **33,** 156–159 (1995).

7. APPENDIX

TUTORIAL psGIC

2D-DIAG FROM 1D HOMODECUPLED

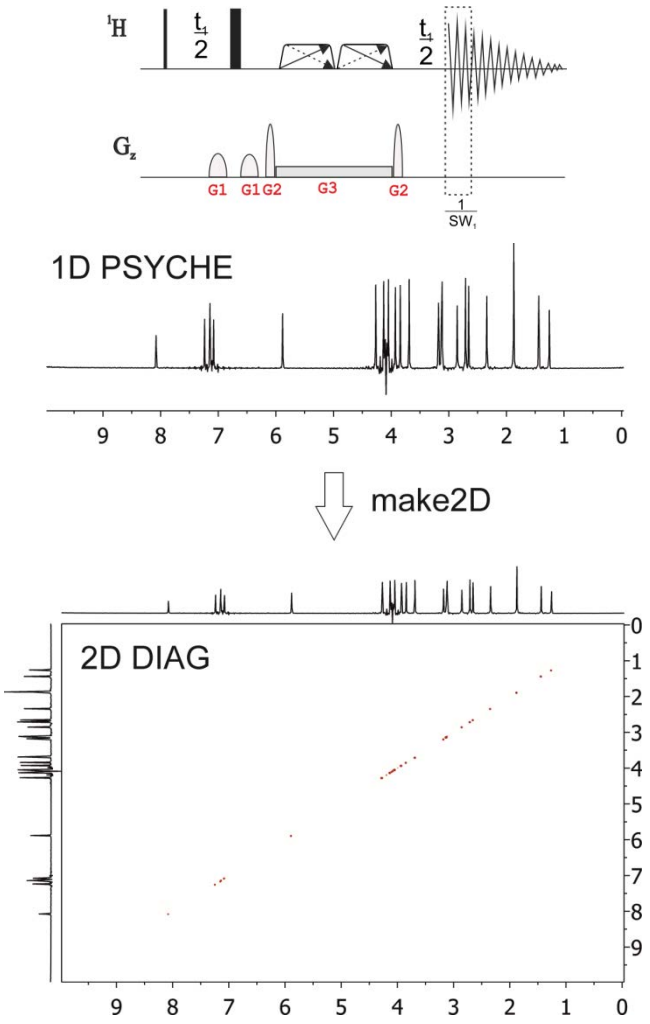

1. To begin, import your 2D homo or heteronuclear spectrum and your 1D homodecoupled ^{1}H spectrum into Mnova 10.1 software.

2. For to reconstruct the 2D DIAG from 1D pure shift spectrum, it is necessary to use the *make2D* script (Figure1). This script is included in Mnova v11.

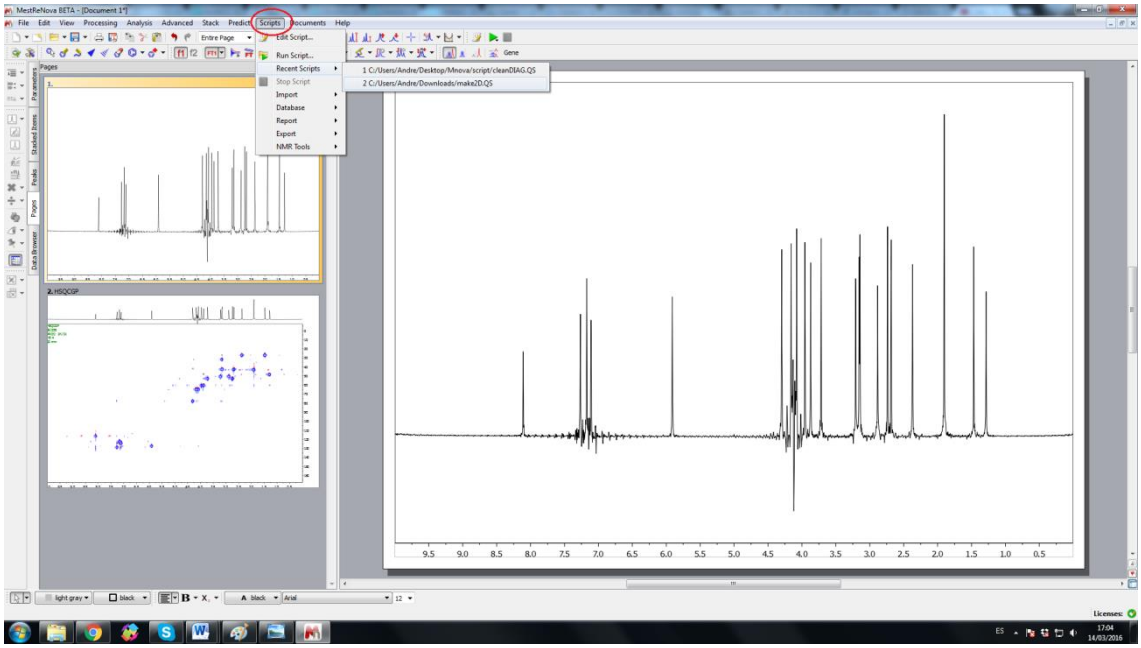

Figure 1: Reconstruct 2D DIAG from 1D pure shift spectrum.

3. Select your pure shift ^{1}H spectrum and follow *scprit>run script* > find the *make2D* script in your computer.

4. To execute the GIC processing, follow the menu '*Processing*/*Covariance NMR*/*Generalized Indirect Covariance*', Figure 2.

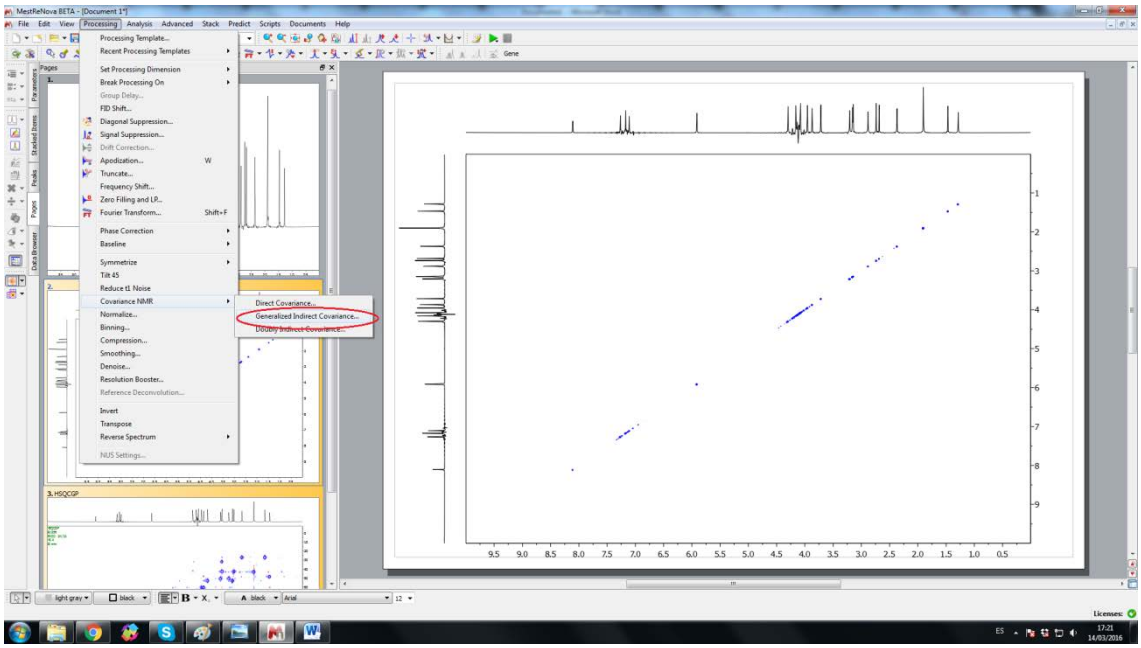

Figure 2: Generalized Indirect Covariance.

5. The ' *Generalized Indirect* Covariance NMR' dialogue box which allows you to select the spectrum and lambda value.

6. Select the target 2D spectrum that you want to transform into a pure-shift format and the 2D DIAG spectrum. Enter the value for the lambda parameter (we advise to use the value of 1), Figure 3.

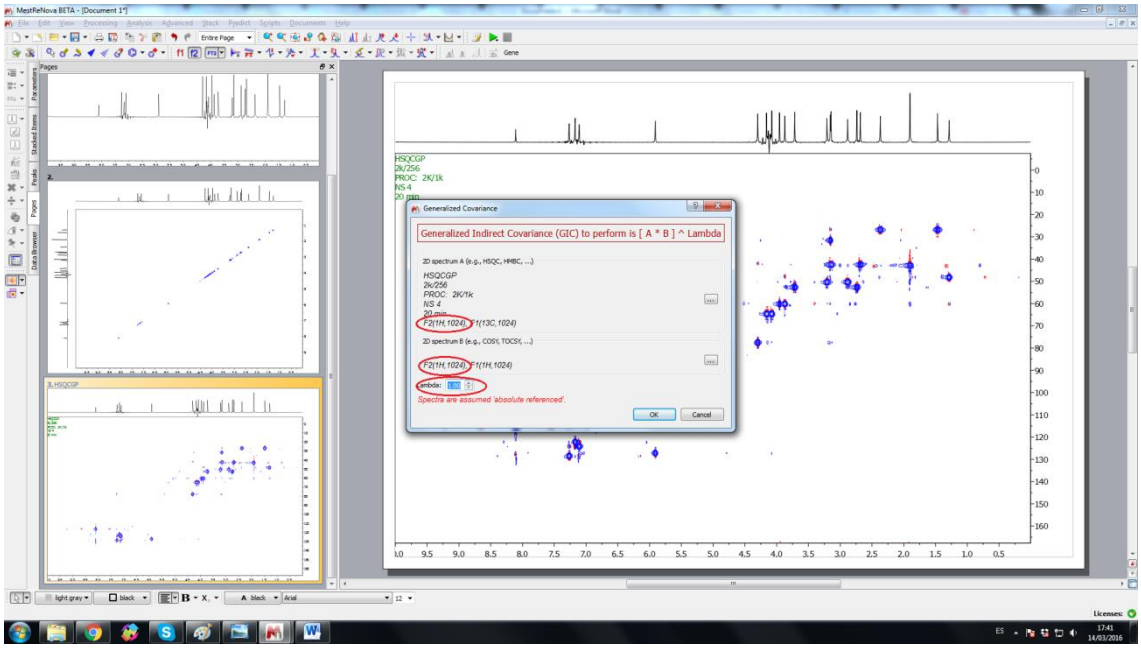

Figure 3: Generalized Indirect Covariance dialogue box.

7. It is important to keep in mind that both spectra must have the same number of points in F2 to apply GIC.

8. After a few seconds, you have the new psGIC spectrum, Figure 4.

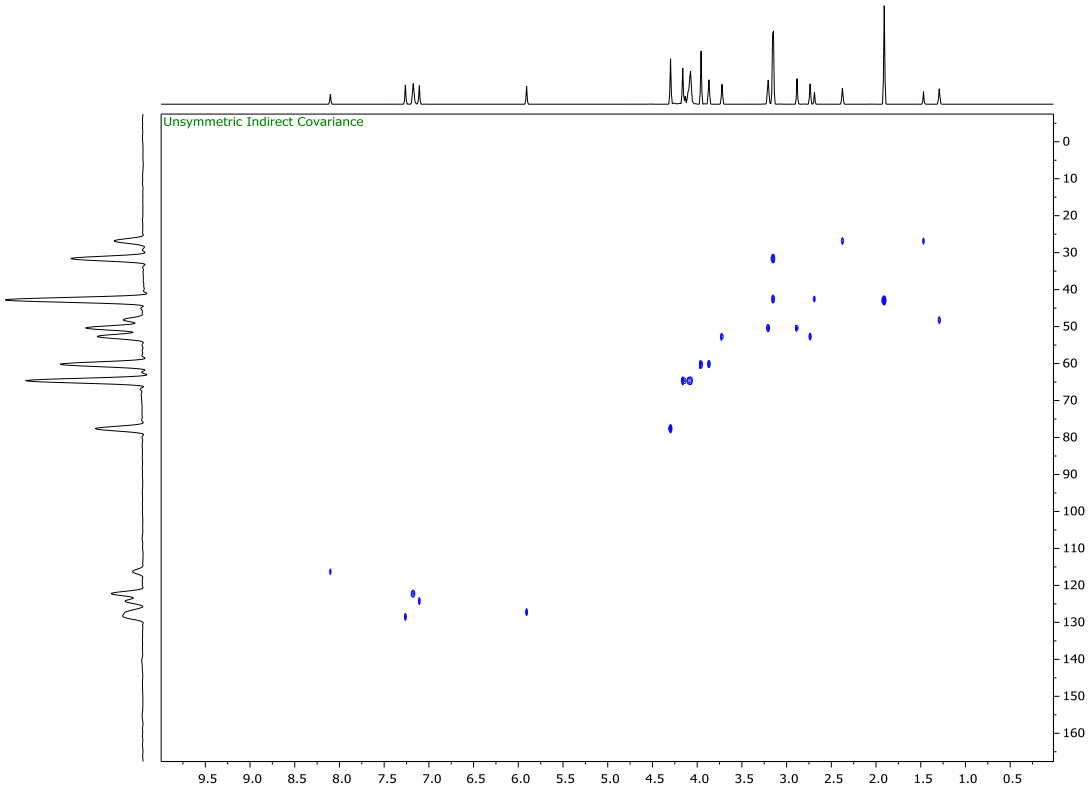

Figure 4: psGIC HSQC.

2D-DIAG FROM 2D PULSE SEQUENCE

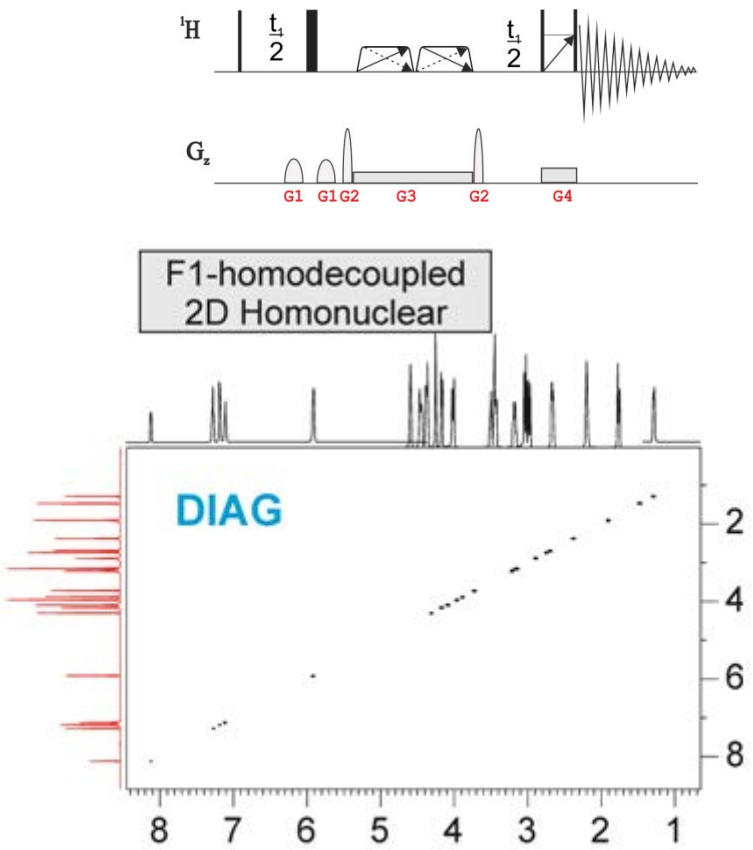

1. Another way to obtain the 2D-DIAG spectrum is from 2D pulse sequence. This experimental DIAG spectrum can be obtained from a modification of the recent PSYCHE-TOCSY pulse sequence with the omission of the DIPSI-2 pulse train.

2. After acquiring the spectrum, the result is a spectrum with any off-diagonals signals (Figure 5B). For to solve this problem, you can use the *Clean2D* script implemented in Mnova v11.

3. The cleanDIAG macro sets all the values in the experimental DIAG spectrum to zero except in a diagonal band with a user-defined width (e.g. 35 Hz).

4. For to run this script is the same as step 3 in **2D-DIAG FROM 1D HOMODECOUPLED**.

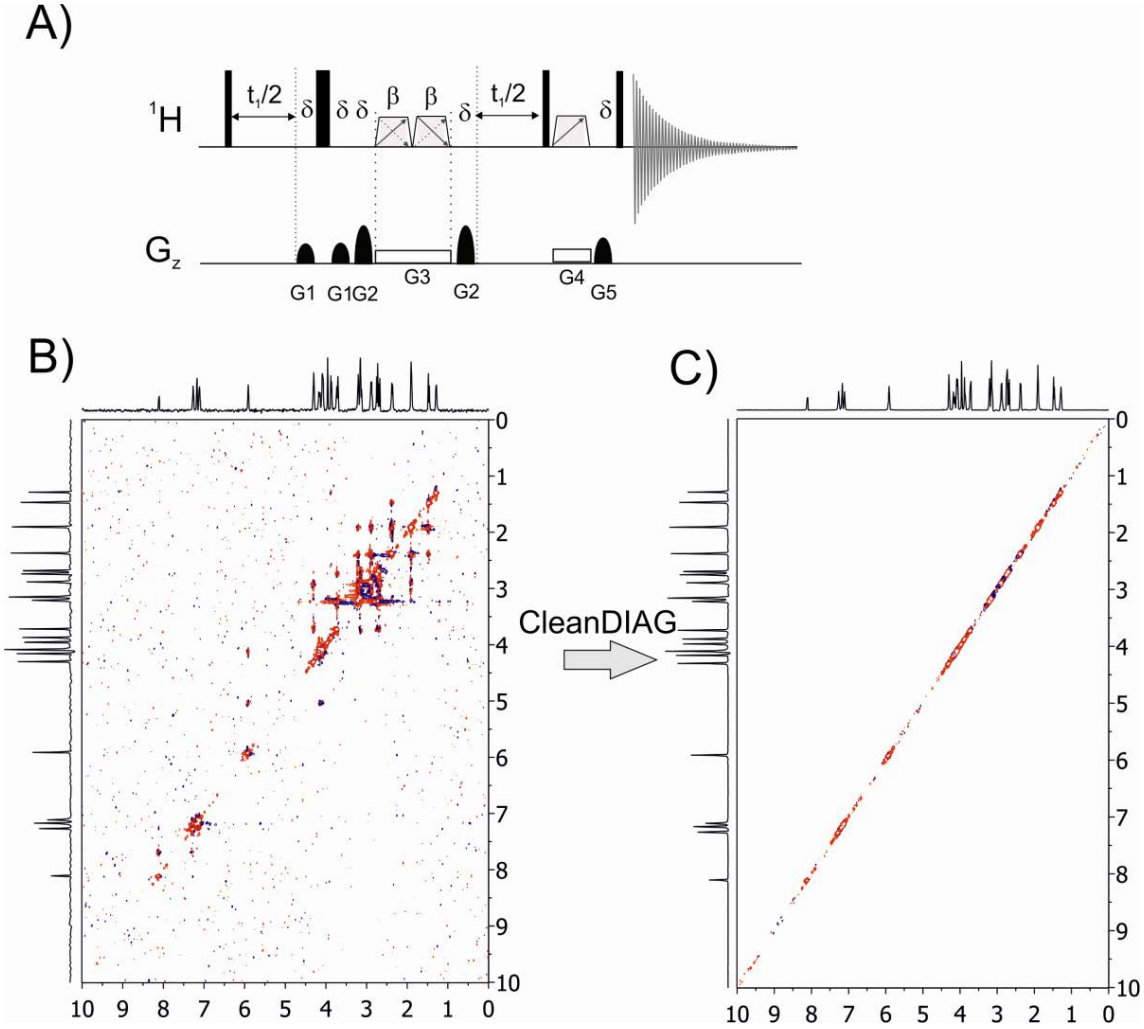

Figure 5: 5A) Pulse sequence used for the DIAG experiment; B-C) Experimental results showing the removal of any off-diagonal signals in the experimental DIAG spectrum by the *Clean2D* script implemented in Mnova. The script is executed with a customised multiple-width factor. The experimental DIAG spectrum in B) was recorded using a double frequency-swept chirp pulse length of 30 ms applied simultaneously to a weak gradient of 1.5 G/cm and with a flip-angle of β=20º. C) DIAG spectrum without off-diagonals signals.

5. After running the *Clean2D* script, it is possible to see the difference between F1 and F2 dimensions (Figure 6). Because of this, it is advisable to use the *Clean 2D* script.

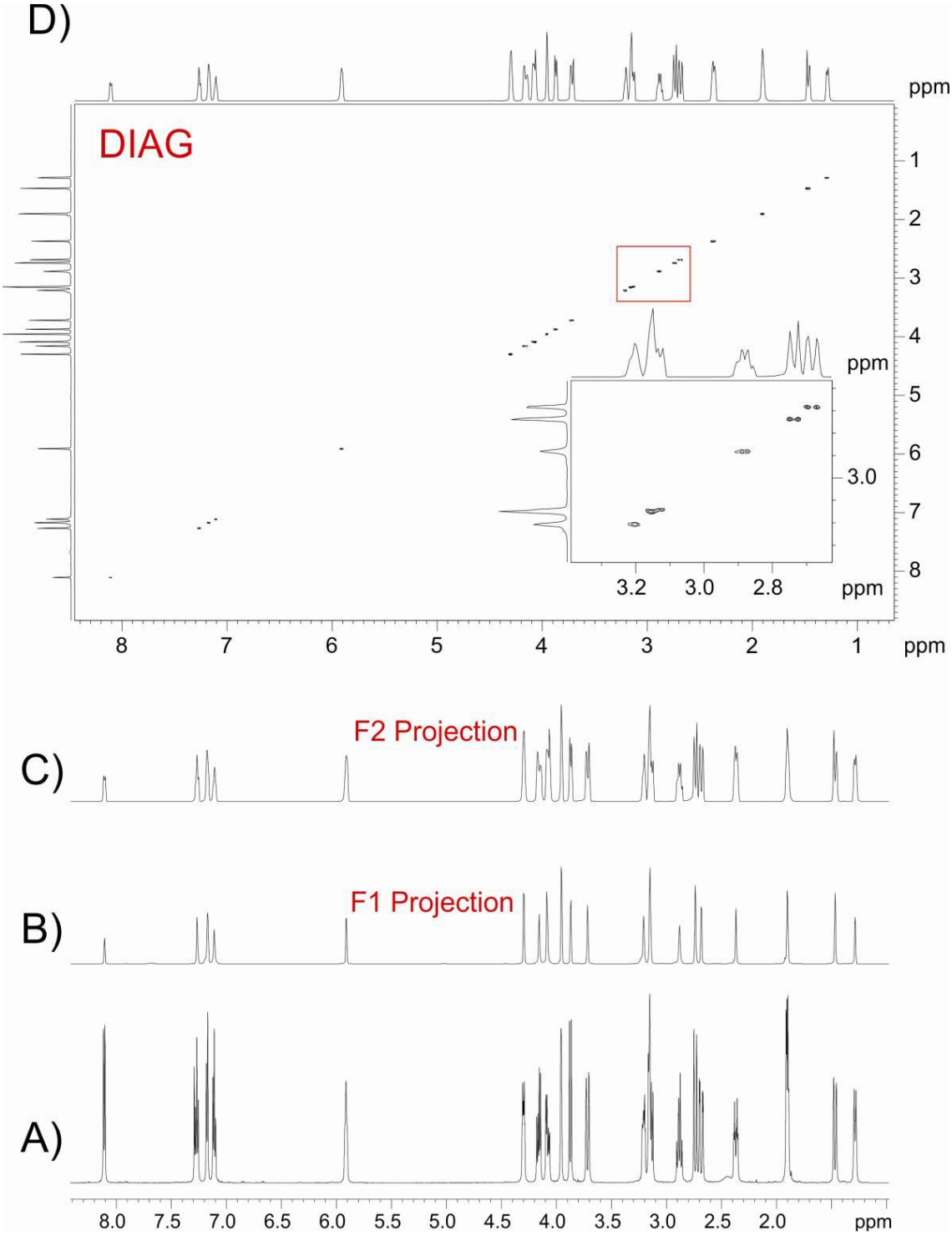

Figure 6: Comparison between the B) internal F1 and C) internal F2 projections in the D) 2D cleanDIAG spectrum of strychnine (see details in Figure 5). The enhanced high resolution obtained along the F1 dimension in DIAG is projected along the detected F2 dimension of regular homo- and heteronuclear NMR spectra.